Title:

Multifunctional requirements for ERK1/2 signaling in the development of ganglionic eminence derived glia and cortical inhibitory neurons

Author Names and Affiliations:

Sara J. Knowles[1], Michael C. Holter[1], Guohui Li[2], George R. Bjorklund[1], Katherina P. Rees[1], Johan S. Martinez-Fuentes[1], Kenji J. Nishimura[1], Ariana E. Afshari[1], Noah Fry[1], April M Stafford[3], Daniel Vogt[3], Marco Mangone[4], Trent Anderson[2], and Jason M. Newbern[1,*]

[1] School of Life Sciences, Arizona State University, Tempe, AZ 85287, USA

[2] College of Medicine, University of Arizona, Phoenix, AZ 85004, USA

[3] Department of Pediatrics and Human Development, Michigan State University, Grand Rapids, MI 49503, USA

[4]Virginia G. Piper Center for Personalized Diagnostics, The Biodesign Institute at Arizona State University, 1001 S McAllister Ave, Tempe, AZ 85281, USA.

*Corresponding Author address:

School of Life Sciences, PO Box 84501

Arizona State University

Tempe, AZ 85287-4501, USA

jason.newbern@asu.edu

Abstract

The RAS/RAF/MEK/ERK1/2 intracellular signaling pathway is activated by numerous cues during brain development and dysregulated in neurodevelopmental syndromes, particularly the RASopathies and certain forms of autism. Cortical excitatory/inhibitory imbalance is thought to be critical in the neuropathogenesis of these conditions. However, the developmental functions of ERK1/2 signaling in cortical inhibitory neurons (CINs) and other medial ganglionic eminence (MGE)-derived non-neuronal cells are poorly understood. Here, we genetically modulated ERK1/2 signaling in mouse MGE neural progenitors or GABAergic neurons in vivo. We find that MEK-ERK1/2 signaling is essential for regulating MGE-derived oligodendrocyte number in the anterior commissure. While *Erk1/2* inactivation does not alter CIN number, we discovered a significant and persistent reduction in somatostatin, but not parvalbumin, expression in a subset of CINs. ERK1/2 signaling is also necessary for chemogenetic activity-dependent FOSB expression in CINs in vivo. Interestingly, one week of chronic chemogenetic stimulation in juvenile or adult animals partially rescues the decrease in somatostatin expression in *Erk1/2* mutant CINs. Our data demonstrate ERK1/2 signaling is required for the establishment of MGE-derived glia, whereas in CINs, ERK1/2 drives activity dependent-responses and the expression of somatostatin in a subset of neurons.

Introduction

The canonical RAS/RAF/MEK/ERK1/2 intracellular kinase cascade is a ubiquitous pathway activated by a wide array of extracellular signals (Lavoie et al., 2020). Mutations in Receptor Tyrosine Kinase (RTK)-associated effectors and upstream regulators of Extracellular Regulated Kinase (ERK1/2, aka *MAPK3/1*) signaling cause a family of developmental syndromes collectively termed the "RASopathies" (Rauen, 2013). Individuals with RASopathies frequently exhibit craniofacial abnormalities, cardiac malformations, and increased cancer risk, in addition to neurological conditions such as epilepsy, developmental delay, intellectual disability, and autism (Tidyman & Rauen, 2016). Most RASopathy mutations increase ERK1/2 signaling, however, microdeletions that disrupt *Erk1* or *Erk2* expression have been linked to neurocognitive delay, intellectual disability, and autism (Ben-Shachar et al., 2008; Fernandez et al., 2010; Linhares et al., 2016; Newbern et al., 2008; Nowaczyk et al., 2014; Pucilowska et al., 2015; Rauen, 2013; Saitta et al., 2004; Samuels et al., 2009; Sánchez et al., 2020). Moreover, ERK1/2 signaling is a point of functional convergence for several autism and schizophrenia-associated copy number variants (Blizinsky et al., 2016; Courchesne et al., 2020; Heavner & Smith, 2020; Lord et al., 2020; Moyses-Oliveira et al., 2020; Rosina et al., 2019). Understanding the normal functions of ERK1/2 signaling in the developing forebrain may be instructive for defining neuropathological mechanisms in multiple neurodevelopmental syndromes.

The patterning of the forebrain is heavily dependent upon canonical trophic cues known to activate RTK signaling, but the precise functions of downstream kinase cascades are less clear (Assimacopoulos et al., 2003; Faedo et al., 2010; Maisonpierre et al., 1990; O'Leary et al., 2007). Studies of the mouse dorsal pallium have shown that FGF and ERK1/2 signaling via

ETV5 are crucial for cortical gliogenesis, while neurogenesis is relatively less affected (Dinh Duong et al., 2019; Fyffe-Maricich et al., 2011; S. Li et al., 2014; X. Li et al., 2012; Pucilowska et al., 2012). Interestingly, cell-specific *Mek1/2*-deletion in embryonic cortical excitatory neurons leads to subtype-specific deficits in morphological and electrophysiological properties during the early postnatal period (L. Xing et al., 2016). In contrast to mouse excitatory neurons, GABAergic cortical inhibitory neurons (CINs) are primarily derived from progenitor domains in the medial and caudal ganglionic eminences (MGE and CGE) (Wonders & Anderson, 2006). CIN patterning cues, migratory paths, master transcription factors, and expression levels of ERK1/2 pathway components differ significantly from dorsally derived glutamatergic neurons (Mardinly et al., 2016; Mayer et al., 2018; Ryu, Kang, et al., 2019; Ryu, Kim, et al., 2019; Talley et al., 2021). It is unknown whether ERK1/2 signaling has similar or unique functions in the development of glial and neuronal derivatives of the ganglionic eminences.

CINs exhibit substantial heterogeneity in their morphology, gene expression profile, electrophysiological properties, and contributions to cognition (Bomkamp et al., 2019; DeFelipe et al., 2013; Gour et al., 2021; Lim et al., 2018; Mayer et al., 2018; Petros et al., 2015). The two largest classes of CINs are identified by parvalbumin (PV) or somatostatin (SST) expression and are distinguished by unique electrophysiological properties (Dehorter et al., 2015; Lim et al., 2018; Okaty et al., 2009; Pan et al., 2018; Urban-Ciecko & Barth, 2016). Differences in their generation and local morphogen gradients bias progeny towards specific subtypes (McKenzie et al., 2019; Miyoshi et al., 2007; Petros et al., 2015). Trophic cues and neurotransmitters (e.g. BDNF/TrkB, Neuregulin-1/ErbB4, glutamate/NMDAR) are also important extracellular influences on CIN development (Cancedda et al., 2007; De Marco García et al., 2011; Exposito-Alonso et al., 2020; Fazzari et al., 2010; Glorioso et al., 2006; Hong et al., 2008; Huang et al.,

1999; Itami et al., 2007; Miller et al., 2011). While the transcriptional mechanisms of CIN development have been intensely studied, the signaling pathways that serve as intermediaries between extracellular stimulation and gene expression changes are relatively less clear. Recent work has shown that hyperactive MEK-ERK1/2 and PI3K-linked signaling pathways have critical roles in CIN development and subtype specification (Angara et al., 2020; Knowles et al., 2022; Malik et al., 2019; Vogt et al., 2015). However, the field still lacks crucial information on whether ERK1/2 signaling is necessary for CIN subtype identity.

The initial stages of postnatal development are characterized by a series of activity-dependent events in which CINs play a critical role (Ben-Ari et al., 2007; Cancedda et al., 2007; Close et al., 2012; Denaxa et al., 2012). Early spontaneous activity causes the release of GABA, which functions as a neurotransmitter and trophic cue to depolarize neurons and promote connections in the nascent cortical circuit (Ben-Ari et al., 2007; Owens & Kriegstein, 2002). Later stages of patterned activity are especially important for establishing the timing of critical periods and excitatory/inhibitory tone in cortical networks (Reh et al., 2020). Activity-dependent responses have been well studied in cortical excitatory neurons, where glutamatergic activation of ERK1/2 has been shown to modulate synaptic strength (Cristo et al., 2001; Thomas & Huganir, 2004; Wu et al., 2001; J. Xing et al., 1996; Yap & Greenberg, 2018). CINs express different levels of glutamate receptor subunits, calcium-binding proteins, and calcium responsive kinases that modulate intracellular signaling responses to glutamate (Cohen et al., 2016; Matthews et al., 1994; Paul et al., 2017; Sik et al., 1998; Tasic et al., 2016; Topolnik, 2012). Indeed, many features of the activity-dependent transcriptome in CINs differ from excitatory neurons (Guenthner et al., 2013; Hrvatin et al., 2018; Mardinly et al., 2016; Spiegel et al., 2014). Nonetheless, the phosphorylation-dependent signaling requirements for ERK1/2

110 in CINs are difficult to assess with transcriptomic approaches.

111 Studying the functions of ERK1/2 specifically in ventral forebrain derivatives using
112 germline knockouts of *Erk1* and *Erk2* is complicated by a combination of embryonic lethality,
113 compensatory interactions, and non-cell autonomous effects (Newbern et al., 2011; Samuels et
114 al., 2008; Selcher, 2001). Here, we used cell-specific genetic modifications to conditionally
115 inactivate ERK1/2 signaling in medial ganglionic eminence (MGE) progenitors (*Nkx2.1*^{Cre}) and
116 GABAergic neurons (*VGAT*^{Cre}) in embryonic mice. We show that ERK1/2 signaling is a critical
117 modulator of MGE-derived oligodendrocyte number in juvenile mice. In contrast, *Erk1/2*
118 appears dispensable for early tangential migration of CINs, the expression of core cortical
119 GABAergic neuron genes, and global CIN number. Further analysis of postnatal stages of
120 cortical maturation, however, revealed that the expression of SST protein in a subset of CINs
121 requires ERK1/2 signaling. We also found that *Erk1/2* is vital for activity-dependent FOSB
122 expression in CINs following chemogenetic stimulation in vivo. Moreover, chronically
123 increasing CIN activity during early postnatal stages or in adulthood was sufficient to partially
124 rescue the proportion of CINs that express SST. Our data reveal previously undescribed roles
125 for ERK1/2 signaling in select aspects of ventral forebrain glial development and the maturation
126 of CINs. These results may also inform our understanding of the cellular events underlying
127 neurodevelopmental disorders linked to aberrant ERK1/2 signaling.

128

Results

ERK1/2 signaling regulates the number of ventral forebrain-derived oligodendrocytes.

The ERK1/2 signaling pathway is an established regulator of dorsal pallium derived glial number, but its role in glial specification from subpallial progenitor domains remains less clear (Dinh Duong et al., 2019; X. Li et al., 2012). Neural progenitors within the subpallial medial ganglionic eminence (MGE) produce both neurons and glia after regional patterning by the transcription factor, Nkx2.1, at ~E8.5 (Shimamura & Rubenstein, 1997). *Nkx2.1*^{Cre} mice provide a valuable tool to selectively induce genetic modifications in MGE-derived glia and cortical inhibitory neurons (CINs) early in development. To completely inhibit ERK1/2 signaling and fluorescently label MGE derivatives, we generated quadruple genetically modified mice with germline *Erk1*/*Mapk3* deletion (*Erk1*$^{-/-}$), loxp-flanked ("floxed") *Erk2/Mapk1* exon 2 alleles (*Erk2*$^{fl/fl}$), *Nkx2.1*$^{Cre\ +/-}$, and a Cre-dependent tdTomato/RFP reporter, *Ai9*$^{+/-}$ (see *Genetically modified mice* in Materials and Methods) (Madisen et al., 2010; Newbern et al., 2008; Samuels et al., 2008; Selcher, 2001; L. Xing et al., 2016; Xu et al., 2008). *Nkx2.1*^{Cre}; *Ai9* mice showed an overall pattern of RFP-labeled neurons and glia consistent with previous reports at P14 (**Figure 1A**) and E13.5 (**Figure 1-figure supplement 1A**) (Madisen et al., 2010; Xu et al., 2008). Mutant mice with complete *Nkx2.1*^{Cre}-mediated *Erk1/2* inactivation (*Erk1*$^{-/-}$*; Erk2*$^{fl/fl}$*; Nkx2.1*^{Cre}*; Ai9*) were born at normal Mendelian ratios, survived into adulthood, and exhibited a reduction in ERK2 protein in CINs compared with *Erk1*$^{+/+}$*; Erk2*$^{wt/wt}$*; Nkx2.1*^{Cre}; *Ai9* (WT) or *Erk1*$^{-/-}$*; Erk2*$^{fl/wt}$*; Nkx2.1*^{Cre}*; Ai9* (HET control) mice of the same age (**Figure 1-figure supplement 1B-J**). Nearby cells, presumptive excitatory neurons, often showed higher levels of ERK2 protein expression, consistent with previous reports (Holter et al., 2021; Mardinly et al., 2016). Past research has demonstrated that DRG sensory or cortical excitatory neuron directed *Erk1*$^{-/-}$*; Erk2*$^{fl/wt}$*; Cre*

Figure 1

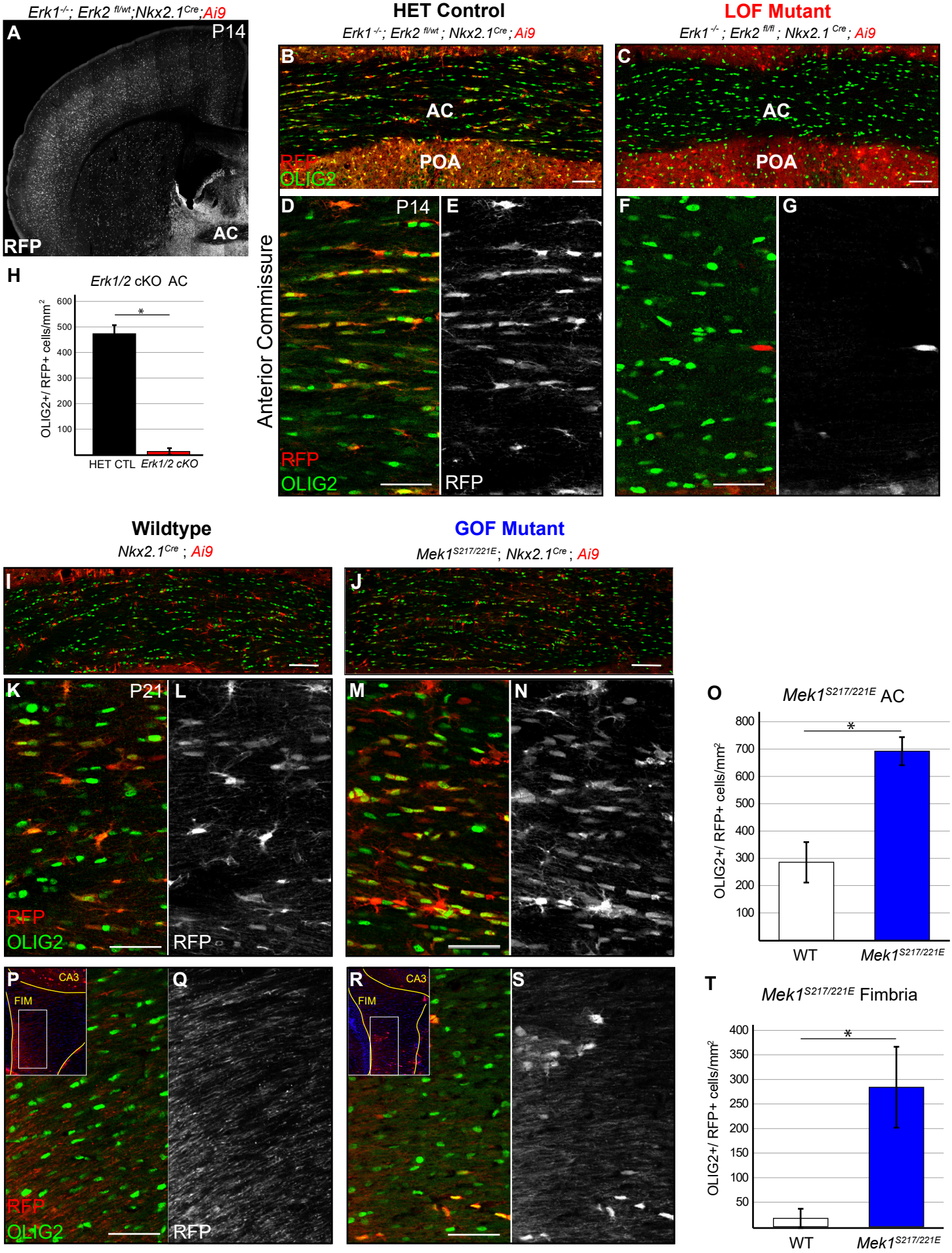
Erk1-/-; Erk2 fl/wt;Nkx2.1Cre;Ai9
A
P14
RFP
AC
HET Control
Erk1 -/-; Erk2 fl/wt ; Nkx2.1Cre ; Ai9
B
AC
POA
RFP
OLIG2
LOF Mutant
Erk1 -/- ; Erk2 fl/fl ; Nkx2.1 Cre ; Ai9
C
AC
POA
Anterior Commissure
D
P14
E
RFP
OLIG2
RFP
F
G
H
Erk1/2 cKO AC
OLIG2+/ RFP+ cells/mm2
600
500
400
300
200
100
*
HET CTL
Erk1/2 cKO
Wildtype
Nkx2.1Cre ; Ai9
GOF Mutant
Mek1S217/221E; Nkx2.1Cre ; Ai9
I
J
Anterior Commissure
K
P21
L
RFP
OLIG2
RFP
M
N
O
Mek1S217/221E AC
OLIG2+/ RFP+ cells/mm2
800
700
600
500
400
300
200
100
*
WT
Mek1S217/221E
Fimbria
P
CA3
FIM
Q
RFP
OLIG2
RFP
R
CA3
FIM
S
T
Mek1S217/221E Fimbria
OLIG2+/ RFP+ cells/mm2
400
350
300
250
200
150
100
50
*
WT
Mek1S217/221E

Figure 1. ERK1/2 signaling regulates MGE-derived oligodendrocyte number. (A) Anatomical image of a P14 *Erk1*$^{-/-}$*; Erk2*$^{fl/wt}$*; Nkx2.1*^{Cre}; *Ai9*$^{+/-}$ coronal section showing the expected neuroanatomical pattern of *Nkx2.1*^{Cre}-mediated recombination. Note the presence of *Nkx2.1*^{Cre}-derived oligodendrocytes in the anterior commissure at this stage. **(B-H)** Representative confocal images of the anterior commissure at P14 display a significant decrease in the density of OLIG2^{+}/RFP^{+} co-labeled cells in *Erk1*$^{-/-}$*; Erk2*$^{fl/fl}$*; Nkx2.1*^{Cre}*; Ai9* mutants (C, F-G) compared to HET controls (B, D-E) (quantification in **H**; N=3, mean ± SEM, *student's t-test, *p*=.0002) (scale bars 100µm (B-C), 50µm (D-G)). **(I-O)** Confocal images of the anterior commissure at P21 revealed a significant increase in the number of OLIG2^{+}/RFP^{+} cells in *Mek1*$^{S217/221E}$*; Nkx2.1*^{Cre}*; Ai9* mutants (J, M-N) relative to wildtype (I, K-L) (scale bar = 100 µm I-J, 50 µm K-N) (Quantification in **O**; N=3-4, mean ± SEM, *student's t-test, *p*=.004). **(P-T)** We observed ectopic expression of OLIG2^{+}/RFP^{+} cells in the fimbria of *Mek1*$^{S217/221E}$*; Nkx2.1*^{Cre}*; Ai9* mutants (scale bar = 50 µm) (quantification in **T**; N=3-4, mean ± SEM, *student's t-test, *p*=.005).

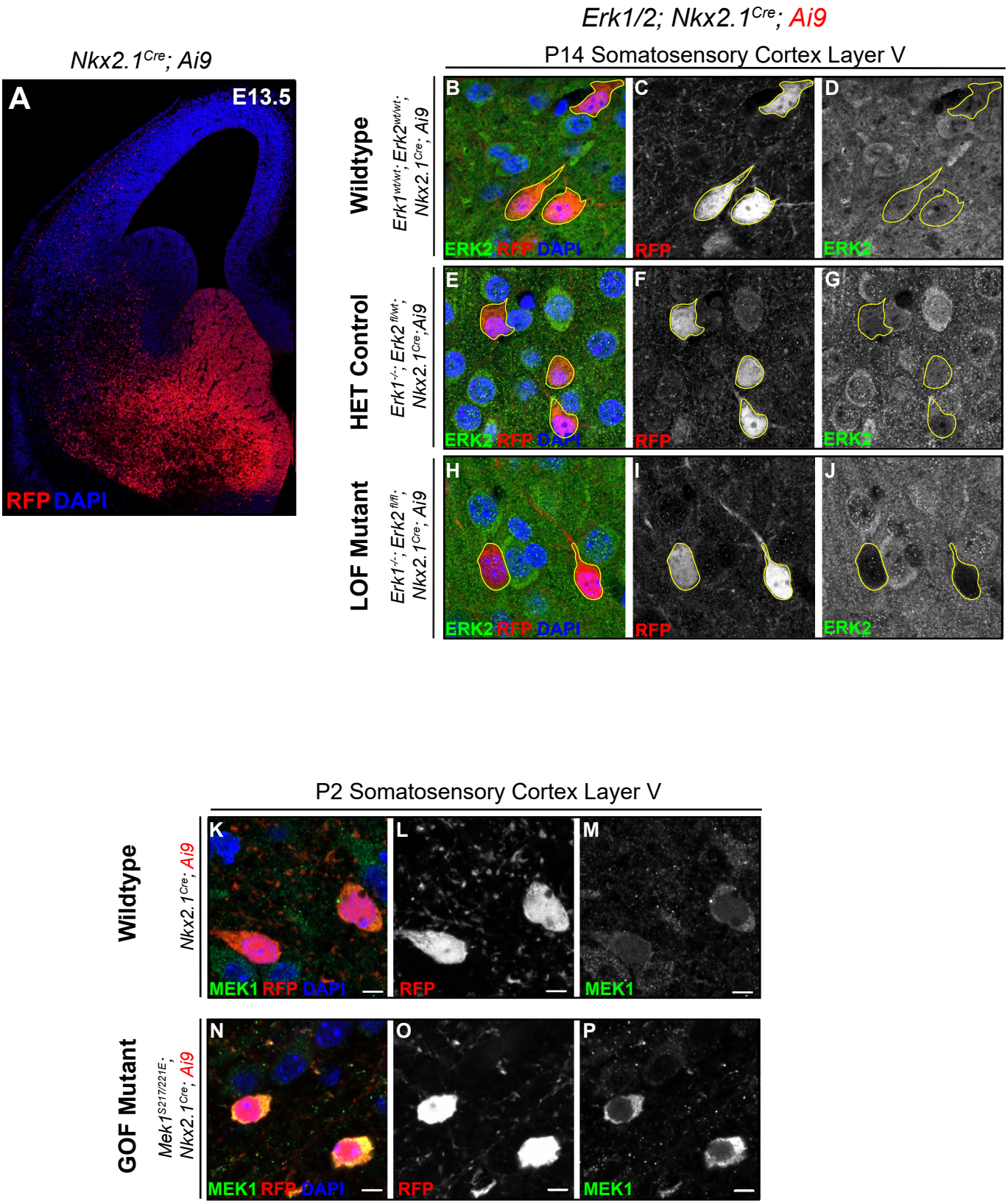
Nkx2.1Cre; Ai9
A
E13.5
RFP DAPI
Erk1/2; Nkx2.1Cre; Ai9
P14 Somatosensory Cortex Layer V
Wildtype
Erk1wt/wt; Erk2wt/wt; Nkx2.1Cre; Ai9
B
C
D
ERK2 RFP DAPI
RFP
ERK2
HET Control
Erk1-/-; Erk2fl/wt; Nkx2.1Cre; Ai9
E
F
G
ERK2 RFP DAPI
RFP
ERK2
LOF Mutant
Erk1-/-; Erk2fl/fl; Nkx2.1Cre; Ai9
H
I
J
ERK2 RFP DAPI
RFP
ERK2
P2 Somatosensory Cortex Layer V
Wildtype
Nkx2.1Cre; Ai9
K
L
M
MEK1 RFP DAPI
RFP
MEK1
GOF Mutant
Mek1S217/221E; Nkx2.1Cre; Ai9
N
O
P
MEK1 RFP DAPI
RFP
MEK1

Figure 1 - figure supplement 1. Cre-targeted modulation of ERK1/2 signaling. (A) Coronal hemisection of an E13.5 *Nkx2.1*^{Cre}*; Ai9* brain showing the expected pattern of *Nkx2.1*^{Cre}-mediated recombination. **(B-J)** High-resolution confocal images of neurons demonstrating reduced ERK2 immunoreactivity in RFP-expressing cells in P14 *Erk1*$^{-/-}$*; Erk2*$^{fl/fl}$*; Nkx2.1*^{Cre}*; Ai9* mice (H-J) compared with wildtype (B-D) or heterozygote controls (E-G) (scale bar = 5µm). **(K-P)** High-resolution confocal images demonstrating an increase in MEK1 expression in RFP-expressing neurons in *Mek1*$^{S217/221E}$; *Nkx2.1*^{Cre}*; Ai9* (N-P) animals compared to wildtype (K-M) (scale bar = 5µm).

A

OLIG2+ Cells in Anterior Commissure							
Age	Genotype	N	Area sampled (mm²)	Total OLIG2+ cells	OLIG2+ cells/mm²	Nkx2.1 cells/mm²	% Nkx2.1 derived
P14	*Erk1*$^{-/-}$; *Erk2*$^{fl/wt}$; *Nkx2.1*^{Cre}; *Ai9*	3	0.118	117	1497 +/- 39	473 +/- 34	31.60
P14	*Erk1*$^{-/-}$; *Erk2*$^{fl/fl}$; *Nkx2.1*^{Cre}; *Ai9*	3	0.237	336	1420 +/- 133	13 +/- 13	0.92
P21	*Nkx2.1*^{Cre}; *Ai9*	4	3.24	649	2077 +/- 164	285 +/- 74	13.72
P21	*MEK*$^{S217/221E}$; *Nkx2.1*^{Cre}; *Ai9*	4	4.45	1042	2385 +/- 92	692 +/- 51	29.01

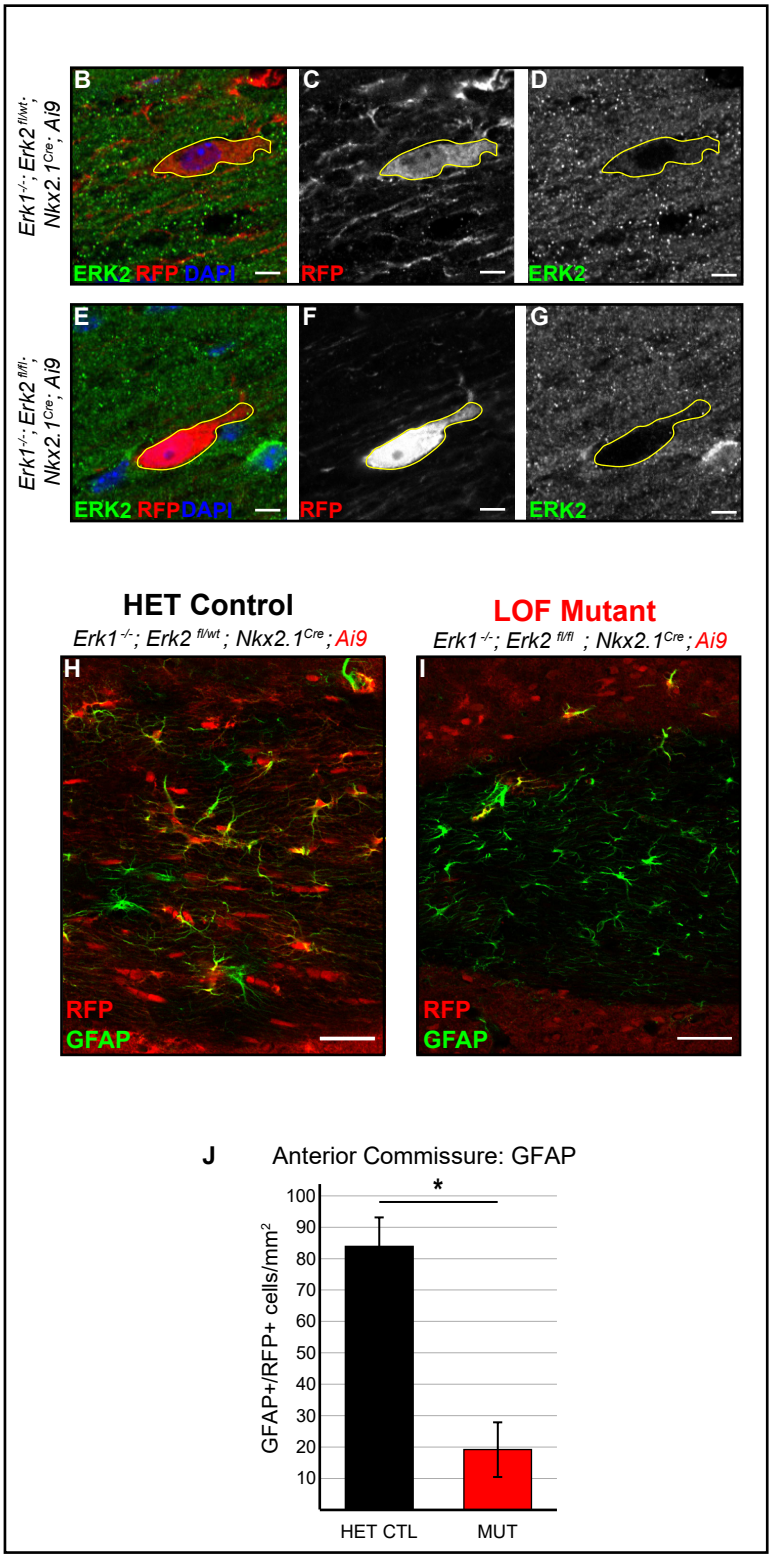

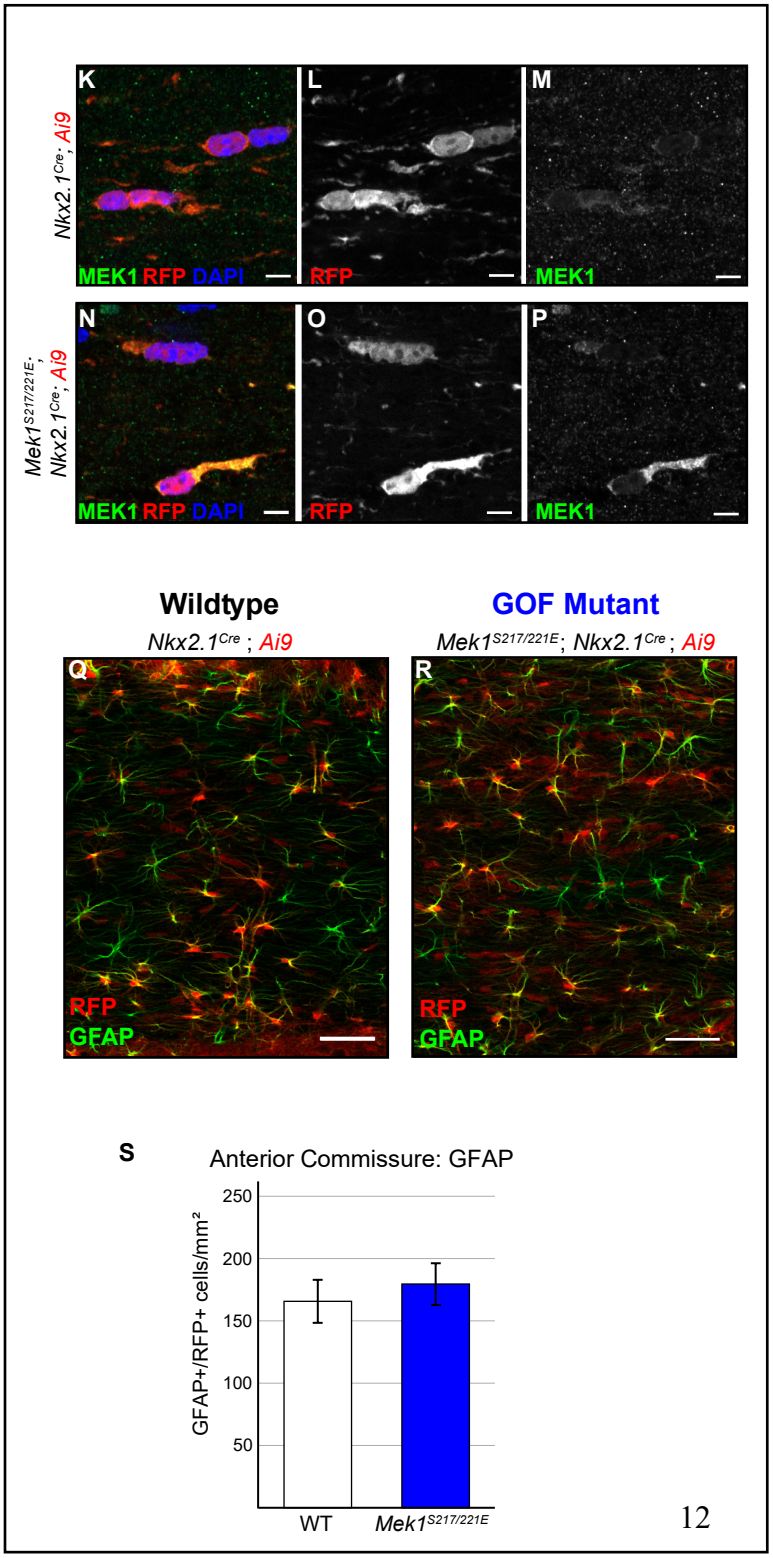

Figure 1 - figure supplement 2. Reduced ERK1/2 signaling regulates MGE-derived GFAP$^+$ astrocyte number. (A) Extended data on *Nkx2.1^{Cre}*-derived OLIG2$^+$ cells in the anterior commissure. **(B-G)** High-resolution confocal images demonstrating reduced ERK2 immunoreactivity in RFP-expressing cells in the anterior commissure of P14 *Erk1$^{-/-}$; Erk2$^{fl/fl}$; Nkx2.1^{Cre}; Ai9* mice (E-G) compared with heterozygote controls (B-D) (scale bar = 5µm). **(H-J)** Images demonstrating reduced density of RFP$^+$/GFAP$^+$ co-labeled cells in the anterior commissure of *Erk1$^{-/-}$; Erk2$^{fl/fl}$; Nkx2.1^{Cre}; Ai9* mice compared with heterozygous controls. (Quantification in **J**, N=3, mean ± SEM, *student's t-test, p<.05) (scale bar = 50µm). **(K-P)** High-resolution confocal images demonstrating an increase in MEK1 protein expression in RFP-expressing neurons in *Mek1$^{S217/221E}$*; *Nkx2.1^{Cre}; Ai9* animals (N-P) compared to wildtype controls (K-M) (scale bar = 5µm). **(Q-S)** Images of RFP+/GFAP+ cells in the anterior commissure of wildtype and *Mek1$^{S217/221E}$*; *Nkx2.1^{Cre}; Ai9* mice compared with heterozygous controls. (Quantification in **S**, N=3-4, mean ± SEM, *student's t-test, p>.05) (scale bar = 50µm).

152 expressing mice were relatively normal (Newbern et al., 2011; L. Xing et al., 2016). *Erk1*$^{-/-}$*;*
153 *Erk2*$^{fl/wt}$*; Nkx2.1*^{Cre}*; Ai9* mice were also grossly intact and used as littermate controls for certain
154 experiments.

155 The anterior commissure is a ventral white matter tract populated by glia from multiple
156 progenitor domains including the MGE (Kessaris et al., 2006; Minocha et al., 2015). Glia from
157 *Erk1*$^{-/-}$*; Erk2*$^{fl/fl}$*; Nkx2.1*^{Cre}*; Ai9* mutants had less ERK2 immunoreactivity than *Erk1*$^{-/-}$*; Erk2*$^{fl/wt}$*;*
158 *Nkx2.1*^{Cre}*; Ai9* HET controls (**Figure 1-figure supplement 2B-G**). We used a marker of the
159 oligodendrocyte lineage, OLIG2, to quantify the density of oligodendrocytes and OPCs at
160 postnatal day 14 (P14). We found a significant reduction in OLIG2^{+}/RFP^{+} co-expressing cells in
161 the anterior commissure of *Erk1*$^{-/-}$*; Erk2*$^{fl/fl}$*; Nkx2.1*^{Cre}*; Ai9* mutants when compared with *Erk1*$^{-/-}$*;*
162 *Erk2*$^{fl/wt}$*; Nkx2.1*^{Cre}*; Ai9* littermate controls (CTL 473 +/- 34 cells/mm^{2}, MUT 13 +/- 13 cells/mm^{2},
163 p=.0002, student's t-test) (**Figure 1 B-H, Figure 1-figure supplement 2A**). GFAP^{+}/RFP^{+}
164 astrocyte density was similarly reduced (CTL 84 +/- 9 cells/mm^{2}, MUT 19 +/- 9 cells/mm^{2}, p=.016,
165 student's t-test) (**Figure 1-figure supplement 2H-J**), suggesting that ERK1/2 signaling is
166 necessary for MGE-derived astrocyte and oligodendrocyte number.

167 RASopathies are primarily caused by mutations that hyperactivate ERK1/2, and often other,
168 signaling cascades. To determine if hyperactive MEK-ERK1/2 signaling is sufficient to modulate
169 MGE-derived glial density in the ventral forebrain, we generated mice expressing a Cre-dependent
170 hyperactivating *Mek1*$^{S217/221E}$ mutation (*CAG-loxpSTOPloxp-Mek1*$^{S217/221E}$*)*. *Mek1*$^{S217/221E}$*;*
171 *Nkx2.1*^{Cre}*; Ai9* mutants display relatively increased MEK1 levels in RFP^{+} CINs and glia (**Figure**
172 **1-figure supplement 1K-P, Figure 1-figure supplement 2K-P**) (Alessi et al., 1994; Bueno, 2000;
173 Cowley, 1994; Holter et al., 2021; Klesse et al., 1999; Krenz et al., 2008; Lajiness et al., 2014; X.
174 Li et al., 2012). In contrast to *Erk1/2* inactivation, *Mek1*$^{S217/221E}$*; Nkx2.1*^{Cre}*; Ai9* mutants showed

175 an increase in OLIG2^{+}/RFP^{+} cell density in the anterior commissure at P21 compared with
176 *Nkx2.1^{Cre}; Ai9* littermate controls (WT 285 +/- 74 cells/mm^2, *Mek1$^{S217/221E}$* 692 +/- 51 cells/mm^2,
177 *p*=.004, student's t-test) (**Figure 1I-O**, **Figure 1-figure supplement 2A**). In addition, we observed
178 ectopic MGE-derived glial profiles in the fimbria of *Mek1$^{S217/221E}$; Nkx2.1^{Cre}; Ai9* mutants (**Figure**
179 **1P-T**). However, we did not observe an increase in RFP+/GFAP+ cell density in the anterior
180 commissure of these animals (**Figure 1-figure supplement 2Q-S**). These data indicate that
181 increased MEK-ERK1/2 signaling enhances MGE-derived oligodendrocyte number.
182
183 *Reduced ERK1/2 signaling does not alter total CIN number in the somatosensory cortex.*
184 ERK1/2 signaling is necessary for the survival and physiological maturation of select
185 excitatory neuron subpopulations, but its requirement for CIN development is unclear (L. Xing et
186 al., 2016). In the primary somatosensory cortex of *Erk1$^{-/-}$; Erk2$^{fl/fl}$; Nkx2.1^{Cre}; Ai9* mice, we found
187 no difference in the density of *Nkx2.1^{Cre}*-recombined cells compared with HET controls at P14
188 (**Figure 2A-E**, *p*=0.476, student's t-test) and P60 (*p*=0.288, student's t-test, data not shown).
189 *Nkx2.1^{Cre}* does not recombine in the fraction of CINs derived from the lateral or caudal ganglionic
190 eminences (Kessaris et al., 2006; Talley et al., 2021). These data suggest ERK1/2 is not required
191 for the generation of the subset of CINs derived from the MGE.
192 To comprehensively assess the role of *Erk1/2* in all postmitotic GABAergic neurons, we
193 generated conditional mutants using *VGAT/Slc32a1^{Cre}* (Madisen et al., 2010; Vong et al., 2011).
194 *VGAT^{Cre}* is expressed in all GABAergic neurons early in development. We found that *Erk1$^{-/-}$;*
195 *Erk2$^{fl/fl}$; VGAT^{Cre}; Ai9* mutant mice were born at normal Mendelian ratios but exhibited profound
196 growth delay by the end of the first postnatal week and lethality in the second week (N=10). No
197 significant difference in the density of *VGAT^{Cre}*-recombined cells was observed between P5 *Erk1^{-}*

Figure 2

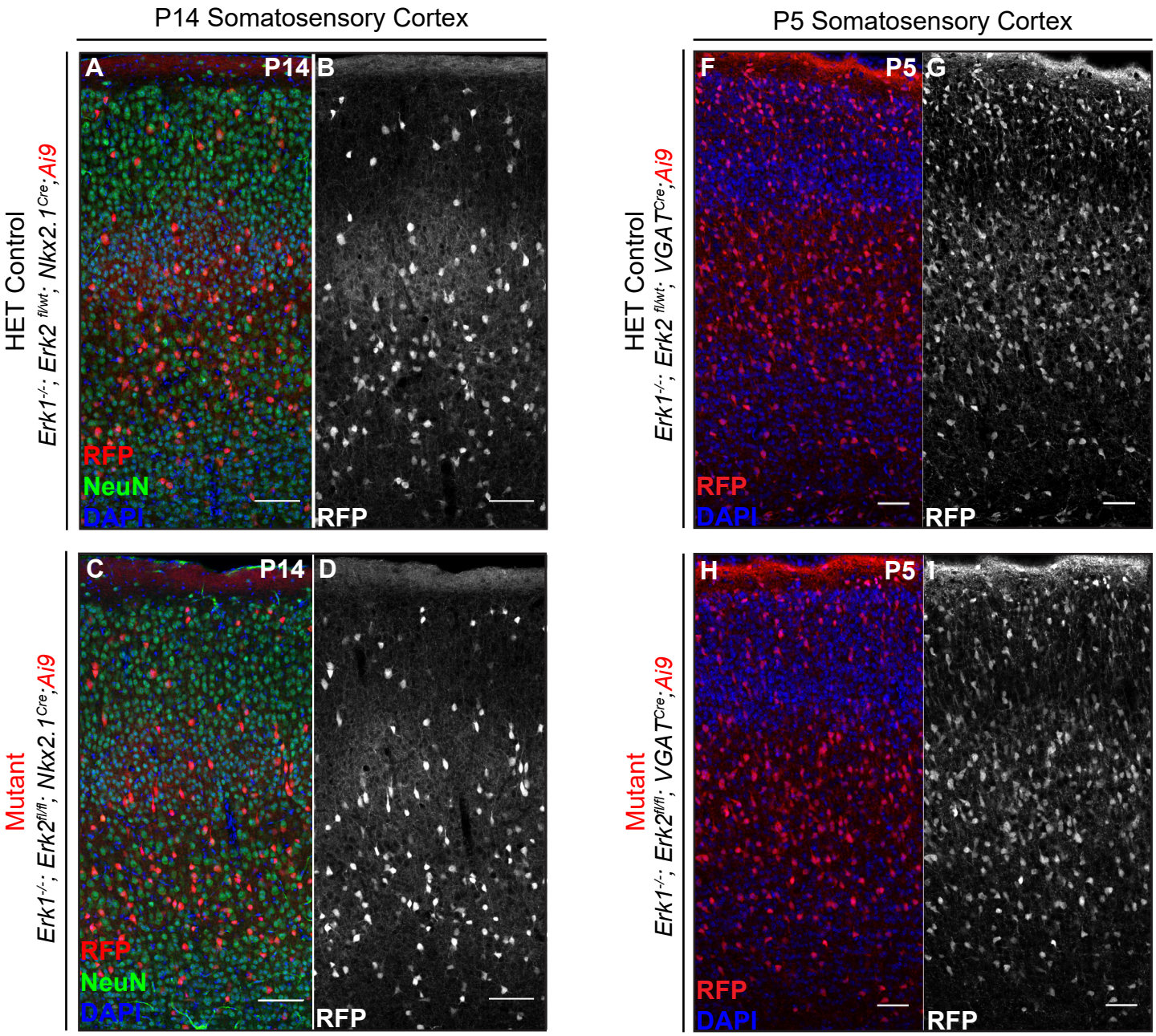
P14 Somatosensory Cortex
P5 Somatosensory Cortex
HET Control
Erk1-/-; Erk2 fl/wt; Nkx2.1Cre;Ai9
HET Control
Erk1-/-; Erk2 fl/wt; VGATCre;Ai9
Mutant
Erk1-/-; Erk2fl/fl; Nkx2.1Cre;Ai9
Mutant
Erk1-/-; Erk2fl/fl; VGATCre;Ai9
A
P14
B
C
P14
D
F
P5
G
H
P5
I
RFP
NeuN
DAPI
RFP

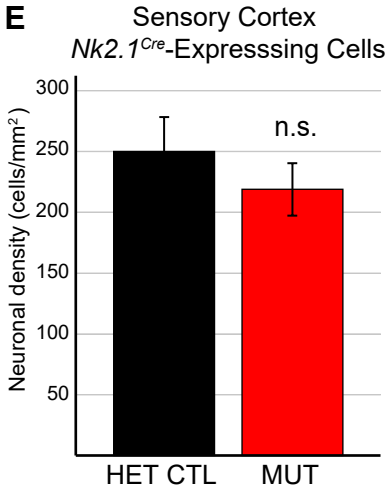
E
Sensory Cortex
Nk2.1Cre-Expresssing Cells
Neuronal density (cells/mm2)
300
250
200
150
100
50
n.s.
HET CTL
MUT

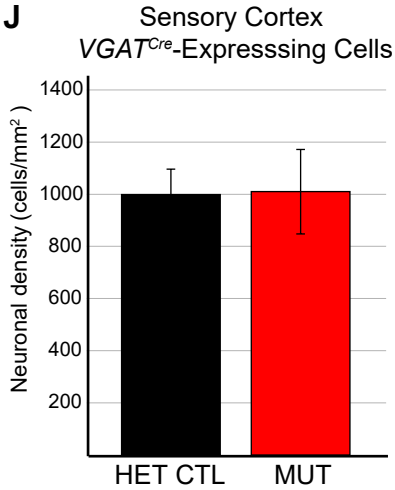
J
Sensory Cortex
VGATCre-Expresssing Cells
Neuronal density (cells/mm2)
1400
1200
1000
800
600
400
200
HET CTL
MUT

Figure 2. *Erk1/2* deletion does not alter CIN number. (A-E) Representative images of P14 somatosensory cortex in HET control (A-B) and *Erk1*$^{-/-}$*; Erk2*$^{fl/fl}$*; Nkx2.1*^{Cre}*; Ai9* (C-D) mutant animals, showing similar density of *Nkx2.1*^{Cre}-positive cells (quantification in **E**, N=4, mean +/- SEM, student's t-test, p=0.476**)** (scale bar = 50µm). **(F-J)** At P5, heterozygote control (F-G) and *Erk1*$^{-/-}$*; Erk2*$^{fl/fl}$*; VGAT*^{Cre}*; Ai9* mutant animals (H-I) showed no significant difference in the density of *VGAT*^{Cre}-positive cells in the somatosensory cortex (quantification in **J**, N=4, mean +/- SEM, student's t-test p=.955) (scale bar = 50µm).

198 $^{/-}$; *Erk2*$^{fl/fl}$; *VGAT*^{Cre}; *Ai9* mutant and *Erk1*$^{-/-}$; *Erk2*$^{fl/wt}$; *VGAT*^{Cre}; *Ai9* HET control cortices (CTL
199 998 +/- 98 cells/mm^2, MUT 1010 +/- 162 cells/mm^2, p=.955, student's t-test) (**Figure 2F-J**).
200 Together, these data suggest that ERK1/2 signaling is dispensable for the initial establishment and
201 maintenance of CIN number.
202
203 *ERK1/2 deletion alters SST expression in a subset of inhibitory neurons.*
204 CINs are a heterogeneous population of neurons that can be divided into numerous subtypes
205 with overlapping but distinct transcriptional profiles. Although CIN number was unaltered in the
206 cortex following ERK1/2 deletion, gene expression changes in these cells remained unknown. To
207 study the CIN translatome, we employed a Cre-dependent 'Ribotag' mouse that expresses an HA-
208 fused ribosomal protein, RPL22^{HA}, for translating ribosome affinity purification followed by RNA
209 sequencing (Sanz et al 2009). Whole cortices were dissected from P7.5 *Erk1*$^{-/-}$; *Erk2*$^{fl/fl}$; *VGAT*^{Cre};
210 *Rpl22*^{HA} (MUT), *Erk1*$^{-/-}$; *Erk2*$^{fl/wt}$; *VGAT*^{Cre}; *Rpl22*^{HA} (HET), or wildtype controls (*Erk1*$^{+/+}$;
211 *Erk2*$^{wt/wt}$; *VGAT*^{Cre}; *Rpl22*^{HA}) (WT). Following homogenization, HA-containing ribosomes were
212 immunoprecipitated and RNA was purified from cortical (INPUT) or immunoprecipitated (IP)
213 samples, amplified, and sequenced. As expected, we observed a near complete absence of reads
214 complementary to *Erk1/Mapk3* exons 1-6 in *Erk1*$^{-/-}$ animals and a gene dose dependent reduction
215 of *Erk2/Mapk1* exon 2 in IP fractions (**Figure 3-figure supplement 1A**). A comparison of the
216 >3400 differentially expressed genes between IP and INPUT fractions within each genotype
217 revealed that IP fractions exhibited significant enrichment of *Cre* and well-established core
218 GABAergic genes (*Gad1/2*, *Slc32a1*, *Erbb4*, *Dlx1/2/5/6*), as well as significant depletion of genes
219 expressed in glia (*Fabp7, Sox10, Pdgfra, S100b*) and excitatory neurons (*Neurod1/6, Camk2a*)
220 (**Table S1** and **Figure 3-figure supplement 1B-C**) (Hrvatin et al., 2018; Mardinly et al., 2016; Mi

221 et al., 2018; Paul et al., 2017; Tasic et al., 2016). These data indicate the Ribotag approach
222 significantly enriched samples for CIN-derived mRNA.

223 We next examined the differential expression of genes between control (HET) and mutant
224 (MUT) IP, CIN-enriched samples, particularly those important for GABAergic specification and
225 subtype identity (**Table S2**). A significant decrease in known ERK1/2 target genes *Spry4*, *Etv5*,
226 and *Egr2* was noted in MUT IP samples (**Figure 3A-magenta**) (X. Li et al., 2012; Newbern et al.,
227 2011; L. Xing et al., 2016). However, the expression of master transcriptional regulators of global
228 CIN identity (*Lhx6*, *Dlx2/5/6)* and GABAergic metabolism *(Gad1/2*, *Slc32a1*) was not
229 significantly different between HET and MUT IP samples (**Figure 3A-green**). GO analysis
230 detected a significant overrepresentation of differentially expressed genes in the category of
231 "regulation of cell differentiation" (GO:0045595, adj. p =.002) and "nervous system development"
232 (GO:0030182, adj. p =.04). Indeed, we observed changes in the expression of genes linked to
233 neural maturation (*Notch1, Smo, Fgf18, Bdnf*) and CIN subtype specification (*Mafb, Sst, Sp9,*
234 *Crhbp, Grin2d*). Together, these data indicate that ERK1/2 inactivation does not significantly
235 disrupt core mediators of CIN identity but may have selective effects on later stages of subtype
236 maturation.

237 We further analyzed CIN subtypes in *Erk1*$^{-/-}$*; Erk2*$^{fl/fl}$*; VGAT*^{Cre}*; Ai9* brains at P5, prior to the
238 observed lethality. At this stage, SST, a canonical marker of a subset of regular spiking (RS) CINs,
239 and Calbindin 1 (CALB1), a calcium binding protein co-expressed in a subset of CINs partially
240 overlapping with SST, are expressed (Forloni et al., 1990; Kawaguchi, 1997; Marsh et al., 2016;
241 Martin et al., 2017; Mi et al., 2018; Munguba et al., 2019; Nigro et al., 2018; Tasic et al., 2016).
242 We assessed these two classes of SST-expressing CINs and found a statistically significant
243 reduction in SST^{+}/CALB1^{-} cells in mutants relative to littermate controls (p=0.017, student's t-

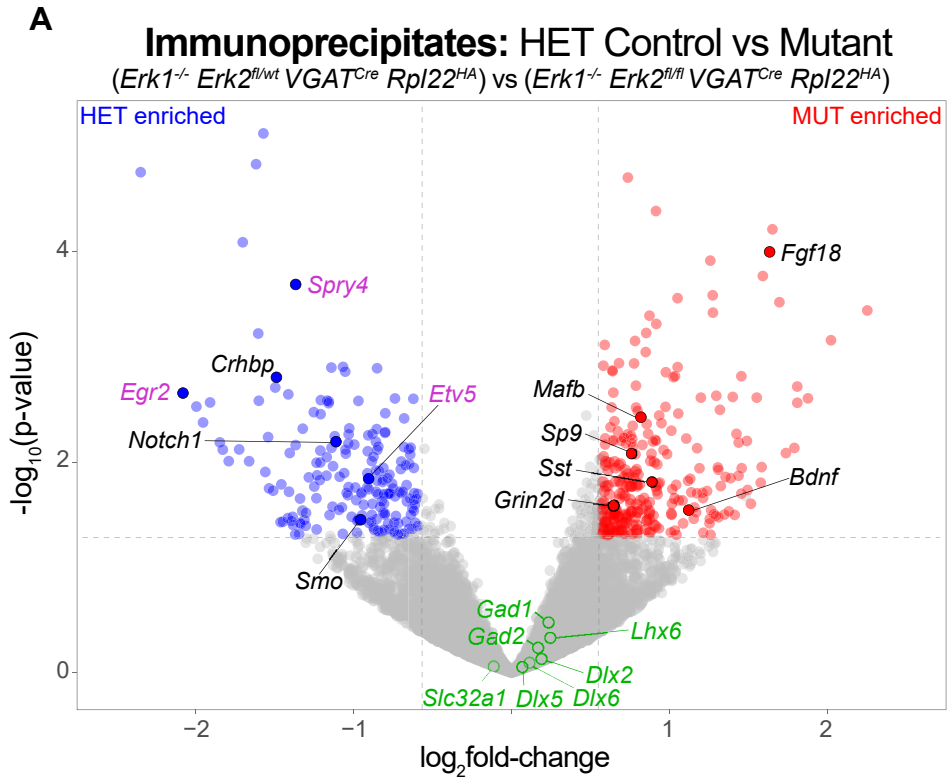
A
Immunoprecipitates: HET Control vs Mutant
(Erk1-/- Erk2fl/wt VGATCre Rpl22HA) vs (Erk1-/- Erk2fl/fl VGATCre Rpl22HA)
HET enriched
MUT enriched
Spry4
Crhbp
Egr2
Notch1
Etv5
Smo
Fgf18
Mafb
Sp9
Sst
Grin2d
Bdnf
Gad1
Gad2
Lhx6
Dlx2
Slc32a1
Dlx5
Dlx6
-log10(p-value)
log2fold-change

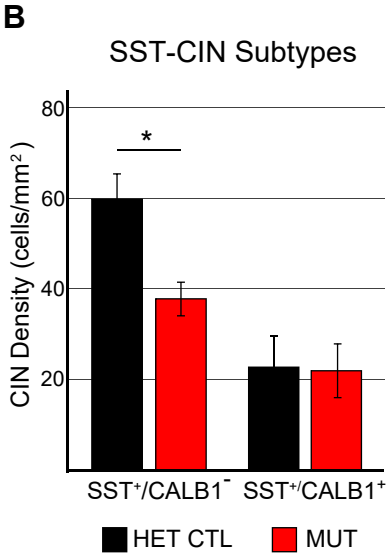
B
SST-CIN Subtypes
CIN Density (cells/mm2)
SST+/CALB1-
SST+/CALB1+
HET CTL
MUT

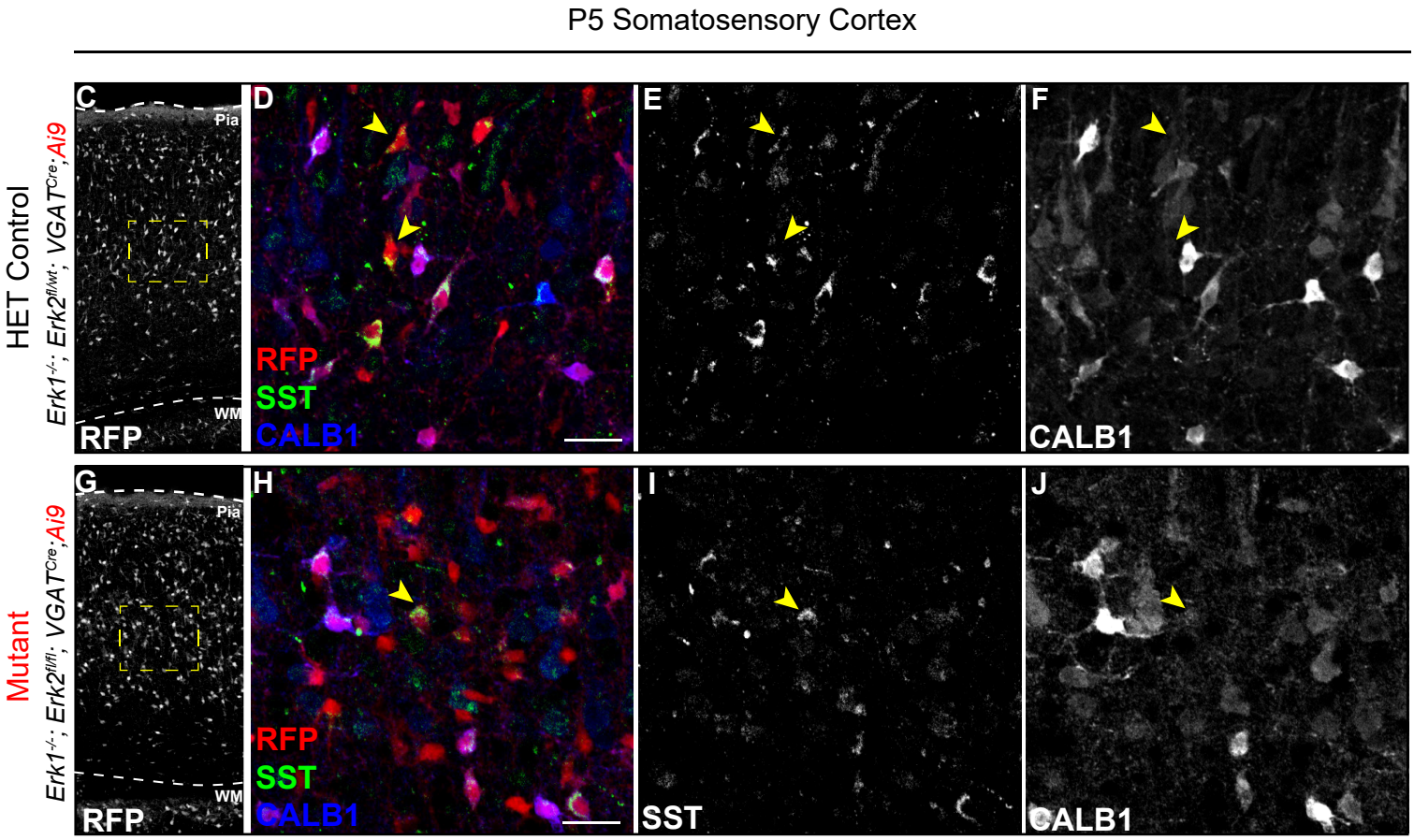
P5 Somatosensory Cortex
HET Control
Erk1-/-; Erk2fl/wt; VGATCre;Ai9
Mutant
Erk1-/-; Erk2fl/fl; VGATCre;Ai9
Pia
WM
RFP
SST
CALB1

Figure 3. Loss of ERK1/2 does not alter the initial expression of generic regulators of GABAergic function. **(A)** HET IP vs MUTANT IP volcano plot of expressed protein-coding genes in Ribotag, CIN-enriched samples illustrates the significant reduction in ERK1/2 pathway target genes in *Erk1/2* inactivated (*Erk1*$^{-/-}$*; Erk2*$^{fl/fl}$*; VGAT*^{Cre}*; Rpl22*^{HA}*)* immunoprecipitated fractions (magenta - *Spry4, Etv5, Egr2*) (N=3, p<.05). A significant difference was not detected in the expression of master regulators of CIN specification (green - *Lhx6, Dlx2/5/6*) and key GABA processing genes (green - *Gad1/2, Slc32a1*). However, the expression CIN-subtype enriched genes (*Crhbp, Sst, Mafb, Grin2d, Sp9*) and canonical developmental signals (*Notch1, Smo, Fgf18, Bdnf*) were significantly altered in mutant CINs. **(B-J)** Immunolabeling analysis of CIN subtype markers revealed a significant reduction in SST^{+}/CALB^{-} cell density (yellow arrowheads) in mutants, while SST^{+}/CALB^{+} co-labeled cell density was unchanged (quantification in **B**, N=4, mean ± SEM, *student's t-test p=0.017). Representative images in (D-F, H-J) are from layer 5 primary somatosensory cortex (scale bar = 25µm).

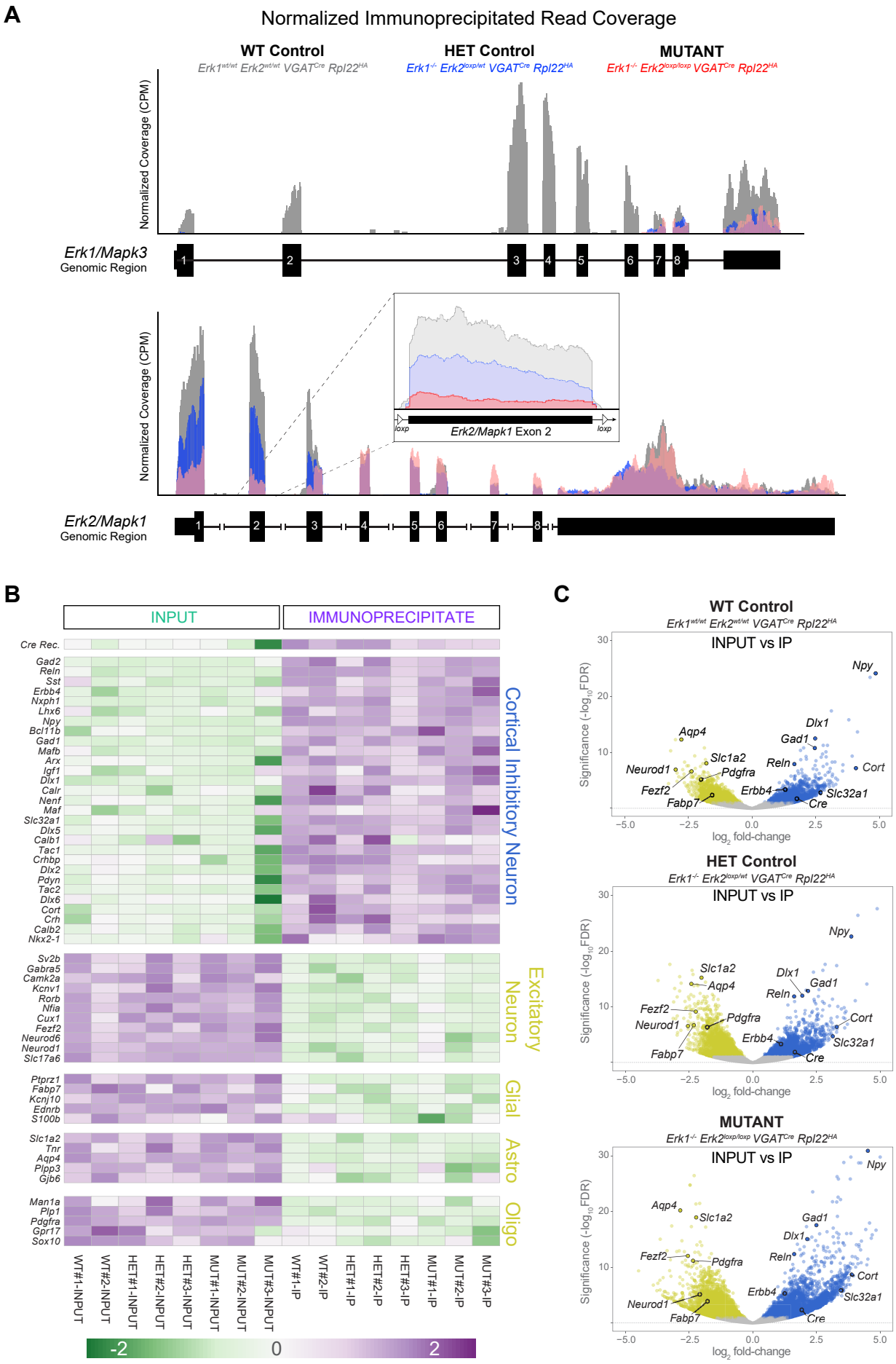
A
Normalized Immunoprecipitated Read Coverage
WT Control
Erk1wt/wt Erk2wt/wt VGATCre Rpl22HA
HET Control
Erk1-/- Erk2loxp/wt VGATCre Rpl22HA
MUTANT
Erk1-/- Erk2loxp/loxp VGATCre Rpl22HA
Normalized Coverage (CPM)
Erk1/Mapk3
Genomic Region
Erk2/Mapk1 Exon 2
loxp
Erk2/Mapk1
Genomic Region
B
INPUT
IMMUNOPRECIPITATE
Cre Rec.
Cortical Inhibitory Neuron
Excitatory Neuron
Glial
Astro
Oligo
WT#1-INPUT
WT#2-INPUT
HET#1-INPUT
HET#2-INPUT
HET#3-INPUT
MUT#1-INPUT
MUT#2-INPUT
MUT#3-INPUT
WT#1-IP
WT#2-IP
HET#1-IP
HET#2-IP
HET#3-IP
MUT#1-IP
MUT#2-IP
MUT#3-IP
-2
0
2
C
WT Control
INPUT vs IP
HET Control
INPUT vs IP
MUTANT
INPUT vs IP
Significance (-log10 FDR)
log2 fold-change

Figure 3 - figure supplement 1. RiboTag in *Erk1/2 VGAT^{Cre}* mice enriches for CIN mRNA. (A) Read coverage maps for *Erk1/Mapk3* and *Erk2/Mapk1* in a representative immunoprecipitated RNA sample from a wildtype (grey), heterozygous control (blue), and mutant *Erk1 Erk2 VGAT^{Cre} Rpl22^{HA}* (red) cortex. As expected, *Erk1* exons 1-6 were not detected in heterozygous (N=3) and mutant (N=3) fractions relative to wildtype (N=2) samples (DEXSeq: $p<0.005$). Analysis of *Erk2/Mapk1* exon 2 (inset), which is *loxp*-flanked in conditional knockouts, revealed a statistically significant reduction in immunoprecipitated mutant samples when compared to heterozygote controls (DEXSeq: 2.5-fold reduction, $p<0.005$, N=3). **(B)** Heatmap of DeSeq2-derived normalized gene expression values for select protein coding genes with known specificity for CINs, excitatory neurons, pan-glia, astrocytes, and oligodendrocytes in all samples. Values were unit-variance scaled for each gene within a row for visualization purposes; purple values indicate relative enrichment while green values indicate relative depletion. **(C)** Volcano plots including >11,000 expressed protein coding genes in IP vs INPUT fractions within each of the three test conditions. Grey dots indicate genes not significantly changed, yellow-green dots are significantly enriched genes in INPUT fractions, while blue dots are significantly enriched genes in IP fractions. Select genes known to be expressed in distinct cell types noted in (B) are highlighted.

244 test), but no change in SST^+/$CALB1^+$ co-expressing cells (p=0.938, student's t-test) (**Figure 3B-**
245 **J**). The early lethality of the *Erk1*$^{-/-}$*; Erk2*$^{fl/fl}$*; VGAT*^{Cre}*; Ai9* mice prohibited our ability to study
246 fully mature CIN markers, as PV is not expressed until the second postnatal week and only a subset
247 of RS CINs have initiated SST protein expression (del Rio et al., 1994; Forloni et al., 1990; Huang
248 et al., 1999). Nonetheless, our data are consistent with a role for ERK1/2 in the early development
249 of SST-CIN subtypes in the first postnatal week.

250 The broad recombination pattern of *VGAT*^{Cre} throughout the entire nervous system leaves open
251 the possibility of non-cell-autonomous effects on CIN development. We therefore performed more
252 detailed studies of subtype specification in *Nkx2.1*^{Cre} mutants, where recombination occurs in a
253 smaller subset of CINs, but survival extends into adulthood. Quantification of PV-CIN number in
254 P14 and adult *Erk1*$^{-/-}$*; Erk2*$^{fl/fl}$*; Nkx2.1*^{Cre}*; Ai3* mice revealed no differences in the proportion of
255 *Nkx2.1*^{Cre}-derived CINs expressing PV or their somal size (CTL: 181.7 +/- 4.4μm^2, MUT: 187.4
256 +/- 5.0μm^2, mean +/- SEM, N=105 cells/group, student's t-test, p=0.398) (**Figure 4A-C, E-G, I-**
257 **K, M-O, Q**). Notably, we observed a significant reduction in the proportion of *Nkx2.1*^{Cre}-derived,
258 SST-expressing CINs at P14, an effect which persisted into adulthood (**Figure 4D, H, L, P, Q**).
259 This phenotype appears to require complete loss of ERK1/2 signaling since overall PV and SST
260 cell densities were unchanged between P60 Cre-negative *Erk1*$^{-/-}$ mice and *Erk1*$^{-/-}$*; Erk2*$^{fl/wt}$*;*
261 *Nkx2.1*^{Cre} (HET control) animals (**Figure 4-figure supplement 1A**). Additionally, *Erk2*$^{fl/fl}$*;*
262 *Nkx2.1*^{Cre}*; Ai14* mutants showed no relative difference in CIN density or subtypes at P30 compared
263 to *Erk2* wildtype controls (**Figure 4-figure supplement 1B-F**). Attempts to generate an *Erk1*$^{-/-}$*;*
264 *Erk2*$^{fl/fl}$*; SST*^{Cre} strain yielded no viable mutants at birth (0 of 49, 12 expected) (Taniguchi et al.,
265 2011). Hyperactivation of MEK-ERK1/2 signaling in P21 *Mek1*$^{S217/221E}$*; Nkx2.1*^{Cre}*; Ai9* mice did
266 not alter the density of SST-expressing CINs, though we observed the previously reported decrease

Figure 4

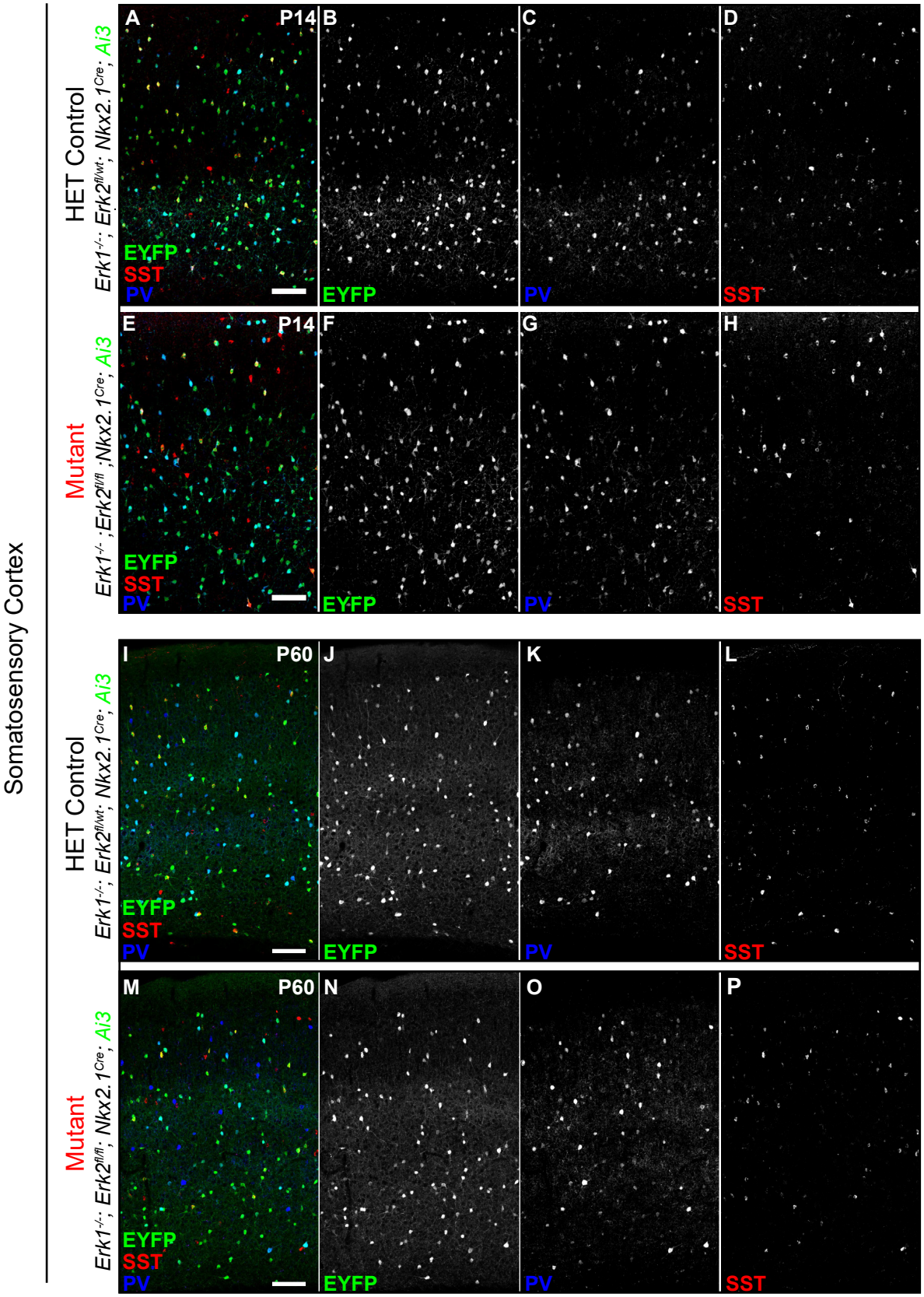
Somatosensory Cortex
HET Control
Erk1-/-; Erk2fl/wt; Nkx2.1Cre; Ai3
Mutant
Erk1-/-; Erk2fl/fl; Nkx2.1Cre; Ai3
A
P14
B
C
D
E
F
G
H
I
P60
J
K
L
M
N
O
P
EYFP
SST
PV

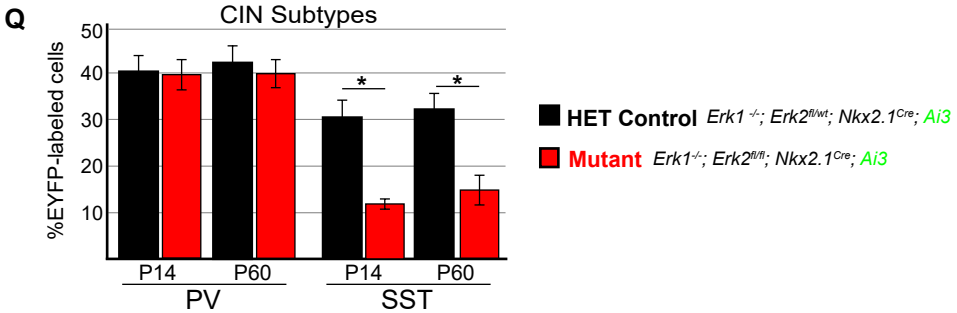
Q
CIN Subtypes
%EYFP-labeled cells
50
40
30
20
10
*
*
P14
P60
P14
P60
PV
SST
HET Control Erk1-/-; Erk2fl/wt; Nkx2.1Cre; Ai3
Mutant Erk1-/-; Erk2fl/fl; Nkx2.1Cre; Ai3

Figure 4. The proportion of SST-expressing CINs decreased following reductions in ERK1/2 signaling. (A-H) Representative confocal images of the somatosensory cortex at P14. The proportion of PV-expressing CINs was similar between genotypes (**C, G**, quantification in **Q**; N=3, mean ± SEM, student's t-test, $p > .05$), while the proportion of $SST^+/EYFP^+$ cells was significantly lower in mutants compared to HET controls (**D, H**, quantification in **Q**; N=3, mean ± SEM, *student's t-test, $p = .005$). **(I-P)** By P60, no difference in PV-CINs was detected (**K, O**, quantification in **Q**; N=3, mean ± SEM, $p > .05$), whereas a significant decrease in the density of $SST^+/EYFP^+$ cells in mutant cortices was still apparent (**L, P**, quantification in **Q**; N=3, mean ± SEM, *student's t-test $p = .03$) (scale bars =50 μm).

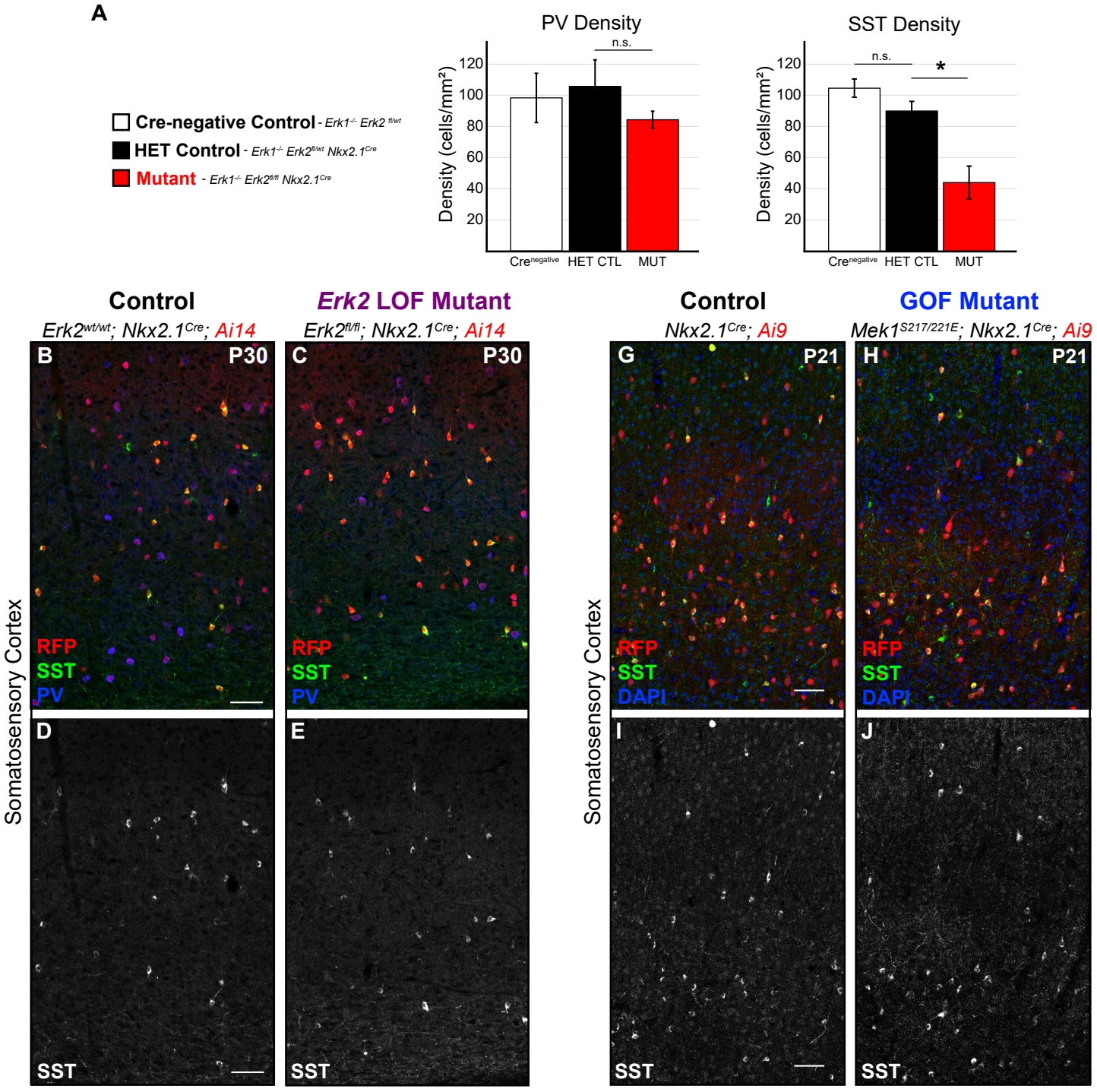
A
Cre-negative Control - Erk1-/- Erk2 fl/wt
HET Control - Erk1-/- Erk2fl/wt Nkx2.1Cre
Mutant - Erk1-/- Erk2fl/fl Nkx2.1Cre
PV Density
SST Density
Density (cells/mm²)
n.s.
*
Cre negative
HET CTL
MUT
Control
Erk2 LOF Mutant
Erk2wt/wt; Nkx2.1Cre; Ai14
Erk2fl/fl; Nkx2.1Cre; Ai14
Control
GOF Mutant
Nkx2.1Cre; Ai9
Mek1S217/221E; Nkx2.1Cre; Ai9
Somatosensory Cortex
B
C
D
E
G
H
I
J
P30
P21
RFP
SST
PV
DAPI
SST

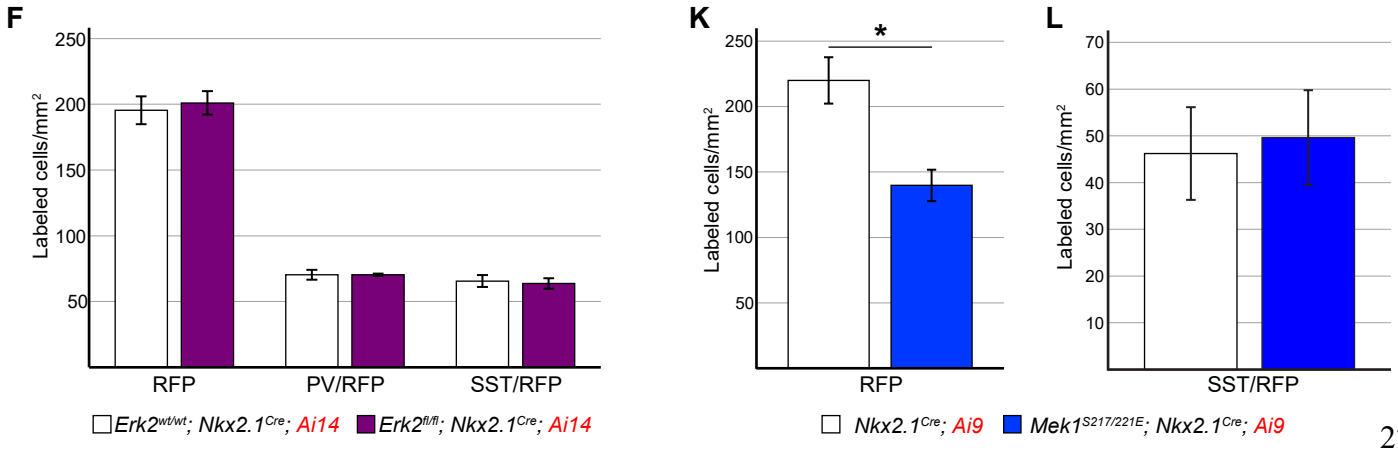
F
K
L
Labeled cells/mm²
RFP
PV/RFP
SST/RFP
*
Erk2wt/wt; Nkx2.1Cre; Ai14
Erk2fl/fl; Nkx2.1Cre; Ai14
Nkx2.1Cre; Ai9
Mek1S217/221E; Nkx2.1Cre; Ai9

Figure 4 - figure supplement 1. Complete loss of ERK1/2 signaling is required to alter the number of SST-expressing cells. (**A**) Quantification of total PV-expressing and SST-expressing cell density in the P60 somatosensory cortex of Cre-negative controls (*Erk1*$^{-/-}$), HET controls (*Erk1*$^{-/-}$; *Erk2*$^{fl/wt}$; *Nkx2.1*^{Cre}) and mutant (*Erk1*$^{-/-}$; *Erk2*$^{fl/fl}$; *Nkx2.1*^{Cre}) mice (N=3, mean +/- SEM, one-way ANOVA followed by Fisher's LSD; PV-$F_{2,6}$=0.621, p>.05; SST-$F_{2,6}$=16.206, p=.004). (**B-F**) Representative images showing CIN subtypes in the P30 primary somatosensory cortex. *Nkx2.1*^{Cre} mediated deletion of *Erk2* did not alter total Cre-expressing CIN number or the density of SST- or PV-expressing CINs (quantification in **F**, N=3, mean +/- SEM, students t-test p >.05) (scale bar = 50 µm). **(G-L)** Hyperactivation of ERK1/2 in *Mek1*$^{S217/221E}$; *Nkx2.1*^{Cre} mice reduced total Cre-expressing CIN density (quantification in **K**; N=3, mean +/- SEM, students t-test p <.05) but did not alter SST^{+}/RFP^{+}-CIN density (quantification in **L**; N=3, mean +/- SEM, students t-test p >.05) (scale bar = 50 µm).

267 in cortical GABAergic neuron number due to embryonic loss of PV-CINs (**Figure 4-figure**
268 **supplement 1G-L**) (Holter et al., 2021). Together, these data demonstrate subtype-selective
269 requirements for ERK1/2 signaling in regulating SST expression.
270
271 *Chemogenetic activation of MGE-derived CINs in acute slices.*
272 The postnatal maturation of CINs is dependent on trophic cues and neurotransmitter signaling.
273 NRG1/ERBB4, BDNF/TRKB, and glutamate/NMDAR signaling promote appropriate activity-
274 dependent responses in CINs through the activation of multiple intracellular signaling cascades
275 (Fazzari et al., 2010; Huang et al., 1999; Ting et al., 2011; Yap & Greenberg, 2018). However, the
276 specific roles of ERK1/2 signaling in this process remain unclear. To interrogate the cell-
277 autonomous contributions of ERK1/2 to CINs' activity-dependent gene expression we directly
278 activated a subpopulation of GABAergic neurons using a chemogenetic approach with Designer
279 Receptors Exclusively Activated by Designer Drugs (DREADDs). DREADDs are based on a
280 modified G-Protein-Coupled Receptor and the engineered ligand, clozapine-*N*-oxide (CNO)
281 (Jendryka et al., 2019; Nawaratne et al., 2008; Roth, 2016). In hM3D$_q$-DREADD expressing
282 neurons, CNO has been shown to activate G$_q$-PLC signaling, resulting in KCNQ channel closure,
283 TRPC channel opening, and ultimately membrane depolarization (Choveau et al., 2012; Mori et
284 al., 2015; Rogers et al., 2021; Roth, 2016; Topolnik et al., 2006; Zou et al., 2016).
285 We generated *Erk1/2; Nkx2.1^{Cre}; G$_q$-DREADD-HA* animals for chemogenetic activation of
286 CINs (Rogan & Roth, 2011; Zhu et al., 2016). We performed patch-clamp recordings of FS-CINs
287 in acute slices from P15-P22 HET control and mutant cortices (**Figure 5A**) (Anderson et al., 2010;
288 Kawaguchi, 1997; McCormick et al., 1985). We did not detect a difference in resting membrane
289 potential (CTL -69.00 ± 1.8 mV, MUT -69.75 ± 1.2 mV, p=0.73), membrane resistance (CTL

140.0 ± 18 MOhm, MUT 132.5 ± 12 Mohm, p= 0.74) or capacitance (CTL 42.5 ± 3.1 pF, MUT 43.5 ± 3.9 pF, p=0.85) between genotypes (**Figure 5-figure supplement 1A**). Bath application of 10μM CNO induced a depolarizing increase in the holding current of both HET control and ERK1/2 inactivated FS-CINs (p<.05, paired t-test) (**Figure 5B**). Current clamp recordings revealed that depolarizing current injections following application of CNO significantly increased firing frequency when compared to baseline conditions (p<.05, paired t-test) (**Figure 5C**). In sum, acute CNO treatment effectively increases the activity of CINs in slices.

ERK1/2 regulates activity-dependent FOSB expression in CINs following chemogenetic depolarization in vivo.

During the emergence of $GABA_AR$-mediated inhibition in the neonatal cortex, activity is especially critical for the survival of CINs (De Marco García et al., 2011; Hanson et al., 2019; Lodato et al., 2011; Okaty et al., 2009; Pan et al., 2018; Southwell et al., 2012). To assess the role of chronic changes in activity on CIN number in vivo, we treated *Erk1/2; Nkx2.1^{Cre}; G_q-DREADD-HA* animals with saline vehicle or 2 mg/kg CNO daily from P8-P14 (**Figure 5D**). We identified *Nkx2.1^{Cre}*-derived CINs using the haemagglutinin (HA) tag fused to the G_q receptor in the Cre-dependent construct. The density of Cre-recombined, HA^+ CINs in the primary somatosensory cortex was not altered by seven days of CNO treatment at this age (**Figure 5-figure supplement 1B**).

In excitatory neurons, ERK1/2 signaling is an important regulator of activity-dependent gene expression (Thomas & Huganir, 2004). However, this relationship is less clear in developing CINs, which exhibit notable differences in activity-dependent gene programs (Hrvatin et al., 2018; Mardinly et al., 2016; Sik et al., 1998). We therefore measured the expression of the activity-

313 dependent, AP-1 family transcription factor, FOSB. Consistent with past studies, we found that
314 5.4 +/- 1.9% of HA^+ CINs in vehicle treated, *Erk1*$^{-/-}$*; Erk2*$^{fl/wt}$*; Nkx2.1*^{Cre}*;* G_q*-DREADD-HA,* HET
315 control mice exhibited detectable FOSB immunoreactivity, whereas we observed many
316 surrounding excitatory neurons with significant FOSB expression (**Figure 5E-H)** (Hrvatin et al.,
317 2018; Mardinly et al., 2016). Vehicle-treated *Erk1*$^{-/-}$*; Erk2*$^{fl/fl}$*; Nkx2.1*^{Cre}*;* G_q*-DREADD-HA* mutant
318 CINs did not exhibit significant differences in the proportion of $FOSB^+/HA^+$ cells when compared
319 to vehicle treated HET controls (**Figure 5E, L-N**). Lastly, we found that hyperactivation of MEK-
320 ERK1/2 signaling in *Mek1*$^{S217/221E}$*; Nkx2.1*^{Cre}*; Ai9* mice also did not alter basal FOSB expression
321 in CINs (**Figure 5-figure supplement 1D-F**).

322 We next analyzed FOSB expression in CINs following one week of chemogenetic stimulation
323 from P8-P14. In HET control mice, CNO led to a significant, 6.3-fold increase in $FOSB^+/HA^+$ co-
324 labeled cells to 23.9 +/- 1.2% of HA^+ CINs (mean +/- SEM, $F_{3,14}$=15.37, post-hoc p<.001) (**Figure**
325 **5E, I-K, magenta arrows**). At P14, $PV^+/FOSB^+/HA^+$ triple-labeled cells represented 3.8 +/- 0.4%
326 (mean +/- SEM, N=4) of HA^+ CINs (**Figure 5I-K**). Importantly, in *Erk1*$^{-/-}$*; Erk2*$^{fl/fl}$*; Nkx2.1*^{Cre}*;* G_q*-*
327 *DREADD-HA* mutant CINs, CNO-induced FOSB expression was dramatically reduced when
328 compared to CNO treated HET controls ($F_{3,14}$=15.37, post-hoc p<.001) (**Figure 5E, O-Q,**
329 **magenta arrows**). Notably, we were unable to detect a statistically significant increase in FOSB-
330 expressing CINs in CNO treated mutants relative to vehicle treated mutants (post-hoc p=.221)
331 (**Figure 5E**). Together, these data demonstrate that ERK1/2 signaling is necessary for
332 chemogenetic activity-dependent FOSB expression in developing CINs.

333

334 *Chemogenetic stimulation during development increases SST-expressing CINs in Erk1/2 mutants.*

335 Our results suggest ERK1/2 mediates select aspects of activity dependent signaling in CINs.

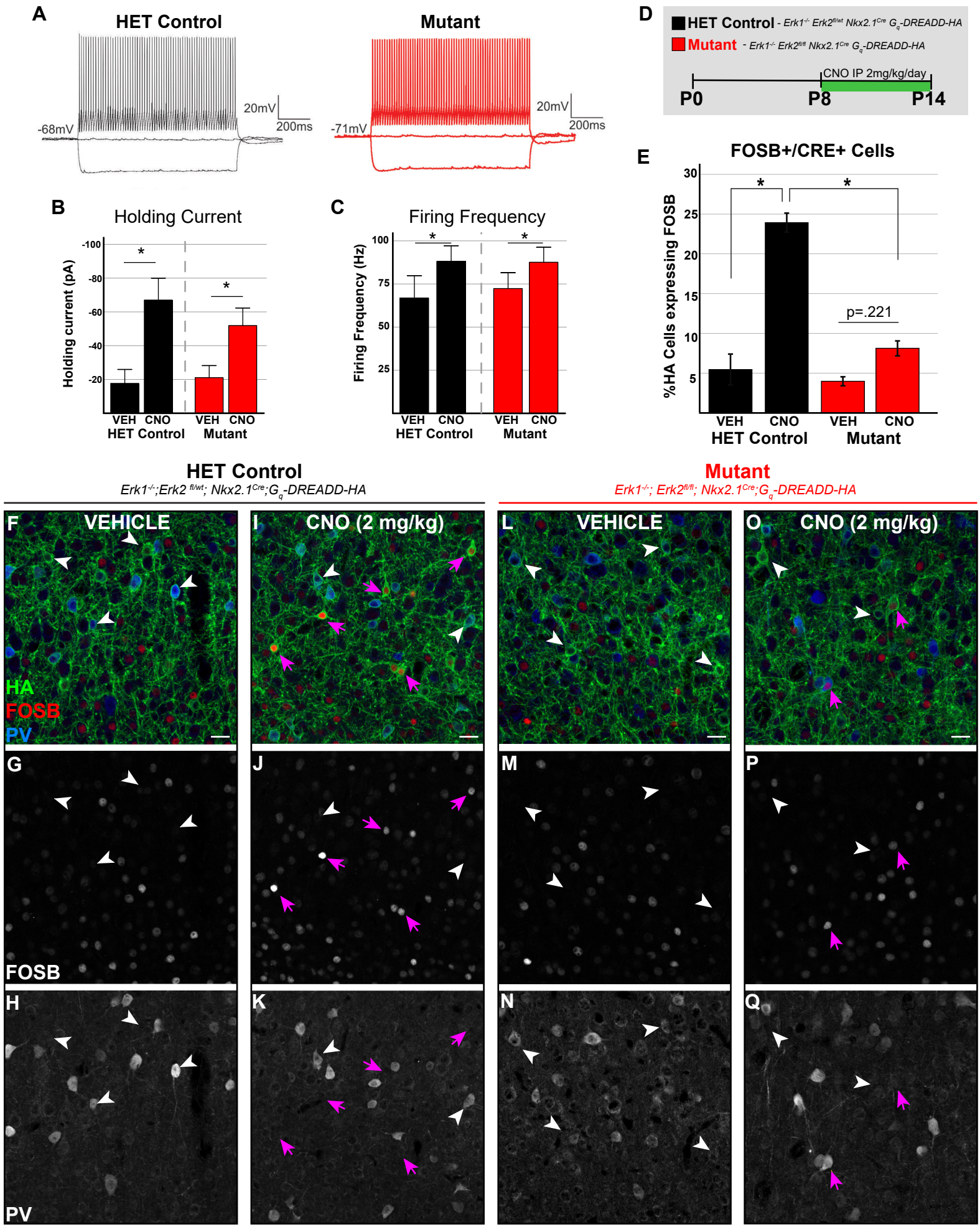
A
HET Control
Mutant
-68mV
20mV
200ms
-71mV
20mV
200ms
B
Holding Current
Holding current (pA)
-100
-80
-60
-40
-20
VEH CNO VEH CNO
HET Control Mutant
C
Firing Frequency
Firing Frequency (Hz)
100
75
50
25
VEH CNO VEH CNO
HET Control Mutant
D
HET Control - Erk1-/- Erk2fl/wt Nkx2.1Cre Gq-DREADD-HA
Mutant - Erk1-/- Erk2fl/fl Nkx2.1Cre Gq-DREADD-HA
CNO IP 2mg/kg/day
P0
P8
P14
E
FOSB+/CRE+ Cells
%HA Cells expressing FOSB
30
25
20
15
10
5
p=.221
VEH CNO VEH CNO
HET Control Mutant
HET Control
Erk1-/-;Erk2 fl/wt; Nkx2.1Cre;Gq-DREADD-HA
Mutant
Erk1-/-; Erk2fl/fl; Nkx2.1Cre;Gq-DREADD-HA
F VEHICLE
I CNO (2 mg/kg)
L VEHICLE
O CNO (2 mg/kg)
HA
FOSB
PV
G
J
M
P
FOSB
H
K
N
Q
PV

Figure 5. ERK1/2 is required to induce FOSB expression in CINs after h3MD$_q$-DREADD mediated stimulation. **(A)** Representative traces of firing response to depolarizing current steps from HET control or mutant neurons indicate that recorded neurons had a fast-spiking electrophysiological phenotype. **(B)** Acute treatment of CINs in acute slices with 10µM CNO led to a depolarizing increase in the holding current in both HET control and mutant neurons (n=8 neurons/genotype, mean +/- SEM, paired t-test, p <.05). **(C)** HET control and mutant neurons were recorded under current clamp and the response to a depolarizing current step (200pA, 1s) was measured. CNO significantly increased the firing frequency induced by the applied current step in both HET control and mutant neurons when compared to baseline (VEH) (n= 8 neurons/genotype, mean +/- SEM, paired t-test, p<.05). **(D)** Diagram of the in vivo experimental design. Animals were treated with 2 mg/kg CNO or saline vehicle by IP injection for 7 days beginning at P8. **(E)** One week of chemogenetic stimulation increased FOSB expression in HET control CINs but not in mutants (mean +/- SEM, N=4-5/group, one-way ANOVA followed by Fisher's LSD, $F_{3,14}$=15.37, *post-hoc p<.001). **(F-Q)** Representative confocal images of FOSB/PV/HA co-expression in layer 5 somatosensory cortex at P14. White arrowheads indicate HA$^+$ cells lacking significant FOSB expression, whereas magenta arrows indicate FOSB$^+$/HA$^+$ co-labeled cells (scale bar = 25 µm).

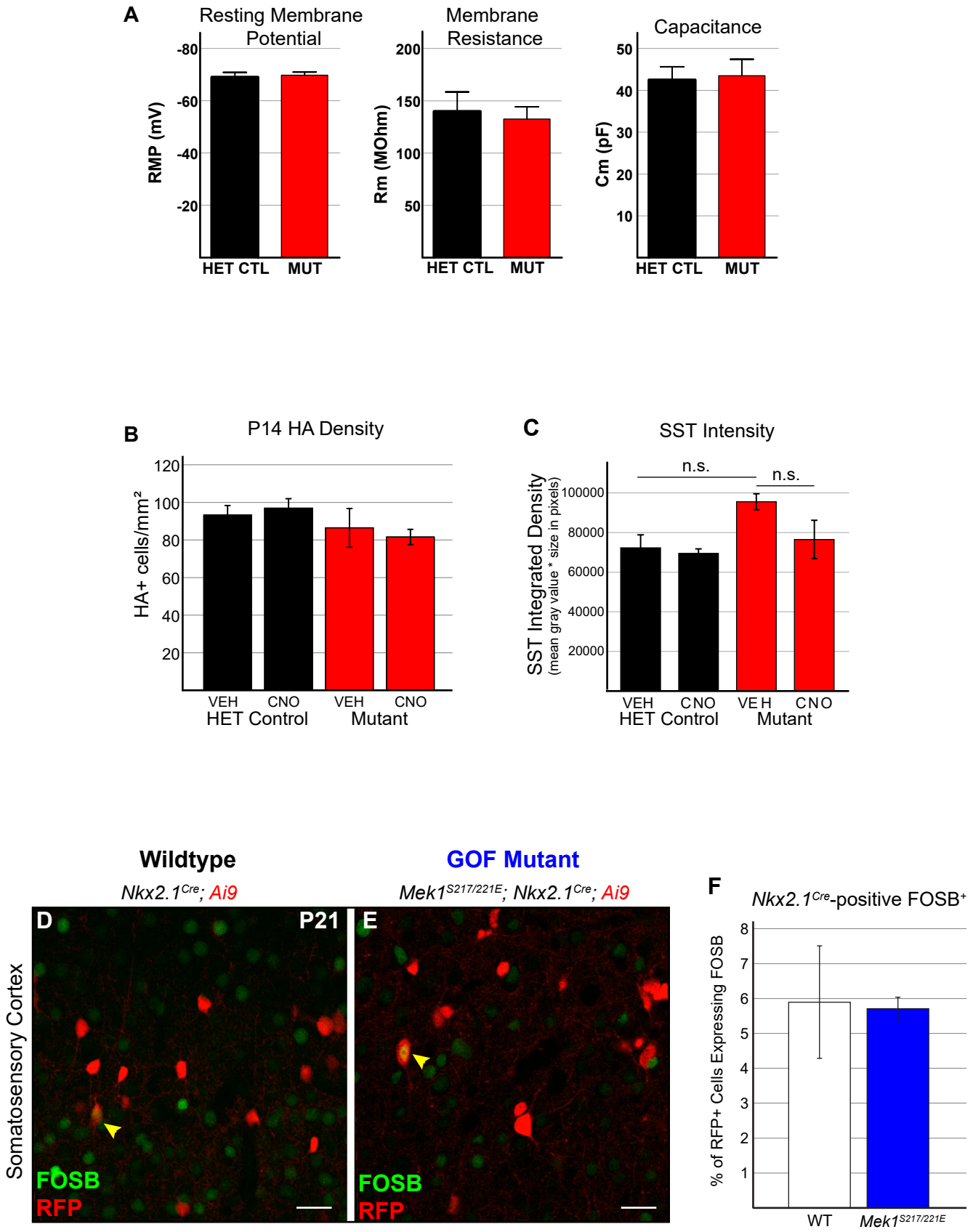
A
Resting Membrane Potential
RMP (mV)
-80
-60
-40
-20
HET CTL
MUT
Membrane Resistance
Rm (MOhm)
200
150
100
50
HET CTL
MUT
Capacitance
Cm (pF)
50
40
30
20
10
HET CTL
MUT
B
P14 HA Density
HA+ cells/mm²
120
100
80
60
40
20
VEH
CNO
VEH
CNO
HET Control
Mutant
C
SST Intensity
SST Integrated Density
(mean gray value * size in pixels)
n.s.
n.s.
100000
80000
60000
40000
20000
VEH
CNO
VEH
CNO
HET Control
Mutant
Wildtype
Nkx2.1Cre; Ai9
GOF Mutant
Mek1S217/221E; Nkx2.1Cre; Ai9
D
P21
E
Somatosensory Cortex
FOSB
RFP
FOSB
RFP
F
Nkx2.1Cre-positive FOSB+
% of RFP+ Cells Expressing FOSB
8
7
6
5
4
3
2
1
WT
Mek1S217/221E

Figure 5 - figure supplement 1. Intrinsic excitability of FS-CINs is not changed following ERK1/2 modulation. (A) Key FS-CIN intrinsic properties appear to be unaffected by ERK1/2 deletion, as there was no difference in resting membrane potential (p=0.73), membrane resistance (p= 0.74), or capacitance (p=0.85) (n=8 neurons/genotype, student's t-test**)**. **(B)** HA^+ cell density was unchanged by 7 days of CNO treatment (N=4-5, one-way ANOVA, $F_{3,24}$=0.62, p>.05). (**C**) CNO did not alter the intensity of SST immunoreactivity across genotypes (N=3 animals, minimum 12 cells/animal, one-way ANOVA, $F_{3,8}$=3.446, p=.072). **(D-F)** Confocal images showing low expression of FOSB in P21 wildtype CINs under basal conditions (D). FOSB expression was relatively unchanged in *Mek1*$^{S217/221E}$*; Nkx2.1*^{Cre} CINs (E) (Quantification in **F**, mean +/- SEM, N=3, student's t-test, p>.05) (scale bar = 25 µm).

However, chronic chemogenetic activation may be capable of activating ERK1/2-independent pathways that compensate for the effects of *Erk1/2* deletion on SST expression during development. We therefore assessed whether one week of daily CNO treatment between P8 and P14 modified the proportion of SST^+/HA^+ cells in the somatosensory cortex. Both calbindin-positive and calbindin-negative SST^+/HA^+ populations were decreased in mutant cortices at P14, suggesting a generalized effect of *Erk1/2* deletion on SST-expressing CIN subtypes (**Figure 6A**, $SST^+/CALB1^-$ p=.007; $SST^+/CALB1^+$ p=.014). In HET control *Erk1*$^{-/-}$*; Erk2*$^{fl/wt}$*; Nkx2.1*^{Cre}*;* G_q*-DREADD-HA* animals, we found that increasing activity during the second postnatal week did not significantly alter the proportion of SST^+/HA^+ CINs ($F_{3,14}$ = 22.83, post-hoc p=0.144) (**Figure 6B-F**). However, chemogenetic stimulation of *Erk1*$^{-/-}$*; Erk2*$^{fl/fl}$*; Nkx2.1*^{Cre}*;* G_q*-DREADD-HA* mutants induced a significant increase in SST^+/HA^+-CINs relative to vehicle-treated mutants (**Figure 6B, G-J**) ($F_{3,14}$ = 22.83, post-hoc p=0.005). We did not observe statistically significant changes in the proportion of PV-expressing neurons or co-expression of PV and SST in HA^+ neurons, indicating that chemogenetic activation did not induce ectopic SST expression in FS CINs (data not shown). The intensity of SST immunoreactivity in CINs reaching a minimum threshold of SST-expression was not significantly different across conditions (**Figure 5-figure supplement 1C**). These data indicate one week of chemogenetic stimulation during early development is sufficient to increase the proportion of CINs expressing SST following the loss of *Erk1/2*.

ERK1/2 signaling is required for activity-dependent FOSB expression in adult CINs.

Early cortical circuits may be uniquely capable of responding to altered activity relative to adult stages. We tested the role of ERK1/2 in activity-dependent FOSB expression in adult CINs between 6-10 months of age following one week of daily CNO administration (**Figure 7A**). In

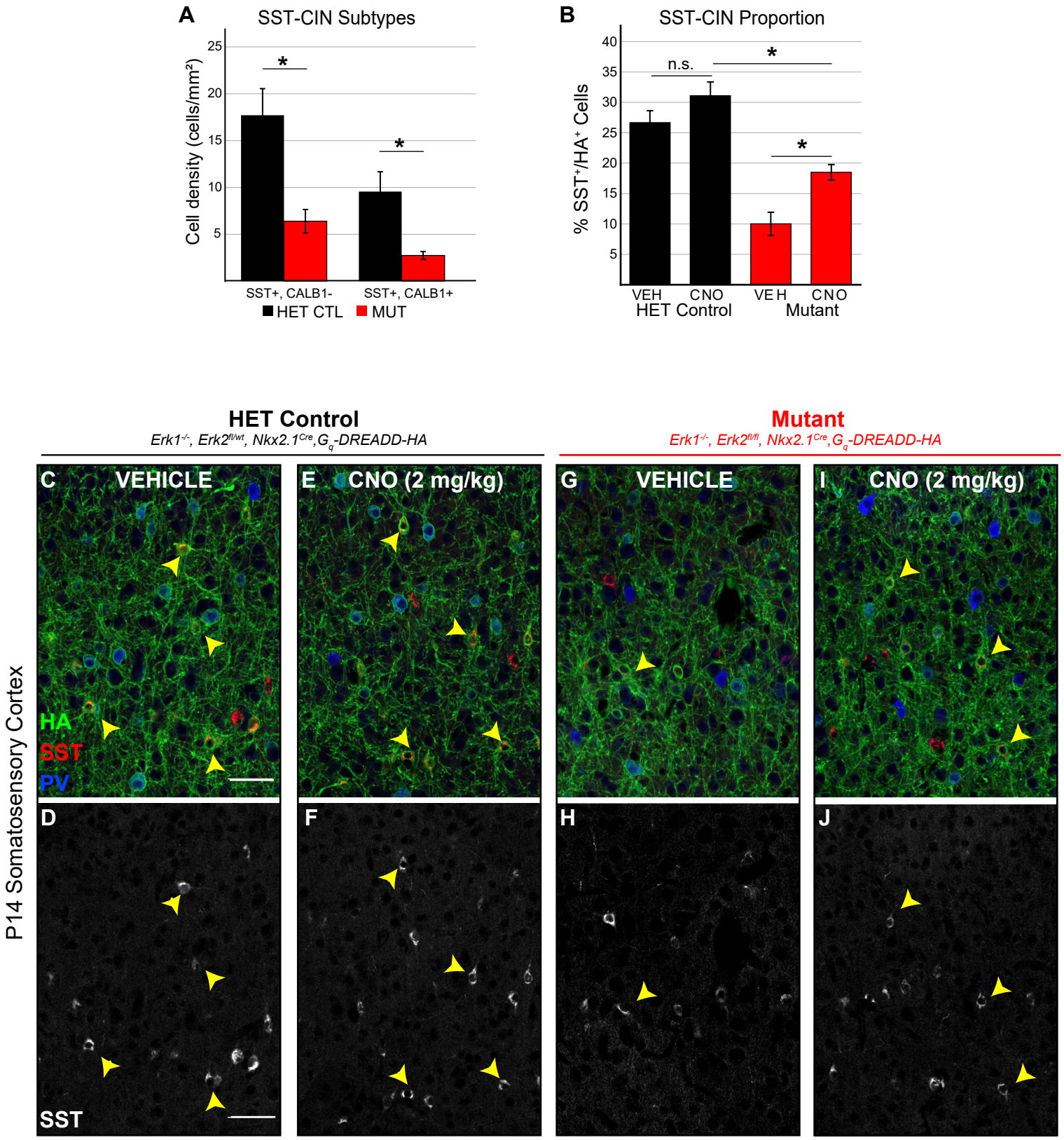
A
SST-CIN Subtypes
Cell density (cells/mm²)
25
20
15
10
5
*
*
SST+, CALB1-
SST+, CALB1+
HET CTL
MUT
B
SST-CIN Proportion
% SST+/HA+ Cells
40
35
30
25
20
15
10
5
n.s.
*
*
VEH
CNO
VEH
CNO
HET Control
Mutant
HET Control
Erk1-/-, Erk2fl/wt, Nkx2.1Cre,Gq-DREADD-HA
Mutant
Erk1-/-, Erk2fl/fl, Nkx2.1Cre,Gq-DREADD-HA
P14 Somatosensory Cortex
C VEHICLE
E CNO (2 mg/kg)
G VEHICLE
I CNO (2 mg/kg)
HA
SST
PV
D
F
H
J
SST

Figure 6. Juvenile chemogenetic stimulation increases SST expression in a subset of CINs. **(A)** Both CALB1+ and CALB1- SST-expressing cells were reduced in P14 mutant animals when compared to HET controls (mean +/- SEM, N=5, student's t-test, SST+/CALB- p=.007, SST+/CALB+ p=.014). (**B**) CNO treatment increased the proportion of CINs expressing SST in ERK1/2 inactivated mutants, though this proportion remained significantly lower than in HET control animals (N=4-5, one-way ANOVA followed by Fisher's LSD, $F_{3,14}$=22.83, *post-hoc p=.005). **(C-J)** Representative confocal images of CIN subtypes in P14 somatosensory cortex, layer 5 (scale bar = 50µm) (D, F, H, J). Monochrome image highlighting somatostatin immunoreactivity in those cells.

359 HET control adult mice, CNO led to a significant 6.5-fold increase in the proportion of CINs
360 expressing FOSB to 27.6 +/- 2.1% of HA^+ CINs (mean +/- SEM, $F_{3,8} = 31.88$, post-hoc $p<0.001$)
361 (**Figure 7B-C, J**). At this stage, 16.4 +/- 1.7% of $FOSB^+/HA^+$ CINs expressed PV (mean +/- SEM,
362 N=3). As in young mice, adult CNO-treated *Erk1*$^{-/-}$*; Erk2*$^{fl/fl}$*; Nkx2.1*^{Cre}*;* G_q*-DREADD-HA* mutant
363 CINs displayed significantly less FOSB induction than HET controls ($F_{3,8} = 31.88$, post-hoc
364 $p<0.001$) (**Figure 7B-E, J**). We noted a reduced proportion of FOSB-expressing HA^+ CINs in both
365 PV-immunolabeled (4.1 +/- 0.5%) as well as PV-negative subtypes (3.1 +/- 0.7%) (mean +/- SEM,
366 N=3). The overall pattern and number of non-recombined $FOSB^+$ cells across the primary
367 somatosensory cortex were relatively unaffected by CIN-specific *Erk1/2* deletion or chronic
368 chemogenetic stimulation (**Figure 7F-I, K**). These data demonstrate that ERK1/2 is required for
369 chemogenetic activation of multiple subtypes of mature CINs.

370 Finally, we tested whether seven days of chemogenetic stimulation during adulthood altered
371 the proportion of SST-expressing CINs. Following one week of daily CNO treatment, HET control
372 animals showed no change in the proportion of SST^+/HA^+ cells in the primary somatosensory
373 cortex (**Figure 8A-F**). In mutant animals, however, we found a modest but statistically significant
374 increase in the proportion of SST^+/HA^+ cells following CNO treatment relative to vehicle treated
375 mutants (**Figure 8B, G-J**) ($F_{3,12} = 126.54$, post-hoc $p=0.024$). These data suggest that activity-
376 mediated increases in the number of SST-expressing CINs in *Erk1/2* mutants can occur well into
377 adulthood.

378

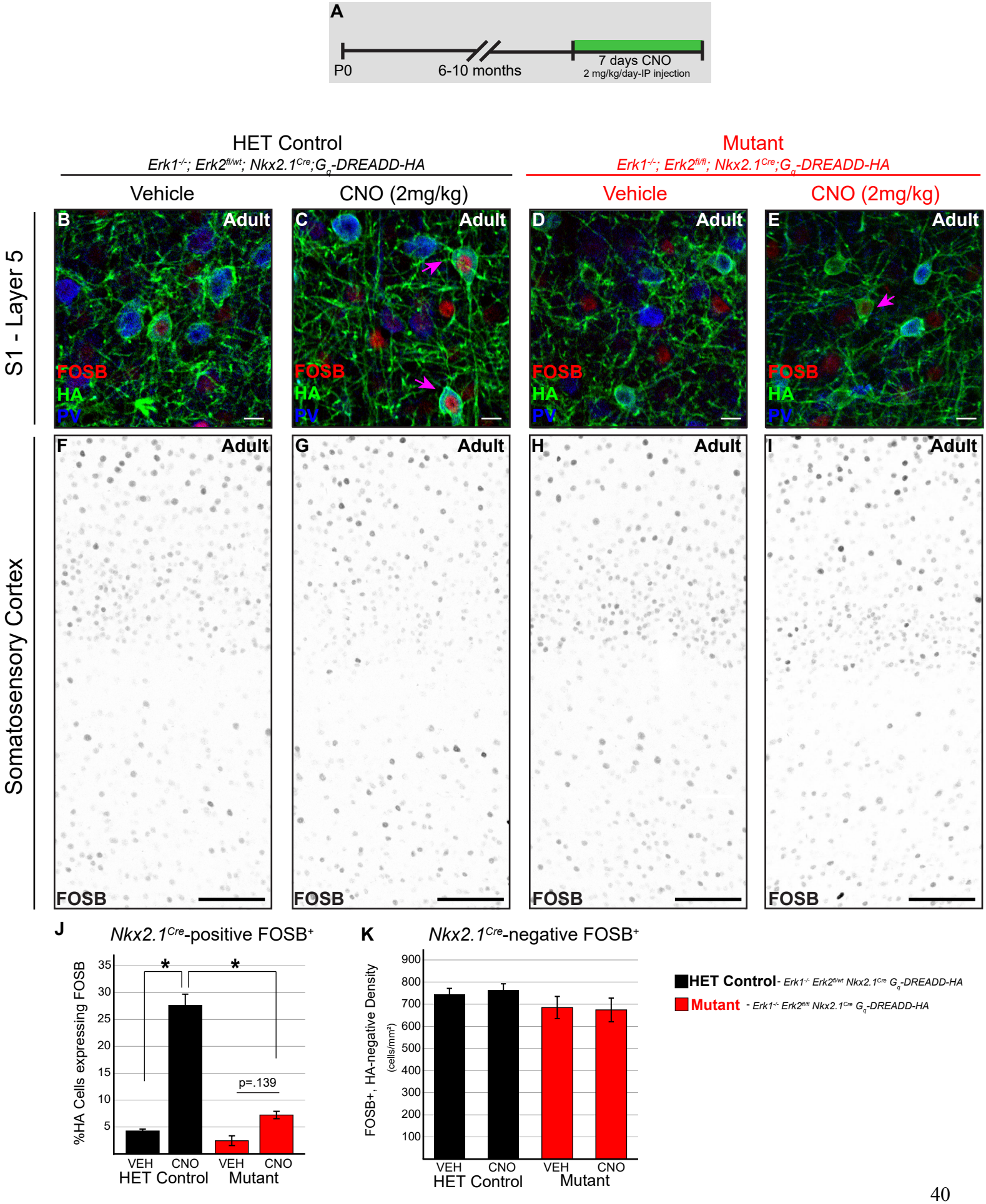
A
P0
6-10 months
7 days CNO
2 mg/kg/day-IP injection
HET Control
Erk1-/-; Erk2fl/wt; Nkx2.1Cre;Gq-DREADD-HA
Mutant
Erk1-/-; Erk2fl/fl; Nkx2.1Cre;Gq-DREADD-HA
Vehicle
CNO (2mg/kg)
Vehicle
CNO (2mg/kg)
S1 - Layer 5
Somatosensory Cortex
B Adult
C Adult
D Adult
E Adult
FOSB
HA
PV
F Adult
G Adult
H Adult
I Adult
FOSB
J
Nkx2.1Cre-positive FOSB+
%HA Cells expressing FOSB
p=.139
VEH CNO VEH CNO
HET Control Mutant
K
Nkx2.1Cre-negative FOSB+
FOSB+, HA-negative Density (cells/mm2)
VEH CNO VEH CNO
HET Control Mutant
HET Control - Erk1-/- Erk2fl/wt Nkx2.1Cre Gq-DREADD-HA
Mutant - Erk1-/- Erk2fl/fl Nkx2.1Cre Gq-DREADD-HA

Figure 7. ERK1/2 is required for activity-dependent responses in adults. (A) Animals aged 6-10 months were administered 2 mg/kg CNO or saline vehicle via daily IP injection for one week. **(B-E)** High magnification images from layer 5 of the adult somatosensory cortex showing FOSB expression within CINs following 7 days of daily CNO treatment (scale bar = 10µm). One week of CNO treatment increased FOSB expression in HET control CINs but not *Erk1*$^{-/-}$*; Erk2*$^{fl/fl}$*; Nkx2.1*^{Cre}*;* G_q*-DREADD-HA* mutant CINs (quantification in J). **(F-I)** Confocal images of the adult somatosensory cortex layers 2-5, showing the distribution of FOSB+ cells (scale bar = 100µm). The density of FOSB^{+}/*Nkx2.1*^{Cre}-negative cells was unchanged in response to *Erk1/2* deletion or chemogenetic stimulation. **(J)** Quantification of *Nkx2.1*^{Cre}-positive cells expressing FOSB (N=3, one-way ANOVA followed by Fisher's LSD, $F_{3,8}$ =31.87, *post-hoc p<.001). **(K)** Quantification of *Nkx2.1*^{Cre}-negative cells expressing FOSB (N=3, one-way ANOVA, $F_{3,8}$ = 0.16, p>.05).

HET Control - *Erk1$^{-/-}$ Erk2$^{fl/wt}$ Nkx2.1^{Cre} G$_q$-DREADD-HA*

Mutant - *Erk1$^{-/-}$ Erk2$^{fl/fl}$ Nkx2.1^{Cre} G$_q$-DREADD-HA*

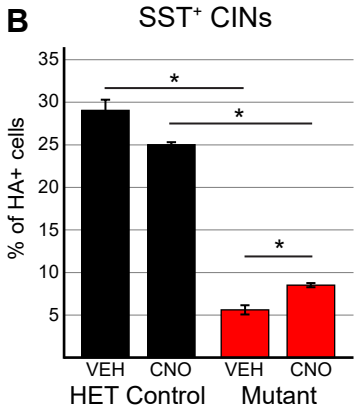

Control

Erk1$^{-/-}$; Erk2$^{fl/wt}$; Nkx2.1^{Cre};G$_q$-DREADD-HA

Mutant

Erk1$^{-/-}$; Erk2$^{fl/fl}$; Nkx2.1^{Cre};G$_q$-DREADD-HA

Adult Somatosensory Cortex

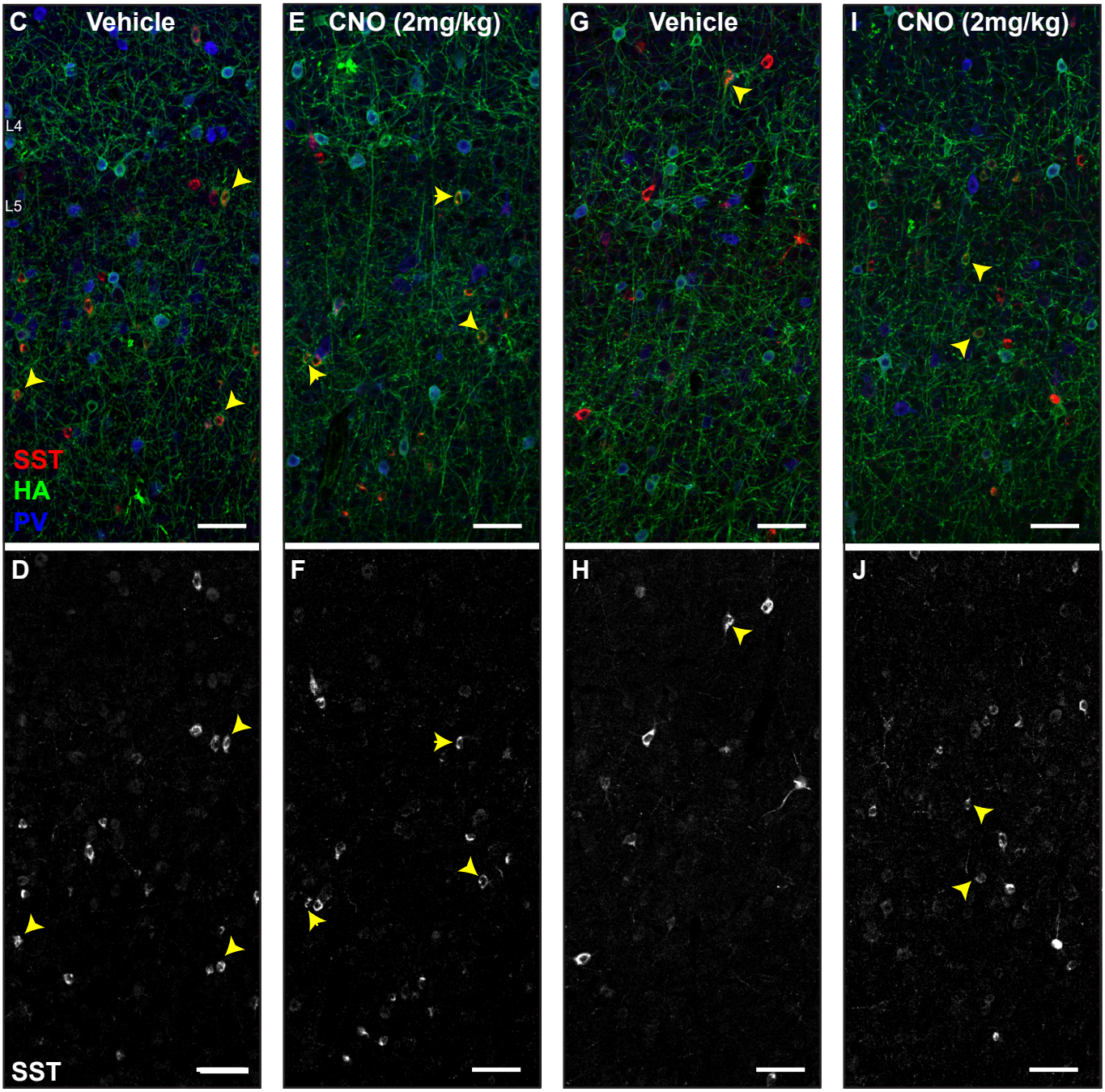

Figure 8. One week of chemogenetic stimulation in adulthood induces a partial rescue of SST expression. **(A)** Diagram of experimental design. **(B)** In adult mice, the proportion of CINs expressing SST is lower in vehicle treated mutants when compared to vehicle treated HET controls. One week of CNO treatment in adult mutants increased SST-CINs relative to vehicle treated mutants (N=4, one-way ANOVA followed by Fisher's LSD, $F_{3,12}$ =126.54, *post-hoc p=.024 MUTVEH/MUTCNO). **(C-J)** Confocal images showing immunolabeling for HA, PV, and SST in HET control and *Erk1*$^{-/-}$*; Erk2*$^{fl/fl}$*; Nkx2.1*^{Cre}*;* G_q*-DREADD-HA* mutant mice. Yellow arrowheads indicate SST^{+}/HA^{+} co-labeled cells in layers 4-5 of the primary somatosensory cortex (scale bar =25µm).

Discussion

Over the course of development, CINs respond to well-defined extracellular cues that regulate proliferation, specification, and the release of neurotransmitters critical for cortical function. Yet the role of associated downstream intracellular signaling cascades in vivo has received less attention. Here, we show that ERK1/2 activity in MGE derivatives is critical for the establishment of glial number but is not necessary for CIN survival or initial commitment to a GABAergic fate. However, we found that ERK1/2 is important for activity dependent expression of FOSB in CINs and regulates the number of SST-expressing, but not PV-expressing, GABAergic neurons. Interestingly, in vivo chemogenetic stimulation of mutant CINs was sufficient to partially overcome the effect of *Erk1/2* inactivation and increase the proportion of CINs expressing SST. These data provide new insight into the specific signaling requirements of developing MGE-derivatives and the cellular functions of ERK1/2 in the development of cortical inhibitory circuits.

Our findings show that loss of ERK1/2 significantly decreases MGE-derived glial number in the anterior commissure, while hyperactive MEK-ERK1/2 signaling is sufficient to increase MGE-derived oligodendrocyte number. Notably, overall oligodendrocyte numbers remained unchanged in ERK1/2 deletion models (**Figure 1–figure supplement 2A**), possibly due to compensatory changes in glia from other progenitor domains (Kessaris et al., 2006; Orduz et al., 2019). These results are consistent with previous findings in neural progenitor domains in the dorsal cortex and peripheral nervous system and further indicate a critical requirement for ERK1/2 signaling in establishing myelinating glial number across the nervous system, despite substantial differences in origin and local extracellular environments (Dinh Duong et al., 2019; Filges et al., 2014; X. Li et al., 2012; Newbern et al., 2011). Whether the reduction in MGE-derived glial number is due to a disruption in the gliogenic transition in neural progenitors or subsequent stages of glial

402 development is unknown (Ishii et al., 2012; S. Li et al., 2014; X. Li et al., 2012), but our results
403 are consistent with a key role for FGF-ERK1/2 signaling in driving forebrain oligodendrocyte
404 development (Furusho et al., 2011, 2017; Ishii et al., 2016). It will be interesting to further dissect
405 the specific molecular mechanisms of ERK1/2 contributions to glial development with Cre lines
406 that recombine at different stages.

407 Upstream RASopathy mutations in *Ras* and *Nf1* alter multiple parallel kinase cascades,
408 including ERK1/2, increase glial number, and alter white matter structure (Angara et al., 2020;
409 Breunig et al., 2015; Fattah et al., 2021; Gutmann et al., 2001; Holter et al., 2019; Krencik et al.,
410 2015; López-Juárez et al., 2017; Rizvi et al., 1999). Whether reduced *ERK1/MAPK3*,
411 *ERK2/MAPK1,* or *MEK2/MAP2K2* gene dosage in individuals with 16p11.2-, distal22q11.2-, or
412 19p13.3-microdeletions, respectively, is sufficient to disrupt myelinating glial number and
413 contribute to abnormal white matter microstructure observed in some of these conditions is unclear
414 (Chang et al., 2016; Owen et al., 2014; Qureshi et al., 2014; Silva et al., 2022). This conserved
415 functional link may also be an important consideration in pediatric RASopathy clinical trials
416 utilizing prolonged pharmacological ERK1/2 pathway inhibition (Payne et al., 2019).

417 Past studies have shown that distinct neuronal populations arising from the same progenitor
418 domain exhibit unexpectedly diverse cellular responses to ERK1/2 modulation (Holter et al., 2021;
419 Hutton et al., 2017; Newbern et al., 2011; Sanchez-Ortiz et al., 2014; Vithayathil et al., 2015; L.
420 Xing et al., 2016). In many non-neuronal cells, ERK1/2 and PI3K/AKT are important regulators
421 of proliferation, migration, and survival (Lavoie et al., 2020). In CINs, PI3K/AKT mediates
422 comparable cellular behaviors (Oishi et al., 2009; Polleux et al., 2002; Vogt et al., 2015; Wei et
423 al., 2020; Wong et al., 2018). Early studies in cancer cell lines suggested a critical role for ERK1/2
424 in migration (Klemke et al., 1997) and an early CNS-wide *Erk1/2* conditional knockout exhibited

425 reduced calbindin- and GAD67-expressing, presumptive GABAergic neurons in the P0.5 cortex
426 (Imamura et al., 2010). In contrast, pharmacological MEK1/2 inhibitors did not disrupt embryonic
427 CIN migration in acute slice assays (Polleux et al., 2002). We used two strains of mice with
428 improved selectivity for the GABAergic lineage to show that ERK1/2 is not necessary for CIN
429 migration or survival in vivo. This outcome differs from our previously reported requirement for
430 ERK1/2 signaling in excitatory corticospinal neuron survival during the neonatal period (L. Xing
431 et al., 2016). The mouse models we have generated will provide important tools for further
432 dissection of the precise mechanisms that regulate these cell context-dependent functions.

433 Early CIN development is determined, in part, by local morphogen gradients acting via specific
434 transcriptional programs (Hu et al., 2017; Lim et al., 2018). For example, SHH signaling is
435 required for the specification of MGE-derived GABAergic neurons during mid embryogenesis and
436 later biases these neurons toward a SST-expressing fate (Tucker et al., 2008; Tyson et al., 2015;
437 Xu et al., 2005, 2010; Yu et al., 2009). Moreover, the pharmacological MEK1/2 inhibitor, U0126,
438 blocks the SHH-induced production of OPCs in cultured dorsal neural progenitors (Kessaris et al.,
439 2004). In certain contexts, ERK1/2 signaling has been shown to non-canonically activate GLI1, a
440 well-known transcriptional target of SHH (Pietrobono et al., 2019; Po et al., 2017). It is possible
441 that SHH and ERK1/2 signaling converge on GLI1 to direct neurons toward a SST-expressing
442 CIN fate. Indeed, conditional loss of *Nf1* or expression of a hyperactivating $BRaf^{V600E}$ variant leads
443 to a reduction in PV-CINs and an increase in the proportion of SST-expressing CINs (Knowles
444 and Stafford et al., 2022). SST expression alone provides an incomplete view of the RS-CIN
445 lineage. Examination of a panel of genes associated with SST-expressing CINs that includes ion
446 channels, transcription factors, and synaptic molecules alongside SST would be informative.
447 Future studies will be necessary to identify the molecular mediators associated with changes in

448 ERK1/2 activity and CIN specification in the developing CNS.

449 Cortical circuit formation establishes a complex balance between GABAergic and
450 glutamatergic signaling. GABA-mediated signals promote the maturation of excitatory neurons,
451 in part via ERK1/2 dependent mechanisms (Cancedda et al., 2007; Obrietan et al., 2002; Peerboom
452 & Wierenga, 2021). Past reports demonstrate that early alterations in CIN number or activity can
453 permanently change circuit architecture and animal behavior (Bitzenhofer et al., 2021; Kaneko et
454 al., 2022; Magno et al., 2021; Tuncdemir et al., 2016). Here, we employed a chemogenetic
455 approach to selectively activate CINs with temporal specificity. We found that *Nkx2.1*^{Cre}-targeted
456 chemogenetic stimulation during the second postnatal week did not alter CIN number. Past studies
457 have identified a role for activity in early CIN survival (Denaxa et al., 2018; Priya et al., 2018;
458 Southwell et al., 2012; Wong et al., 2018). However, we modulated the activity of endogenous
459 CINs at a stage past the reported peak of CIN apoptosis and after $GABA_A$Rs acquire inhibitory
460 responses (Ben-Ari et al., 2007, p.; Denaxa et al., 2018; Southwell et al., 2012; Wong et al., 2018).
461 It is not clear whether CIN-specific ERK1/2 signaling is required for global cortical circuit activity
462 or cognitive behaviors (Adler et al., 2019; Chen et al., 2019; Cummings & Clem, 2020; Fu et al.,
463 2014; Kluge et al., 2008; C. Lee et al., 2022; Magno et al., 2021).

464 Recent work has led to a deeper appreciation for the unique contributions of CIN subtypes to
465 cortical microcircuits. While our past studies have clearly identified significant effects of MEK-
466 ERK1/2 hyperactivation on PV-CIN lineage specification, we failed to observe changes in PV-
467 CIN number, intrinsic membrane properties, or the expression of PV following *Erk1/2* deletion
468 (Angara et al., 2020; Holter et al., 2021; Knowles et al., 2022). However, we now show that
469 ERK1/2 signaling is necessary for activity-dependent FOSB expression in adult PV-CINs.

470 Unexpectedly, we found that ERK1/2 is critical for SST protein expression in a subset of CINs.

471 Somatostatin is developmentally regulated; *Sst* mRNA is first detected in immature CINs by mid-
472 embryogenesis, but substantial levels of SST protein are not observed in CINs until early neonatal
473 stages and patterns of SST expression do not fully mature until P30 (Batista-Brito et al., 2008;
474 Denaxa et al., 2012; Forloni et al., 1990; D. R. Lee et al., 2022; Ma et al., 2022; Neves et al., 2013;
475 Taniguchi et al., 2011). A loss of SST protein has been seen in a number of other neuropathological
476 conditions, but has not been directly assessed in conditions characterized by reduced ERK1/2
477 signaling (Davies et al., 1980; Fee et al., 2017; Pantazopoulos et al., 2017; Peng et al., 2013;
478 Robbins et al., 1991; Sun et al., 2020; Tripp et al., 2011; Wengert et al., 2021). SST is not only a
479 marker of RS-CINs, but an active neuropeptide with biological functions (Baraban & Tallent,
480 2004; Grilli et al., 2004; Liguz-Lecznar et al., 2016; Smith et al., 2019; Song et al., 2021; Tereshko
481 et al., 2021). The release of bioactive neuropeptides from subtypes of CINs likely contributes to
482 cortical computation (Ouwenga et al., 2018; Smith et al., 2019). SST has an overall inhibitory role
483 on cortical circuits and loss of SST protein can cause subtle deficits in motor learning (Tallent &
484 Qiu, 2008; Zeyda et al., 2001). Indeed, a recent report demonstrated that exogenous SST infusion
485 into V1 can improve performance in a visual discrimination task, independent of GABA (Song et
486 al., 2020). Administration of SST or synthetic analogues may compensate for the aberrant
487 development of SST-expressing CINs in *Erk1/2* loss of function models (Banks et al., 1990; Engin
488 & Treit, 2009; Kiviniemi et al., 2015; McKeage, 2015). Approaches that target SST may have
489 broader applications in the treatment of neurodevelopmental disorders, particularly select cases of
490 epilepsy, autism, and schizophrenia where deficits in SST-CIN function are well described (Song
491 et al., 2021).

492 Interestingly, one week of chemogenetic stimulation partially restored SST expression in
493 *Erk1/2*-deleted CINs at both juvenile and adult stages. Chemogenetic depolarization may engage

494 several parallel cascades including cAMP/PKA, Ca^{2+}, PKC, and ERK1/2, which often converge
495 on common transcriptional targets, such as CREB, SRF, and AP-1 family members (Yap &
496 Greenberg, 2018). We demonstrated that the activity-dependent expression of FOSB, a CREB
497 target, requires ERK1/2 signaling in CINs, similar to glutamatergic neurons (Guenthner et al.,
498 2013; Hrvatin et al., 2018; Mardinly et al., 2016; Spiegel et al., 2014). Reduced SST expression in
499 a subset of CINs in *Erk1/2* deleted animals limited our ability to directly assess whether ERK1/2
500 signaling is required for FOSB expression in this specific CIN subtype. Interestingly, one of the
501 first CREB target genes to be identified was SST (Montminy & Bilezikjian, 1987; Yamamoto et
502 al., 1988). Chemogenetic activation of ERK1/2-independent cascades appears sufficient to
503 partially compensate for the loss of *Erk1/2* and modestly increase SST expression in CINs.
504 Whether other activity-dependent genes critical for CIN plasticity are similarly modified remains
505 to be seen. Our finding that adult chemogenetic activation partially restored SST expression raises
506 the possibility that adult modulation of neural activity may be capable of reversing select
507 developmental deficits in ERK1/2-related syndromes.

Acknowledgements:

We thank Chris Wedwick, Anna Bayne, Mya Breitweiser, and Elise Bouchal for technical assistance with mouse sample processing and image analysis. This research is supported by the National Institute of Health grants R00NS076661 and R01NS097537 awarded to JMN. SK is supported by the ARCS Foundation. AMS and DV are supported by the Spectrum Health-Michigan State Alliance Corporation, Autism Research Institute pilot grant and Department of Defense grant NF200109. TA and GL are supported by the University of Arizona – COM Phoenix "Springboard" award. We deeply appreciate the support of the ASU Keck Bioimaging facility and ASU Personalized Diagnostic Core for outstanding technical advice and support.

Conflict of Interest Statement

The authors declare no competing interests.

521 **Materials and Methods**

522 *Genetically modified mice*

523 All mice were fed *ad libitum,* housed under a 12-hour light-dark cycle, and studied in
524 accordance with ARRIVE and Institutional Animal Care and Use Committee guidelines at Arizona
525 State Univ., Michigan State Univ., and the Univ. of Arizona. Mature mice examined in this study
526 were euthanized via CO2 inhalation or approved chemical anesthetics prior to transcardial
527 perfusion, while embryonic/neonatal mice were cryoanesthetized, as described in the AVMA
528 Guidelines on Euthanasia. Male and female mice on mixed genetic backgrounds were utilized in
529 all experiments in this work and generated from crosses between the following individual strains
530 of mice.

Mouse Strains	Details	Reference	Identifier
Erk1/Mapk3$^{-/-}$	Neo cassette inserted into Exon 1-6 of *Erk1/Mapk3*	Selcher et al, 2001	RRID:IMSR_JAX:019113
Erk2/Mapk1$^{loxp/loxp}$	*Erk2/Mapk1* exon 2 flanked by loxp ("*fl*")	Samuels et al., 2008	RRID:IMSR_JAX:019112
CAG-LSL-Mek1$^{S217/221E}$	Cre-dependent hyperactive *Mek1*$^{S217/221E}$ overexpressing mice	Krenz et al., 2008	MGI:3822131
Nkx2.1^{Cre}	Cre recombinase expression in radial glia in the MGE, POA, and other regions by E8.5	Xu et al., 2008	RRID:IMSR_JAX:008661
Slc32a1/VGAT^{Cre}	Cre recombinase expression in all postmitotic GABAergic neurons, including CINs by E11.5	Vong et al., 2011	RRID:IMSR_JAX:016962
CAG-LSL-Gq-DREADD	Cre-dependent HA-hM3Dq-pta-mCitrine expressing line	Zhu et al., 2016	RRID:IMSR_JAX:026220
Rpl22^{HA}	Cre-dependent RNA immunoprecipitation line	Sanz et al., 2009	RRID:IMSR_JAX:011029
Ai3 / Ai9 / Ai14	Cre-dependent fluorescent protein (EYFP or tdTomato) expressing lines	Madisen et al., 2010	RRID:IMSR_JAX:007903, 007908, 007903

531

532 To generate *Erk1/Erk2* loss-of-function mutants, mice expressing *Nkx2.1*^{Cre} or
533 *Slc32A1/VGAT*^{Cre} were bred with mice possessing a neo-insertion in exons 1-6 in the *Erk1/Mapk3*
534 gene (referred to as *Erk1*$^{-}$) and/or a loxp flanked exon 2 in the *Erk2/Mapk1* gene (referred to as

535 *Erk2*^{fl}) (Monory et al., 2006; Samuels et al., 2008; Selcher, 2001; Xu et al., 2008). Littermates
536 expressing Cre recombinase and heterozygous *Erk2*$^{fl/wt}$ were often used as controls for complete
537 *Erk1/2* loss-of-function experiments unless stated otherwise. Cre-dependent tdTomato/RFP (*Ai9*
538 *or Ai14*) or eYFP (*Ai3*) strains were employed to fluorescently-label Cre-expressing cells (Madisen
539 et al., 2010).

540 Conditionally hyperactive MEK-ERK1/2 mutants were generated by crossing *Nkx2.1:Cre*
541 mice with *CAG-loxp-STOP-loxp-Mek1*$^{S217/221E}$ (referred to as *Mek1*$^{S217/221E}$*)* mice on a mixed
542 genetic background to generate double heterozygous mutants expressing *Mek1*$^{S217/221E}$ in a Cre-
543 dependent pattern. *Mek1*$^{S217/221E}$ mice were kindly provided by Dr. Maike Krenz and Dr. Jeffrey
544 Robbins (Krenz et al., 2008).

545 For chemogenetic experiments, an *loxp-STOP-loxp-*G_q*-DREADD-HA* line was used, which
546 produces the engineered G-protein coupled receptor, hM3D_q, with a hemagglutinin (HA) tag in
547 Cre-expressing cells (Zhu et al., 2016). To chemogenetically stimulate these neurons in vivo, mice
548 of the indicated age were randomly assigned to receive an intraperitoneal injection of 2 mg/kg
549 body weight clozapine-*N*-oxide (CNO) or 0.09% NaCl saline vehicle every 24 hours for 7
550 consecutive days. Body weight and time of injection were recorded each day and tissue was
551 collected 2 hours after the last dose of CNO.

552

553 *PCR Genotyping*

554 Genomic DNA was rapidly extracted from mouse tissue samples for PCR genotyping with
555 25mM NaOH, 0.2 mM EDTA, pH=12 and subsequently neutralized with 40 mM Tris-Cl, pH=5.
556 The primers used for genotyping were as follows: (listed 5'-3'): *Cre* –
557 TTCGCAAGAACCTGATGGAC and CATTGCTGTCACTTGGTCGT to amplify a 266 bp

558 fragment; *Erk1*$^{-}$ – AAGGTTAACATCCGGTCCAGCA, AAGCAAGGCTAAGCCGTACC, and
559 CATGCTCCAGACTGCCTTGG to amplify a 571 bp segment wildtype and a 250 bp segment KO
560 allele; *Erk2*^{fl} – AGCCAACAATCCCAAACCTG, and GGCTGCAACCATCTCACAAT amplify
561 275 bp wildtype and 350 bp floxed alleles; *Ai3/Ai9* – four primers were used -
562 AAGGGAGCTGCAGTGGAGTA, CCGAAAATCTGTGGGAAGTC,
563 ACATGGTCCTGCTGGAGTTC, and GGCATTAAAGCAGCGTATCC amplify a 297 bp
564 wildtype Rosa26 segment and a 212 bp *Ai3*/*Ai9* allele; *hM3Dq* – CGCCACCATGTACCCATAC
565 and GTGGTACCGTCTGGAGAGGA amplify a 204 bp fragment; *Mek1*$^{S217/221E}$ –
566 GTACCAGCTCGGCGGAGACCAA and TTGATCACAGCAATGCTAACTTTC amplify a 600
567 bp fragment.
568
569 *Tissue Preparation and Immunostaining*
570 Mice of the specified age were fully anesthetized and perfused with cold 1X PBS followed by
571 4% PFA in a 1X PBS solution. Brains were then removed and post-fixed at 4C. Brains were sliced
572 with a vibratome or were cryoprotected for preparation on a cryostat. Sectioned brain tissue was
573 then incubated for 24-48 hours at 4ºC in a primary antibody solution diluted in .05 – 0.2% Triton
574 in 1X PBS with 5% Normal Donkey Serum (NDS). Primary antibody information is provided in
575 the table below.
576 Sections were then washed three times in 1X PBS .05% Triton and incubated in a solution
577 containing secondary antibodies diluted to 1:1000 in 1X PBS .05 – 0.2% Triton and 5% NDS. A
578 Zeiss LSM710 or LSM800 laser scanning confocal microscope was used to collect images.
579 Representative confocal images were optimized for brightness and contrast in Adobe Photoshop
580 and compiled into figures with Adobe Illustrator.

Primary Antibody and Host	Source	Identifier
Rabbit Anti-Somatostatin	Peninsula/BMA Biomed.	Cat# T-4103.0050, RRID:AB_518614
Guinea Pig Anti-Somatostatin	Synaptic Systems	Cat# 366 004, RRID:AB_2620126
Goat Anti-Parvalbumin	SWANT	Cat# PVG-213, RRID:AB_2650496
Chicken Anti-GFP	Aves	Cat# GFP-1020, RRID:AB_10000240
Chicken Anti-RFP	Rockland	Cat# 600-901-379, RRID:AB_10704808
Rabbit Anti-RFP	Rockland	Cat# 600-401-379, RRID:AB_2209751
Rabbit Anti-ERK2	Abcam	Cat# ab32081, RRID:AB_732210
Chicken Anti-Calbindin 1	Novus	NBP2-50028
Mouse Anti-NeuN	Millipore	Cat# MAB377, RRID:AB_2298772
Mouse Anti-HA	Biolegend	Cat# 901513, RRID:AB_2565335
Rabbit Anti-FOSB	Abcam	Cat# ab184938, RRID:AB_2721123
Rabbit Anti-MEK1	Abcam	Cat# ab32091, RRID:AB_776273
Rabbit Anti-GFAP	Abcam	Cat# ab7260, RRID:AB_305808
Rabbit Anti-OLIG2	Millipore	Cat# AB9610, RRID:AB_570666

Image Analysis

For all immunolabeling experiments, images from multiple tissue sections per mouse containing the anatomical region of interest were quantified by an observer blinded to the genotype. At least three biological replicates per genotype were derived from at least three independent litters to minimize litter batch effects and littermate controls were frequently utilized. To estimate labeled cell density, regions of interest were defined using standard anatomical and architectonic landmarks, the area was measured in Photoshop, and labeled cells were quantified. Sampling information for assessments of anterior commissure glia can be found in Figure 1 – figure supplement 2A. Cortical density measurements are derived from counts collected across an entire cortical column. For analyses of postnatal samples, total CIN density and co-labeled proportions were measured from a minimum of three mice per genotype and at least 500 Cre-expressing CINs derived from confocal images of at least three sections per mouse. Power analyses

were performed prior to conducting most experiments to estimate sample size using a significance level of 5%, power of 80%, and standard deviation based on pilot studies or previously published work. For quantitative analysis of the intensity of SST immunoreactivity in CINs, we analyzed images which were acquired with the same settings across trials. We sampled from a minimum of 10 randomly selected cells per animal that met a minimal threshold for SST-expression and three animals per condition. Integrated density of SST immunoreactivity was measured using Photoshop. For comparisons involving two groups, statistical significance was determined using an unpaired, two-tailed t-test. For comparison of three or more groups, we performed a one-way ANOVA followed by Fisher's LSD post-hoc tests using IBM SPSS Statistics 28.

RNA collection and sequencing

RNA collection and ribosome immunoprecipitation from brain samples was performed essentially as described in Sanz et al., 2009. Whole P7.5 cortices were rapidly dissected, rinsed, and Dounce homogenized in 500 µL of ice-cold RNase-free buffer polysome buffer (50 mM Tris pH 7.5, 100 mM KCl, 12 mM MgCl2, 1% NP-40, 1 mM DTT, 200U/ml Promega RNasin, 1 mg/ml heparin, 100 µg/ml cycloheximide, and protease inhibitors). The lysate was cleared via centrifugation at 10,000g for 20 min at 4ºC. 60 µl of supernatant ("INPUT") containing RNA derived from the entire cortical sample was collected and lysed with 350 µl of buffer RLT from Qiagen RNeasy Kit supplemented with 10µl/ml bME. Rpl22^{HA}-containing ribosomes were immunoprecipitated ("IP") from the remaining supernatant by gently mixing with 5µl of rabbit anti-HA antibody (#71–5500 Thermo Fisher Sci) and incubating with gentle rocking at 4°C for 2 hours before isolation with 50 µl of protein A/G magnetic beads previously equilibrated in polysome buffer and a magnetic stand. Immunoprecipitates were rinsed 3x with 800 µl of a high

salt buffer (50 mM Tris pH 7.5, 300 mM KCl, 12 mM MgCl2, 1% NP-40, 1 mM DTT, 100 µg/ml cycloheximide) and then lysed in 350 µl of buffer RLT. RNA isolation from INPUT and IP fractions was performed following manufacturer's instructions using Qiagen's RNeasy extraction kit with DNAse digestion. RNA quantitation was performed using a Ribogreen RNA reagent and samples with an RNA integrity number < 7 on an Agilent Bioanalyzer were selected for sequencing.

2 ng of purified RNA were used for single primer isothermal amplification (SPIA) and generation of double-stranded cDNA with the Ovation RNAseq System V2 per manufacturer instructions (Nugen Technologies). Library construction and sequencing were performed on the Illumina NextSeq 500 platform at the Arizona State University's Genomics Core facility. RNAseq reads were quality checked, filtered, aligned to the mouse genome Ensembl GRCm38 primary assembly using RNA-STAR, and read counts were estimated using featureCounts (Dobin et al., 2013). DEXseq was employed to measure differential exon usage in *Erk1* exons 1-6 and *Erk2* exon 2 (Anders et al., 2012). Analysis with DeSeq2 resulted in >11,000 protein-coding genes in each sample with a normalized count > 50 (**Table S1**) (Love et al., 2014). Protein-coding genes were considered differentially expressed if the DeSeq2 derived fold-change between conditions was >1.5, unadjusted p-value <.05, and the CoV of normalized DeSeq2 counts within a condition were < 90 (**Table S2**). All code is publicly available, please see original papers for full information. Raw sequencing data are available in NCBI's Gene Expression Omnibus repository at accession number GSE206633 (Edgar et al., 2002).

Electrophysiology

For electrophysiological experiments, postnatal day 15-22 (P15-22) mice were used for the

640 preparation of in vitro whole-cell patch-clamp experiments as previously reported (Anderson et
641 al., 2010; Goddeyne et al., 2015; Holter et al., 2021; Nichols et al., 2018). The somatosensory
642 cortices of these mice were injected with a Cre-dependent AAV9-FLEX-tdTomato (Addgene
643 catalog #28306-AAV9) viral vector solution between P0-P2 to unambiguously label a subset of
644 recombined CINs for fluorescently-guided patch clamping. In brief, mice were then deeply
645 anesthetized by isoflurane inhalation before decapitation. Brains were quickly removed and
646 immersed in the saturated (95% O_2, 5% CO_2), ice-cold artificial cerebral spinal fluid (aCSF), which
647 contains (in mM): 126 NaCl, 26 $NaHCO_3$, 2.5 KCl, 10 Glucose, 1.25 $Na_2H_2PO_4H_2O$, 1
648 $MgSO_4 \cdot 7H_2O$, 2 $CaCl_2H_2O$, pH 7.4. Coronal slices from the region of the somatosensory cortex
649 (350 μm in thickness) were collected with a vibratome (VT 1200; Leica, Nussloch, Germany).
650 Following the preparation of brain slices, they were allowed to recover in the same aCSF at 32ºC
651 for 30 minutes before being moved to room temperature for an additional 30 minutes. For patch-
652 clamp recordings, slices were transferred into a submerged recording chamber and perfused
653 continuously with aCSF at 32ºC at a rate of 1-2 ml/min. Whole-cell patch-clamp recordings were
654 obtained from fluorescent positive neurons in layer V (L5) of the somatosensory cortex by using
655 an Axon 700B amplifier. The data were filtered at 2 kHz and sampled at 10 kHz via a digitizer
656 (Digidata 1440, Molecular Devices) and recorded using Clampex 10.6 software (Molecular
657 Devices). The pipettes had a resistance of 2-5 MΩ when filled with the internal solution which
658 contains (in mM): 135 K-Gluconate, 4 KCl, 2 NaCl, 10 HEPES, 4 EGTA, 4 Mg ATP and 0.3 Na
659 Tris. Pipettes were pulled from borosilicate glass (BF150-110-10, Sutter Instruments) by using a
660 Sutter Instrument puller (Model P-1000). The stability of the recordings was monitored throughout
661 the experiment and recordings with series resistances (Rs) larger than 25 MΩ or a change of more
662 than 20% were abandoned.

663 Data were analyzed using Clampfit software (Molecular Devices) and results were presented
664 as mean ± SEM. Membrane resistance (Rm) and capacitance (Cm) were calculated from the
665 response to a voltage step (5mV). Resting membrane potential was measured during current-clamp
666 recording prior to the introduction of steps (-200pA, 0 or 200pA, 1 s duration) used in examining
667 the firing properties of the neurons. For calculation of CNO induced changes in holding current,
668 neurons were recorded under voltage clamp at -70mV. The change in holding current was
669 calculated by subtracting the baseline value (i.e., in aCSF) from that measured after 20 minutes of
670 bath application of CNO (10 μM). At this time point, CNO-induced changes in holding current
671 had reached a steady-state plateau. Data were compiled and appropriate statistical analysis was
672 performed using Prism software (Graphpad) and figures compiled in CorelDraw (Corel
673 Corporation) and Adobe Illustrator. For all electrophysiological statistics, $p < .05$ was considered
674 statistically significant and tested with an unpaired student t-test unless otherwise indicated.
675

References

Adler, A., Zhao, R., Shin, M. E., Yasuda, R., & Gan, W.-B. (2019). Somatostatin-Expressing Interneurons Enable and Maintain Learning-Dependent Sequential Activation of Pyramidal Neurons. *Neuron*, *102*(1), 202-216.e7. https://doi.org/10.1016/j.neuron.2019.01.036

Alessi, D. R., Saito, Y., Campbell, D. G., Cohen, P., Sithanandam, G., Rapp, U., Ashworth, A., Marshall, C. J., & Cowley, S. (1994). Identification of the sites in MAP kinase kinase-1 phosphorylated by p74raf-1. *The EMBO Journal*, *13*(7), 1610–1619.

Anders, S., Reyes, A., & Huber, W. (2012). Detecting differential usage of exons from RNA-seq data. *Genome Research*, *22*(10), 2008–2017. https://doi.org/10.1101/gr.133744.111

Anderson, T. R., Huguenard, J. R., & Prince, D. A. (2010). Differential effects of Na+-K+ ATPase blockade on cortical layer V neurons. *The Journal of Physiology*, *588*(Pt 22), 4401–4414. https://doi.org/10.1113/jphysiol.2010.191858

Angara, K., Pai, E. L.-L., Bilinovich, S. M., Stafford, A. M., Nguyen, J. T., Li, K. X., Paul, A., Rubenstein, J. L., & Vogt, D. (2020). Nf1 deletion results in depletion of the Lhx6 transcription factor and a specific loss of parvalbumin+ cortical interneurons. *Proceedings of the National Academy of Sciences*, *117*(11), 6189–6195. https://doi.org/10.1073/pnas.1915458117

Assimacopoulos, S., Grove, E. A., & Ragsdale, C. W. (2003). Identification of a *Pax6* -Dependent Epidermal Growth Factor Family Signaling Source at the Lateral Edge of the Embryonic Cerebral Cortex. *The Journal of Neuroscience*, *23*(16), 6399–6403. https://doi.org/10.1523/JNEUROSCI.23-16-06399.2003

Banks, W. A., Schally, A. V., Barrera, C. M., Fasold, M. B., Durham, D. A., Csernus, V. J., Groot, K., & Kastin, A. J. (1990). Permeability of the murine blood-brain barrier to some octapeptide analogs of somatostatin. *Proceedings of the National Academy of Sciences*, *87*(17), 6762–6766. https://doi.org/10.1073/pnas.87.17.6762

Baraban, S. C., & Tallent, M. K. (2004). Interneuron Diversity series: Interneuronal neuropeptides – endogenous regulators of neuronal excitability. *Trends in Neurosciences*, *27*(3), 135–142. https://doi.org/10.1016/j.tins.2004.01.008

Batista-Brito, R., Machold, R., Klein, C., & Fishell, G. (2008). Gene Expression in Cortical Interneuron Precursors is Prescient of their Mature Function. *Cerebral Cortex*, *18*(10), 2306–2317. https://doi.org/10.1093/cercor/bhm258

Ben-Ari, Y., Gaiarsa, J.-L., Tyzio, R., & Khazipov, R. (2007). GABA: A Pioneer Transmitter That Excites Immature Neurons and Generates Primitive Oscillations. *Physiological Reviews*, *87*(4), 1215–1284. https://doi.org/10.1152/physrev.00017.2006

Ben-Shachar, S., Ou, Z., Shaw, C. A., Belmont, J. W., Patel, M. S., Hummel, M., Amato, S., Tartaglia, N., Berg, J., Sutton, V. R., Lalani, S. R., Chinault, A. C., Cheung, S. W., Lupski, J. R., & Patel, A. (2008). 22q11.2 Distal Deletion: A Recurrent Genomic Disorder Distinct from DiGeorge Syndrome and Velocardiofacial Syndrome. *The American Journal of Human Genetics*, *82*(1), 214–221. https://doi.org/10.1016/j.ajhg.2007.09.014

Bitzenhofer, S. H., Pöpplau, J. A., Chini, M., Marquardt, A., & Hanganu-Opatz, I. L. (2021). A transient developmental increase in prefrontal activity alters network maturation and causes cognitive dysfunction in adult mice. *Neuron*, *109*(8), 1350-1364.e6. https://doi.org/10.1016/j.neuron.2021.02.011

Blizinsky, K. D., Diaz-Castro, B., Forrest, M. P., Schürmann, B., Bach, A. P., Martin-de-Saavedra, M. D., Wang, L., Csernansky, J. G., Duan, J., & Penzes, P. (2016). Reversal of dendritic phenotypes in 16p11.2 microduplication mouse model neurons by pharmacological targeting of a network hub. *Proceedings of the National Academy of Sciences*, *113*(30), 8520–8525. https://doi.org/10.1073/pnas.1607014113

Bomkamp, C., Tripathy, S. J., Bengtsson Gonzales, C., Hjerling-Leffler, J., Craig, A. M., & Pavlidis, P. (2019). Transcriptomic correlates of electrophysiological and morphological diversity within and

725 across excitatory and inhibitory neuron classes. *PLOS Computational Biology*, *15*(6), e1007113.
726 https://doi.org/10.1371/journal.pcbi.1007113
727 Breunig, J. J., Levy, R., Antonuk, C. D., Molina, J., Dutra-Clarke, M., Park, H., Akhtar, A. A., Kim, G.
728 B., Town, T., Hu, X., Bannykh, S. I., Verhaak, R. G. W., & Danielpour, M. (2015). Ets Factors
729 Regulate Neural Stem Cell Depletion and Gliogenesis in Ras Pathway Glioma. *Cell Reports*,
730 *12*(2), 258–271. https://doi.org/10.1016/j.celrep.2015.06.012
731 Bueno, O. F. (2000). The MEK1-ERK1/2 signaling pathway promotes compensated cardiac hypertrophy
732 in transgenic mice. *The EMBO Journal*, *19*(23), 6341–6350.
733 https://doi.org/10.1093/emboj/19.23.6341
734 Cancedda, L., Fiumelli, H., Chen, K., & Poo, M. -m. (2007). Excitatory GABA Action Is Essential for
735 Morphological Maturation of Cortical Neurons In Vivo. *Journal of Neuroscience*, *27*(19), 5224–
736 5235. https://doi.org/10.1523/JNEUROSCI.5169-06.2007
737 Chang, Y. S., Owen, J. P., Pojman, N. J., Thieu, T., Bukshpun, P., Wakahiro, M. L. J., Marco, E. J.,
738 Berman, J. I., Spiro, J. E., Chung, W. K., Buckner, R. L., Roberts, T. P. L., Nagarajan, S. S.,
739 Sherr, E. H., & Mukherjee, P. (2016). Reciprocal white matter alterations due to 16p11.2
740 chromosomal deletions versus duplications. *Human Brain Mapping*, *37*(8), 2833–2848.
741 https://doi.org/10.1002/hbm.23211
742 Chen, K., Yang, G., So, K.-F., & Zhang, L. (2019). Activation of Cortical Somatostatin Interneurons
743 Rescues Synapse Loss and Motor Deficits after Acute MPTP Infusion. *IScience*, *17*, 230–241.
744 https://doi.org/10.1016/j.isci.2019.06.040
745 Choveau, F. S., Abderemane-Ali, F., Coyan, F. C., Es-Salah-Lamoureux, Z., Baró, I., & Loussouarn, G.
746 (2012). Opposite Effects of the S4–S5 Linker and PIP2 on Voltage-Gated Channel Function:
747 KCNQ1/KCNE1 and Other Channels. *Frontiers in Pharmacology*, *3*.
748 https://doi.org/10.3389/fphar.2012.00125
749 Close, J., Xu, H., De Marco Garcia, N., Batista-Brito, R., Rossignol, E., Rudy, B., & Fishell, G. (2012).
750 Satb1 Is an Activity-Modulated Transcription Factor Required for the Terminal Differentiation

and Connectivity of Medial Ganglionic Eminence-Derived Cortical Interneurons. *Journal of Neuroscience*, *32*(49), 17690–17705. https://doi.org/10.1523/JNEUROSCI.3583-12.2012

Cohen, S. M., Ma, H., Kuchibhotla, K. V., Watson, B. O., Buzsáki, G., Froemke, R. C., & Tsien, R. W. (2016). Excitation-Transcription Coupling in Parvalbumin-Positive Interneurons Employs a Novel CaM Kinase-Dependent Pathway Distinct from Excitatory Neurons. *Neuron*, *90*(2), 292–307. https://doi.org/10.1016/j.neuron.2016.03.001

Courchesne, E., Gazestani, V. H., & Lewis, N. E. (2020). Prenatal Origins of ASD: The When, What, and How of ASD Development. *Trends in Neurosciences*, *43*(5), 326–342. https://doi.org/10.1016/j.tins.2020.03.005

Cowley, S. (1994). Activation of MAP kinase kinase is necessary and sufficient for PC12 differentiation and for transformation of NIH 3T3 cells. *Cell*, *77*(6), 841–852. https://doi.org/10.1016/0092-8674(94)90133-3

Cristo, G. D., Berardi, N., Cancedda, L., Pizzorusso, T., Putignano, E., Ratto, G. M., & Maffei, L. (2001). Requirement of ERK Activation for Visual Cortical Plasticity. *Science*, *292*(5525), 2337–2340. https://doi.org/10.1126/science.1059075

Cummings, K. A., & Clem, R. L. (2020). Prefrontal somatostatin interneurons encode fear memory. *Nature Neuroscience*, *23*(1), 61–74. https://doi.org/10.1038/s41593-019-0552-7

Davies, P., Katzman, R., & Terry, R. D. (1980). Reduced somatostatin-like immunoreactivity in cerebral cortex from cases of Alzheimer disease and Alzheimer senile dementa. *Nature*, *288*(5788), 279–280. https://doi.org/10.1038/288279a0

De Marco García, N. V., Karayannis, T., & Fishell, G. (2011). Neuronal activity is required for the development of specific cortical interneuron subtypes. *Nature*, *472*(7343), 351–355. https://doi.org/10.1038/nature09865

DeFelipe, J., López-Cruz, P. L., Benavides-Piccione, R., Bielza, C., Larrañaga, P., Anderson, S., Burkhalter, A., Cauli, B., Fairén, A., Feldmeyer, D., Fishell, G., Fitzpatrick, D., Freund, T. F., González-Burgos, G., Hestrin, S., Hill, S., Hof, P. R., Huang, J., Jones, E. G., … Ascoli, G. A.

(2013). New insights into the classification and nomenclature of cortical GABAergic interneurons. *Nature Reviews Neuroscience*, *14*(3), 202–216. https://doi.org/10.1038/nrn3444

Dehorter, N., Ciceri, G., Bartolini, G., Lim, L., del Pino, I., & Marín, O. (2015). Tuning of fast-spiking interneuron properties by an activity-dependent transcriptional switch. *Science*, *349*(6253), 1216–1220. https://doi.org/10.1126/science.aab3415

del Rio, J., de Lecea, L., Ferrer, I., & Soriano, E. (1994). The development of parvalbumin-immunoreactivity in the neocortex of the mouse. *Developmental Brain Research*, *81*(2), 247–259. https://doi.org/10.1016/0165-3806(94)90311-5

Denaxa, M., Kalaitzidou, M., Garefalaki, A., Achimastou, A., Lasrado, R., Maes, T., & Pachnis, V. (2012). Maturation-Promoting Activity of SATB1 in MGE-Derived Cortical Interneurons. *Cell Reports*, *2*(5), 1351–1362. https://doi.org/10.1016/j.celrep.2012.10.003

Denaxa, M., Neves, G., Rabinowitz, A., Kemlo, S., Liodis, P., Burrone, J., & Pachnis, V. (2018). Modulation of Apoptosis Controls Inhibitory Interneuron Number in the Cortex. *Cell Reports*, *22*(7), 1710–1721. https://doi.org/10.1016/j.celrep.2018.01.064

Dinh Duong, T. A., Hoshiba, Y., Saito, K., Kawasaki, K., Ichikawa, Y., Matsumoto, N., Shinmyo, Y., & Kawasaki, H. (2019). FGF Signaling Directs the Cell Fate Switch from Neurons to Astrocytes in the Developing Mouse Cerebral Cortex. *The Journal of Neuroscience*, *39*(31), 6081–6094. https://doi.org/10.1523/JNEUROSCI.2195-18.2019

Dobin, A., Davis, C. A., Schlesinger, F., Drenkow, J., Zaleski, C., Jha, S., Batut, P., Chaisson, M., & Gingeras, T. R. (2013). STAR: Ultrafast universal RNA-seq aligner. *Bioinformatics (Oxford, England)*, *29*(1), 15–21. https://doi.org/10.1093/bioinformatics/bts635

Edgar, R., Domrachev, M., & Lash, A. E. (2002). Gene Expression Omnibus: NCBI gene expression and hybridization array data repository. *Nucleic Acids Research*, *30*(1), 207–210. https://doi.org/10.1093/nar/30.1.207

Engin, E., & Treit, D. (2009). Anxiolytic and antidepressant actions of somatostatin: The role of sst2 and sst3 receptors. *Psychopharmacology*, *206*(2), 281–289. https://doi.org/10.1007/s00213-009-1605-5

Exposito-Alonso, D., Osório, C., Bernard, C., Pascual-García, S., del Pino, I., Marín, O., & Rico, B. (2020). Subcellular sorting of neuregulins controls the assembly of excitatory-inhibitory cortical circuits. *ELife*, *9*, e57000. https://doi.org/10.7554/eLife.57000

Faedo, A., Borello, U., & Rubenstein, J. L. R. (2010). Repression of Fgf Signaling by Sprouty1-2 Regulates Cortical Patterning in Two Distinct Regions and Times. *Journal of Neuroscience*, *30*(11), 4015–4023. https://doi.org/10.1523/JNEUROSCI.0307-10.2010

Fattah, M., Raman, M. M., Reiss, A. L., & Green, T. (2021). PTPN11 Mutations in the Ras-MAPK Signaling Pathway Affect Human White Matter Microstructure. *Cerebral Cortex*, *31*(3), 1489–1499. https://doi.org/10.1093/cercor/bhaa299

Fazzari, P., Paternain, A. V., Valiente, M., Pla, R., Luján, R., Lloyd, K., Lerma, J., Marín, O., & Rico, B. (2010). Control of cortical GABA circuitry development by Nrg1 and ErbB4 signalling. *Nature*, *464*(7293), 1376–1380. https://doi.org/10.1038/nature08928

Fee, C., Banasr, M., & Sibille, E. (2017). Somatostatin-Positive Gamma-Aminobutyric Acid Interneuron Deficits in Depression: Cortical Microcircuit and Therapeutic Perspectives. *Biological Psychiatry*, *82*(8), 549–559. https://doi.org/10.1016/j.biopsych.2017.05.024

Fernandez, B. A., Roberts, W., Chung, B., Weksberg, R., Meyn, S., Szatmari, P., Joseph-George, A. M., MacKay, S., Whitten, K., Noble, B., Vardy, C., Crosbie, V., Luscombe, S., Tucker, E., Turner, L., Marshall, C. R., & Scherer, S. W. (2010). Phenotypic spectrum associated with de novo and inherited deletions and duplications at 16p11.2 in individuals ascertained for diagnosis of autism spectrum disorder. *Journal of Medical Genetics*, *47*(3), 195–203. https://doi.org/10.1136/jmg.2009.069369

Filges, I., Sparagana, S., Sargent, M., Selby, K., Schlade-Bartusiak, K., Lueder, G. T., Robichaux-Viehoever, A., Schlaggar, B. L., Shimony, J. S., & Shinawi, M. (2014). Brain MRI abnormalities

and spectrum of neurological and clinical findings in three patients with proximal 16p11.2 microduplication. *American Journal of Medical Genetics. Part A*, *164A*(8), 2003–2012. https://doi.org/10.1002/ajmg.a.36605

Forloni, G., Hohmann, C., & Coyle, J. T. (1990). Developmental expression of somatostatin in mouse brain. I. Immunocytochemical studies. *Developmental Brain Research*, *53*(1), 6–25. https://doi.org/10.1016/0165-3806(90)90120-N

Fu, Y., Tucciarone, J. M., Espinosa, J. S., Sheng, N., Darcy, D. P., Nicoll, R. A., Huang, Z. J., & Stryker, M. P. (2014). A cortical circuit for gain control by behavioral state. *Cell*, *156*(6), 1139–1152. https://doi.org/10.1016/j.cell.2014.01.050

Furusho, M., Ishii, A., & Bansal, R. (2017). Signaling by FGF Receptor 2, Not FGF Receptor 1, Regulates Myelin Thickness through Activation of ERK1/2-MAPK, Which Promotes mTORC1 Activity in an Akt-Independent Manner. *The Journal of Neuroscience: The Official Journal of the Society for Neuroscience*, *37*(11), 2931–2946. https://doi.org/10.1523/JNEUROSCI.3316-16.2017

Furusho, M., Kaga, Y., Ishii, A., Hébert, J. M., & Bansal, R. (2011). Fibroblast growth factor signaling is required for the generation of oligodendrocyte progenitors from the embryonic forebrain. *The Journal of Neuroscience: The Official Journal of the Society for Neuroscience*, *31*(13), 5055–5066. https://doi.org/10.1523/JNEUROSCI.4800-10.2011

Fyffe-Maricich, S. L., Karlo, J. C., Landreth, G. E., & Miller, R. H. (2011). The ERK2 Mitogen-Activated Protein Kinase Regulates the Timing of Oligodendrocyte Differentiation. *Journal of Neuroscience*, *31*(3), 843–850. https://doi.org/10.1523/JNEUROSCI.3239-10.2011

Glorioso, C., Sabatini, M., Unger, T., Hashimoto, T., Monteggia, L. M., Lewis, D. A., & Mirnics, K. (2006). Specificity and timing of neocortical transcriptome changes in response to BDNF gene ablation during embryogenesis or adulthood. *Molecular Psychiatry*, *11*(7), 633–648. https://doi.org/10.1038/sj.mp.4001835

852 Goddeyne, C., Nichols, J., Wu, C., & Anderson, T. (2015). Repetitive mild traumatic brain injury induces
853 ventriculomegaly and cortical thinning in juvenile rats. *Journal of Neurophysiology*, *113*(9),
854 3268–3280. https://doi.org/10.1152/jn.00970.2014
855 Gour, A., Boergens, K. M., Heike, N., Hua, Y., Laserstein, P., Song, K., & Helmstaedter, M. (2021).
856 Postnatal connectomic development of inhibition in mouse barrel cortex. *Science*, *371*(6528),
857 eabb4534. https://doi.org/10.1126/science.abb4534
858 Grilli, M., Raiteri, L., & Pittaluga, A. (2004). Somatostatin inhibits glutamate release from mouse
859 cerebrocortical nerve endings through presynaptic sst2 receptors linked to the adenylyl cyclase–
860 protein kinase A pathway. *Neuropharmacology*, *46*(3), 388–396.
861 https://doi.org/10.1016/j.neuropharm.2003.09.012
862 Guenthner, C. J., Miyamichi, K., Yang, H. H., Heller, H. C., & Luo, L. (2013). Permanent Genetic Access
863 to Transiently Active Neurons via TRAP: Targeted Recombination in Active Populations.
864 *Neuron*, *78*(5), 773–784. https://doi.org/10.1016/j.neuron.2013.03.025
865 Gutmann, D. H., Wu, Y. L., Hedrick, N. M., Zhu, Y., Guha, A., & Parada, L. F. (2001). Heterozygosity
866 for the neurofibromatosis 1 (NF1) tumor suppressor results in abnormalities in cell attachment,
867 spreading and motility in astrocytes. *Human Molecular Genetics*, *10*(26), 3009–3016.
868 https://doi.org/10.1093/hmg/10.26.3009
869 Hanson, E., Armbruster, M., Lau, L. A., Sommer, M. E., Klaft, Z.-J., Swanger, S. A., Traynelis, S. F.,
870 Moss, S. J., Noubary, F., Chadchankar, J., & Dulla, C. G. (2019). Tonic Activation of
871 GluN2C/GluN2D-Containing NMDA Receptors by Ambient Glutamate Facilitates Cortical
872 Interneuron Maturation. *The Journal of Neuroscience: The Official Journal of the Society for*
873 *Neuroscience*, *39*(19), 3611–3626. https://doi.org/10.1523/JNEUROSCI.1392-18.2019
874 Heavner, W. E., & Smith, S. E. P. (2020). Resolving the Synaptic versus Developmental Dichotomy of
875 Autism Risk Genes. *Trends in Neurosciences*, *43*(4), 227–241.
876 https://doi.org/10.1016/j.tins.2020.01.009

877 Holter, M. C., Hewitt, L. T., Nishimura, K. J., Knowles, S. J., Bjorklund, G. R., Shah, S., Fry, N. R.,
878 Rees, K. P., Gupta, T. A., Daniels, C. W., Li, G., Marsh, S., Treiman, D. M., Olive, M. F.,
879 Anderson, T. R., Sanabria, F., Snider, W. D., & Newbern, J. M. (2021). Hyperactive MEK1
880 Signaling in Cortical GABAergic Neurons Promotes Embryonic Parvalbumin Neuron Loss and
881 Defects in Behavioral Inhibition. *Cerebral Cortex*, bhaa413.
882 https://doi.org/10.1093/cercor/bhaa413
883 Holter, M. C., Hewitt, Lauren. T., Koebele, S. V., Judd, J. M., Xing, L., Bimonte-Nelson, H. A., Conrad,
884 C. D., Araki, T., Neel, B. G., Snider, W. D., & Newbern, J. M. (2019). The Noonan Syndrome-
885 linked Raf1L613V mutation drives increased glial number in the mouse cortex and enhanced
886 learning. *PLOS Genetics*, *15*(4), e1008108. https://doi.org/10.1371/journal.pgen.1008108
887 Hong, E. J., McCord, A. E., & Greenberg, M. E. (2008). A Biological Function for the Neuronal Activity-
888 Dependent Component of Bdnf Transcription in the Development of Cortical Inhibition. *Neuron*,
889 *60*(4), 610–624. https://doi.org/10.1016/j.neuron.2008.09.024
890 Hrvatin, S., Hochbaum, D. R., Nagy, M. A., Cicconet, M., Robertson, K., Cheadle, L., Zilionis, R.,
891 Ratner, A., Borges-Monroy, R., Klein, A. M., Sabatini, B. L., & Greenberg, M. E. (2018). Single-
892 cell analysis of experience-dependent transcriptomic states in the mouse visual cortex. *Nature*
893 *Neuroscience*, *21*(1), 120–129. https://doi.org/10.1038/s41593-017-0029-5
894 Hu, J. S., Vogt, D., Sandberg, M., & Rubenstein, J. L. (2017). Cortical interneuron development: A tale of
895 time and space. *Development*, *144*(21), 3867–3878. https://doi.org/10.1242/dev.132852
896 Huang, Z. J., Kirkwood, A., Pizzorusso, T., Porciatti, V., Morales, B., Bear, M. F., Maffei, L., &
897 Tonegawa, S. (1999). BDNF Regulates the Maturation of Inhibition and the Critical Period of
898 Plasticity in Mouse Visual Cortex. *Cell*, *98*(6), 739–755. https://doi.org/10.1016/S0092-
899 8674(00)81509-3
900 Hutton, S. R., Otis, J. M., Kim, E. M., Lamsal, Y., Stuber, G. D., & Snider, W. D. (2017). ERK/MAPK
901 Signaling Is Required for Pathway-Specific Striatal Motor Functions. *The Journal of*

Neuroscience: The Official Journal of the Society for Neuroscience, *37*(34), 8102–8115. https://doi.org/10.1523/JNEUROSCI.0473-17.2017

Imamura, O., Pagès, G., Pouysségur, J., Endo, S., & Takishima, K. (2010). ERK1 and ERK2 are required for radial glial maintenance and cortical lamination. *Genes to Cells: Devoted to Molecular & Cellular Mechanisms*, *15*(10), 1072–1088. https://doi.org/10.1111/j.1365-2443.2010.01444.x

Ishii, A., Furusho, M., Dupree, J. L., & Bansal, R. (2016). Strength of ERK1/2 MAPK Activation Determines Its Effect on Myelin and Axonal Integrity in the Adult CNS. *The Journal of Neuroscience: The Official Journal of the Society for Neuroscience*, *36*(24), 6471–6487. https://doi.org/10.1523/JNEUROSCI.0299-16.2016

Ishii, A., Fyffe-Maricich, S. L., Furusho, M., Miller, R. H., & Bansal, R. (2012). ERK1/ERK2 MAPK Signaling is Required to Increase Myelin Thickness Independent of Oligodendrocyte Differentiation and Initiation of Myelination. *Journal of Neuroscience*, *32*(26), 8855–8864. https://doi.org/10.1523/JNEUROSCI.0137-12.2012

Itami, C., Kimura, F., & Nakamura, S. (2007). Brain-Derived Neurotrophic Factor Regulates the Maturation of Layer 4 Fast-Spiking Cells after the Second Postnatal Week in the Developing Barrel Cortex. *Journal of Neuroscience*, *27*(9), 2241–2252. https://doi.org/10.1523/JNEUROSCI.3345-06.2007

Jendryka, M., Palchaudhuri, M., Ursu, D., van der Veen, B., Liss, B., Kätzel, D., Nissen, W., & Pekcec, A. (2019). Pharmacokinetic and pharmacodynamic actions of clozapine-N-oxide, clozapine, and compound 21 in DREADD-based chemogenetics in mice. *Scientific Reports*, *9*(1), 4522. https://doi.org/10.1038/s41598-019-41088-2

Kaneko, K., Currin, C. B., Goff, K. M., Wengert, E. R., Somarowthu, A., Vogels, T. P., & Goldberg, E. M. (2022). Developmentally regulated impairment of parvalbumin interneuron synaptic transmission in an experimental model of Dravet syndrome. *Cell Reports*, *38*(13), 110580. https://doi.org/10.1016/j.celrep.2022.110580

927 Kawaguchi, Y. (1997). GABAergic cell subtypes and their synaptic connections in rat frontal cortex.
928 *Cerebral Cortex*, *7*(6), 476–486. https://doi.org/10.1093/cercor/7.6.476
929 Kessaris, N., Fogarty, M., Iannarelli, P., Grist, M., Wegner, M., & Richardson, W. D. (2006). Competing
930 waves of oligodendrocytes in the forebrain and postnatal elimination of an embryonic lineage.
931 *Nature Neuroscience*, *9*(2), 173–179. https://doi.org/10.1038/nn1620
932 Kessaris, N., Jamen, F., Rubin, L. L., & Richardson, W. D. (2004). Cooperation between sonic hedgehog
933 and fibroblast growth factor/MAPK signalling pathways in neocortical precursors. *Development*
934 *(Cambridge, England)*, *131*(6), 1289–1298. https://doi.org/10.1242/dev.01027
935 Kiviniemi, A., Gardberg, M., Frantzén, J., Pesola, M., Vuorinen, V., Parkkola, R., Tolvanen, T., Suilamo,
936 S., Johansson, J., Luoto, P., Kemppainen, J., Roivainen, A., & Minn, H. (2015). Somatostatin
937 receptor subtype 2 in high-grade gliomas: PET/CT with 68Ga-DOTA-peptides, correlation to
938 prognostic markers, and implications for targeted radiotherapy. *EJNMMI Research*, *5*(1), 25.
939 https://doi.org/10.1186/s13550-015-0106-2
940 Klemke, R. L., Cai, S., Giannini, A. L., Gallagher, P. J., de Lanerolle, P., & Cheresh, D. A. (1997).
941 Regulation of cell motility by mitogen-activated protein kinase. *The Journal of Cell Biology*,
942 *137*(2), 481–492. https://doi.org/10.1083/jcb.137.2.481
943 Klesse, L. J., Meyers, K. A., Marshall, C. J., & Parada, L. F. (1999). Nerve growth factor induces survival
944 and differentiation through two distinct signaling cascades in PC12 cells. *Oncogene*, *18*(12),
945 2055–2068. https://doi.org/10.1038/sj.onc.1202524
946 Kluge, C., Stoppel, C., Szinyei, C., Stork, O., & Pape, H.-C. (2008). Role of the somatostatin system in
947 contextual fear memory and hippocampal synaptic plasticity. *Learning & Memory*, *15*(4), 252–
948 260. https://doi.org/10.1101/lm.793008
949 Knowles, S. J., Stafford, A. M., Zaman, T., Angara, K., Williams, M. R., Newbern, J. M., & Vogt, D.
950 (2022). *Distinct hyperactive RAS/MAPK alleles converge on common GABAergic interneuron*
951 *core programs* [Preprint]. Neuroscience. https://doi.org/10.1101/2022.08.04.502867

Krencik, R., Hokanson, K. C., Narayan, A. R., Dvornik, J., Rooney, G. E., Rauen, K. A., Weiss, L. A., Rowitch, D. H., & Ullian, E. M. (2015). Dysregulation of astrocyte extracellular signaling in Costello syndrome. *Science Translational Medicine*, *7*(286), 286ra66. https://doi.org/10.1126/scitranslmed.aaa5645

Krenz, M., Gulick, J., Osinska, H. E., Colbert, M. C., Molkentin, J. D., & Robbins, J. (2008). Role of ERK1/2 signaling in congenital valve malformations in Noonan syndrome. *Proceedings of the National Academy of Sciences*, *105*(48), 18930–18935. https://doi.org/10.1073/pnas.0806556105

Lajiness, J. D., Snider, P., Wang, J., Feng, G.-S., Krenz, M., & Conway, S. J. (2014). SHP-2 deletion in postmigratory neural crest cells results in impaired cardiac sympathetic innervation. *Proceedings of the National Academy of Sciences*, *111*(14), E1374–E1382. https://doi.org/10.1073/pnas.1319208111

Lavoie, H., Gagnon, J., & Therrien, M. (2020). ERK signalling: A master regulator of cell behaviour, life and fate. *Nature Reviews Molecular Cell Biology*, *21*(10), 607–632. https://doi.org/10.1038/s41580-020-0255-7

Lee, C., Harkin, E. F., Yin, X., Naud, R., & Chen, S. (2022). Cell-type-specific responses to associative learning in the primary motor cortex. *ELife*, *11*, e72549. https://doi.org/10.7554/eLife.72549

Lee, D. R., Rhodes, C., Mitra, A., Zhang, Y., Maric, D., Dale, R. K., & Petros, T. J. (2022). Transcriptional heterogeneity of ventricular zone cells in the ganglionic eminences of the mouse forebrain. *ELife*, *11*, e71864. https://doi.org/10.7554/eLife.71864

Li, S., Mattar, P., Dixit, R., Lawn, S. O., Wilkinson, G., Kinch, C., Eisenstat, D., Kurrasch, D. M., Chan, J. A., & Schuurmans, C. (2014). RAS/ERK Signaling Controls Proneural Genetic Programs in Cortical Development and Gliomagenesis. *Journal of Neuroscience*, *34*(6), 2169–2190. https://doi.org/10.1523/JNEUROSCI.4077-13.2014

Li, X., Newbern, J. M., Wu, Y., Morgan-Smith, M., Zhong, J., Charron, J., & Snider, W. D. (2012). MEK Is a Key Regulator of Gliogenesis in the Developing Brain. *Neuron*, *75*(6), 1035–1050. https://doi.org/10.1016/j.neuron.2012.08.031

Liguz-Lecznar, M., Urban-Ciecko, J., & Kossut, M. (2016). Somatostatin and Somatostatin-Containing Neurons in Shaping Neuronal Activity and Plasticity. *Frontiers in Neural Circuits*, *10*. https://doi.org/10.3389/fncir.2016.00048

Lim, L., Mi, D., Llorca, A., & Marín, O. (2018). Development and Functional Diversification of Cortical Interneurons. *Neuron*, *100*(2), 294–313. https://doi.org/10.1016/j.neuron.2018.10.009

Linhares, N. D., Freire, M. C. M., Cardenas, R. G. C. do C. L., Pena, H. B., Lachlan, K., Dallapiccola, B., Bacino, C., Delobel, B., James, P., Thuresson, A.-C., Annerén, G., & Pena, S. D. J. (2016). 1p13.2 deletion displays clinical features overlapping Noonan syndrome, likely related to NRAS gene haploinsufficiency. *Genetics and Molecular Biology*, *39*(3), 349–357. https://doi.org/10.1590/1678-4685-GMB-2016-0049

Lodato, S., Rouaux, C., Quast, K. B., Jantrachotechatchawan, C., Studer, M., Hensch, T. K., & Arlotta, P. (2011). Excitatory Projection Neuron Subtypes Control the Distribution of Local Inhibitory Interneurons in the Cerebral Cortex. *Neuron*, *69*(4), 763–779. https://doi.org/10.1016/j.neuron.2011.01.015

López-Juárez, A., Titus, H. E., Silbak, S. H., Pressler, J. W., Rizvi, T. A., Bogard, M., Bennett, M. R., Ciraolo, G., Williams, M. T., Vorhees, C. V., & Ratner, N. (2017). Oligodendrocyte Nf1 Controls Aberrant Notch Activation and Regulates Myelin Structure and Behavior. *Cell Reports*, *19*(3), 545–557. https://doi.org/10.1016/j.celrep.2017.03.073

Lord, C., Brugha, T. S., Charman, T., Cusack, J., Dumas, G., Frazier, T., Jones, E. J. H., Jones, R. M., Pickles, A., State, M. W., Taylor, J. L., & Veenstra-VanderWeele, J. (2020). Autism spectrum disorder. *Nature Reviews Disease Primers*, *6*(1), 5. https://doi.org/10.1038/s41572-019-0138-4

Love, M. I., Huber, W., & Anders, S. (2014). Moderated estimation of fold change and dispersion for RNA-seq data with DESeq2. *Genome Biology*, *15*(12), 550. https://doi.org/10.1186/s13059-014-0550-8

Ma, S., Skarica, M., Li, Q., Xu, C., Risgaard, R. D., Tebbenkamp, A. T. N., Mato-Blanco, X., Kovner, R., Krsnik, Ž., de Martin, X., Luria, V., Martí-Pérez, X., Liang, D., Karger, A., Schmidt, D. K.,

Gomez-Sanchez, Z., Qi, C., Gobeske, K. T., Pochareddy, S., … Sestan, N. (2022). Molecular and cellular evolution of the primate dorsolateral prefrontal cortex. *Science*, *377*(6614), eabo7257. https://doi.org/10.1126/science.abo7257

Madisen, L., Zwingman, T. A., Sunkin, S. M., Oh, S. W., Zariwala, H. A., Gu, H., Ng, L. L., Palmiter, R. D., Hawrylycz, M. J., Jones, A. R., Lein, E. S., & Zeng, H. (2010). A robust and high-throughput Cre reporting and characterization system for the whole mouse brain. *Nature Neuroscience*, *13*(1), 133–140. https://doi.org/10.1038/nn.2467

Magno, L., Asgarian, Z., Pendolino, V., Velona, T., Mackintosh, A., Lee, F., Stryjewska, A., Zimmer, C., Guillemot, F., Farrant, M., Clark, B., & Kessaris, N. (2021). Transient developmental imbalance of cortical interneuron subtypes presages long-term changes in behavior. *Cell Reports*, *35*(11), 109249. https://doi.org/10.1016/j.celrep.2021.109249

Maisonpierre, P. C., Belluscio, L., Friedman, B., Alderson, R. F., Wiegand, S. J., Furth, M. E., Lindsay, R. M., & Yancopoulos, G. D. (1990). NT-3, BDNF, and NGF in the developing rat nervous system: Parallel as well as reciprocal patterns of expression. *Neuron*, *5*(4), 501–509. https://doi.org/10.1016/0896-6273(90)90089-X

Malik, R., Pai, E. L.-L., Rubin, A. N., Stafford, A. M., Angara, K., Minasi, P., Rubenstein, J. L., Sohal, V. S., & Vogt, D. (2019). Tsc1 represses parvalbumin expression and fast-spiking properties in somatostatin lineage cortical interneurons. *Nature Communications*, *10*(1), 4994. https://doi.org/10.1038/s41467-019-12962-4

Mardinly, A. R., Spiegel, I., Patrizi, A., Centofante, E., Bazinet, J. E., Tzeng, C. P., Mandel-Brehm, C., Harmin, D. A., Adesnik, H., Fagiolini, M., & Greenberg, M. E. (2016). Sensory experience regulates cortical inhibition by inducing IGF1 in VIP neurons. *Nature*, *531*(7594), 371–375. https://doi.org/10.1038/nature17187

Marsh, E. D., Nasrallah, M. P., Walsh, C., Murray, K. A., Nicole Sunnen, C., McCoy, A., & Golden, J. A. (2016). Developmental interneuron subtype deficits after targeted loss of Arx. *BMC Neuroscience*, *17*(1), 35. https://doi.org/10.1186/s12868-016-0265-8

Martin, D., Xu, J., Porretta, C., & Nichols, C. D. (2017). Neurocytometry: Flow Cytometric Sorting of Specific Neuronal Populations from Human and Rodent Brain. *ACS Chemical Neuroscience*, *8*(2), 356–367. https://doi.org/10.1021/acschemneuro.6b00374

Matthews, R. P., Guthrie, C. R., Wailes, L. M., Zhao, X., Means, A. R., & McKnight, G. S. (1994). Calcium/calmodulin-dependent protein kinase types II and IV differentially regulate CREB-dependent gene expression. *Molecular and Cellular Biology*, *14*(9), 6107–6116. https://doi.org/10.1128/MCB.14.9.6107

Mayer, C., Hafemeister, C., Bandler, R. C., Machold, R., Batista Brito, R., Jaglin, X., Allaway, K., Butler, A., Fishell, G., & Satija, R. (2018). Developmental diversification of cortical inhibitory interneurons. *Nature*, *555*(7697), 457–462. https://doi.org/10.1038/nature25999

McCormick, D. A., Connors, B. W., Lighthall, J. W., & Prince, D. A. (1985). Comparative electrophysiology of pyramidal and sparsely spiny stellate neurons of the neocortex. *Journal of Neurophysiology*, *54*(4), 782–806. https://doi.org/10.1152/jn.1985.54.4.782

McKeage, K. (2015). Pasireotide in Acromegaly: A Review. *Drugs*, *75*(9), 1039–1048. https://doi.org/10.1007/s40265-015-0413-y

McKenzie, M. G., Cobbs, L. V., Dummer, P. D., Petros, T. J., Halford, M. M., Stacker, S. A., Zou, Y., Fishell, G. J., & Au, E. (2019). Non-canonical Wnt Signaling through Ryk Regulates the Generation of Somatostatin- and Parvalbumin-Expressing Cortical Interneurons. *Neuron*, *103*(5), 853-864.e4. https://doi.org/10.1016/j.neuron.2019.06.003

Mi, D., Li, Z., Lim, L., Li, M., Moissidis, M., Yang, Y., Gao, T., Hu, T. X., Pratt, T., Price, D. J., Sestan, N., & Marín, O. (2018). Early emergence of cortical interneuron diversity in the mouse embryo. *Science*, *360*(6384), 81–85. https://doi.org/10.1126/science.aar6821

Miller, M. N., Okaty, B. W., Kato, S., & Nelson, S. B. (2011). Activity-dependent changes in the firing properties of neocortical fast-spiking interneurons in the absence of large changes in gene expression. *Developmental Neurobiology*, *71*(1), 62–70. https://doi.org/10.1002/dneu.20811

1055 Minocha, S., Valloton, D., Ypsilanti, A. R., Fiumelli, H., Allen, E. A., Yanagawa, Y., Marin, O.,
1056 Chédotal, A., Hornung, J.-P., & Lebrand, C. (2015). Nkx2.1-derived astrocytes and neurons
1057 together with Slit2 are indispensable for anterior commissure formation. *Nature Communications*,
1058 *6*, 6887. https://doi.org/10.1038/ncomms7887
1059 Miyoshi, G., Butt, S. J. B., Takebayashi, H., & Fishell, G. (2007). Physiologically Distinct Temporal
1060 Cohorts of Cortical Interneurons Arise from Telencephalic Olig2-Expressing Precursors. *Journal*
1061 *of Neuroscience*, *27*(29), 7786–7798. https://doi.org/10.1523/JNEUROSCI.1807-07.2007
1062 Monory, K., Massa, F., Egertová, M., Eder, M., Blaudzun, H., Westenbroek, R., Kelsch, W., Jacob, W.,
1063 Marsch, R., Ekker, M., Long, J., Rubenstein, J. L., Goebbels, S., Nave, K.-A., During, M.,
1064 Klugmann, M., Wölfel, B., Dodt, H.-U., Zieglgänsberger, W., … Lutz, B. (2006). The
1065 Endocannabinoid System Controls Key Epileptogenic Circuits in the Hippocampus. *Neuron*,
1066 *51*(4), 455–466. https://doi.org/10.1016/j.neuron.2006.07.006
1067 Montminy, M. R., & Bilezikjian, L. M. (1987). Binding of a nuclear protein to the cyclic-AMP response
1068 element of the somatostatin gene. *Nature*, *328*(6126), 175–178. https://doi.org/10.1038/328175a0
1069 Mori, M. X., Itsuki, K., Hase, H., Sawamura, S., Kurokawa, T., Mori, Y., & Inoue, R. (2015). Dynamics
1070 of receptor-operated Ca2+ currents through TRPC channels controlled via the PI(4,5)P2-PLC
1071 signaling pathway. *Frontiers in Pharmacology*, *6*. https://doi.org/10.3389/fphar.2015.00022
1072 Moyses-Oliveira, M., Yadav, R., Erdin, S., & Talkowski, M. E. (2020). New gene discoveries highlight
1073 functional convergence in autism and related neurodevelopmental disorders. *Current Opinion in*
1074 *Genetics & Development*, *65*, 195–206. https://doi.org/10.1016/j.gde.2020.07.001
1075 Munguba, H., Nikouei, K., Hochgerner, H., Oberst, P., Kouznetsova, A., Ryge, J., Batista-Brito, R.,
1076 Munoz-Manchado, A. B., Close, J., Linnarsson, S., & Hjerling-Leffler, J. (2019). *Transcriptional*
1077 *maintenance of cortical somatostatin interneuron subtype identity during migration* [Preprint].
1078 Neuroscience. https://doi.org/10.1101/593285
1079 Nawaratne, V., Leach, K., Suratman, N., Loiacono, R. E., Felder, C. C., Armbruster, B. N., Roth, B. L.,
1080 Sexton, P. M., & Christopoulos, A. (2008). New Insights into the Function of M_4 Muscarinic

Acetylcholine Receptors Gained Using a Novel Allosteric Modulator and a DREADD (Designer Receptor Exclusively Activated by a Designer Drug). *Molecular Pharmacology*, *74*(4), 1119–1131. https://doi.org/10.1124/mol.108.049353

Neves, G., Shah, M. M., Liodis, P., Achimastou, A., Denaxa, M., Roalfe, G., Sesay, A., Walker, M. C., & Pachnis, V. (2013). The LIM Homeodomain Protein Lhx6 Regulates Maturation of Interneurons and Network Excitability in the Mammalian Cortex. *Cerebral Cortex*, *23*(8), 1811–1823. https://doi.org/10.1093/cercor/bhs159

Newbern, J., Li, X., Shoemaker, S. E., Zhou, J., Zhong, J., Wu, Y., Bonder, D., Hollenback, S., Coppola, G., Geschwind, D. H., Landreth, G. E., & Snider, W. D. (2011). Specific functions for ERK/MAPK signaling during PNS development. *Neuron*, *69*(1), 91–105. https://doi.org/10.1016/j.neuron.2010.12.003

Newbern, J., Zhong, J., Wickramasinghe, R. S., Li, X., Wu, Y., Samuels, I., Cherosky, N., Karlo, J. C., O'Loughlin, B., Wikenheiser, J., Gargesha, M., Doughman, Y. Q., Charron, J., Ginty, D. D., Watanabe, M., Saitta, S. C., Snider, W. D., & Landreth, G. E. (2008). Mouse and human phenotypes indicate a critical conserved role for ERK2 signaling in neural crest development. *Proceedings of the National Academy of Sciences of the United States of America*, *105*(44), 17115–17120. https://doi.org/10.1073/pnas.0805239105

Nichols, J., Bjorklund, G. R., Newbern, J., & Anderson, T. (2018). Parvalbumin fast-spiking interneurons are selectively altered by paediatric traumatic brain injury. *The Journal of Physiology*, *596*(7), 1277–1293. https://doi.org/10.1113/JP275393

Nigro, M. J., Hashikawa-Yamasaki, Y., & Rudy, B. (2018). Diversity and Connectivity of Layer 5 Somatostatin-Expressing Interneurons in the Mouse Barrel Cortex. *The Journal of Neuroscience*, *38*(7), 1622–1633. https://doi.org/10.1523/JNEUROSCI.2415-17.2017

Nowaczyk, M. J. M., Thompson, B. A., Zeesman, S., Moog, U., Sanchez-Lara, P. A., Magoulas, P. L., Falk, R. E., Hoover-Fong, J. E., Batista, D. A. S., Amudhavalli, S. M., White, S. M., Graham, G.

1106 E., & Rauen, K. A. (2014). Deletion of MAP2K2/MEK2: A novel mechanism for a RASopathy?
1107 *Clinical Genetics*, *85*(2), 138–146. https://doi.org/10.1111/cge.12116
1108 Obrietan, K., Gao, X.-B., & van den Pol, A. N. (2002). Excitatory Actions of GABA Increase BDNF
1109 Expression via a MAPK-CREB–Dependent Mechanism—A Positive Feedback Circuit in
1110 Developing Neurons. *Journal of Neurophysiology*, *88*(2), 1005–1015.
1111 https://doi.org/10.1152/jn.2002.88.2.1005
1112 Oishi, K., Watatani, K., Itoh, Y., Okano, H., Guillemot, F., Nakajima, K., & Gotoh, Y. (2009). Selective
1113 induction of neocortical GABAergic neurons by the PDK1-Akt pathway through activation of
1114 Mash1. *Proceedings of the National Academy of Sciences*, *106*(31), 13064–13069.
1115 https://doi.org/10.1073/pnas.0808400106
1116 Okaty, B. W., Miller, M. N., Sugino, K., Hempel, C. M., & Nelson, S. B. (2009). Transcriptional and
1117 Electrophysiological Maturation of Neocortical Fast-Spiking GABAergic Interneurons. *Journal*
1118 *of Neuroscience*, *29*(21), 7040–7052. https://doi.org/10.1523/JNEUROSCI.0105-09.2009
1119 O'Leary, D. D. M., Chou, S.-J., & Sahara, S. (2007). Area Patterning of the Mammalian Cortex. *Neuron*,
1120 *56*(2), 252–269. https://doi.org/10.1016/j.neuron.2007.10.010
1121 Orduz, D., Benamer, N., Ortolani, D., Coppola, E., Vigier, L., Pierani, A., & Angulo, M. C. (2019).
1122 Developmental cell death regulates lineage-related interneuron-oligodendroglia functional
1123 clusters and oligodendrocyte homeostasis. *Nature Communications*, *10*(1), 4249.
1124 https://doi.org/10.1038/s41467-019-11904-4
1125 Ouwenga, R., Lake, A. M., Aryal, S., Lagunas, T., & Dougherty, J. D. (2018). The Differences in Local
1126 Translatome across Distinct Neuron Types Is Mediated by Both Baseline Cellular Differences
1127 and Post-transcriptional Mechanisms. *Eneuro*, *5*(6), ENEURO.0320-18.2018.
1128 https://doi.org/10.1523/ENEURO.0320-18.2018
1129 Owen, J. P., Chang, Y. S., Pojman, N. J., Bukshpun, P., Wakahiro, M. L. J., Marco, E. J., Berman, J. I.,
1130 Spiro, J. E., Chung, W. K., Buckner, R. L., Roberts, T. P. L., Nagarajan, S. S., Sherr, E. H.,
1131 Mukherjee, P., & Simons VIP Consortium. (2014). Aberrant white matter microstructure in

children with 16p11.2 deletions. *The Journal of Neuroscience: The Official Journal of the Society for Neuroscience*, *34*(18), 6214–6223. https://doi.org/10.1523/JNEUROSCI.4495-13.2014

Owens, D. F., & Kriegstein, A. R. (2002). Is there more to gaba than synaptic inhibition? *Nature Reviews Neuroscience*, *3*(9), 715–727. https://doi.org/10.1038/nrn919

Pan, N. C., Fang, A., Shen, C., Sun, L., Wu, Q., & Wang, X. (2018). Early Excitatory Activity-Dependent Maturation of Somatostatin Interneurons in Cortical Layer 2/3 of Mice. *Cerebral Cortex*. https://doi.org/10.1093/cercor/bhy293

Pantazopoulos, H., Wiseman, J. T., Markota, M., Ehrenfeld, L., & Berretta, S. (2017). Decreased Numbers of Somatostatin-Expressing Neurons in the Amygdala of Subjects With Bipolar Disorder or Schizophrenia: Relationship to Circadian Rhythms. *Biological Psychiatry*, *81*(6), 536–547. https://doi.org/10.1016/j.biopsych.2016.04.006

Paul, A., Crow, M., Raudales, R., He, M., Gillis, J., & Huang, Z. J. (2017). Transcriptional Architecture of Synaptic Communication Delineates GABAergic Neuron Identity. *Cell*, *171*(3), 522-539.e20. https://doi.org/10.1016/j.cell.2017.08.032

Payne, J. M., Hearps, S. J. C., Walsh, K. S., Paltin, I., Barton, B., Ullrich, N. J., Haebich, K. M., Coghill, D., Gioia, G. A., Cantor, A., Cutter, G., Tonsgard, J. H., Viskochil, D., Rey-Casserly, C., Schorry, E. K., Ackerson, J. D., Klesse, L., Fisher, M. J., Gutmann, D. H., … the NF Clinical Trials Consortium. (2019). Reproducibility of cognitive endpoints in clinical trials: Lessons from neurofibromatosis type 1. *Annals of Clinical and Translational Neurology*, *6*(12), 2555–2565. https://doi.org/10.1002/acn3.50952

Peerboom, C., & Wierenga, C. J. (2021). The postnatal GABA shift: A developmental perspective. *Neuroscience & Biobehavioral Reviews*, *124*, 179–192. https://doi.org/10.1016/j.neubiorev.2021.01.024

Peng, Z., Zhang, N., Wei, W., Huang, C. S., Cetina, Y., Otis, T. S., & Houser, C. R. (2013). A Reorganized GABAergic Circuit in a Model of Epilepsy: Evidence from Optogenetic Labeling

and Stimulation of Somatostatin Interneurons. *Journal of Neuroscience*, *33*(36), 14392–14405. https://doi.org/10.1523/JNEUROSCI.2045-13.2013

Petros, T. J., Bultje, R. S., Ross, M. E., Fishell, G., & Anderson, S. A. (2015). Apical versus Basal Neurogenesis Directs Cortical Interneuron Subclass Fate. *Cell Reports*, *13*(6), 1090–1095. https://doi.org/10.1016/j.celrep.2015.09.079

Pietrobono, S., Gagliardi, S., & Stecca, B. (2019). Non-canonical Hedgehog Signaling Pathway in Cancer: Activation of GLI Transcription Factors Beyond Smoothened. *Frontiers in Genetics*, *10*, 556. https://doi.org/10.3389/fgene.2019.00556

Po, A., Silvano, M., Miele, E., Capalbo, C., Eramo, A., Salvati, V., Todaro, M., Besharat, Z. M., Catanzaro, G., Cucchi, D., Coni, S., Di Marcotullio, L., Canettieri, G., Vacca, A., Stassi, G., De Smaele, E., Tartaglia, M., Screpanti, I., De Maria, R., & Ferretti, E. (2017). Noncanonical GLI1 signaling promotes stemness features and in vivo growth in lung adenocarcinoma. *Oncogene*, *36*(32), 4641–4652. https://doi.org/10.1038/onc.2017.91

Polleux, F., Whitford, K. L., Dijkhuizen, P. A., Vitalis, T., & Ghosh, A. (2002). Control of cortical interneuron migration by neurotrophins and PI3-kinase signaling. *Development (Cambridge, England)*, *129*(13), 3147–3160.

Priya, R., Paredes, M. F., Karayannis, T., Yusuf, N., Liu, X., Jaglin, X., Graef, I., Alvarez-Buylla, A., & Fishell, G. (2018). Activity Regulates Cell Death within Cortical Interneurons through a Calcineurin-Dependent Mechanism. *Cell Reports*, *22*(7), 1695–1709. https://doi.org/10.1016/j.celrep.2018.01.007

Pucilowska, J., Puzerey, P. A., Karlo, J. C., Galan, R. F., & Landreth, G. E. (2012). Disrupted ERK Signaling during Cortical Development Leads to Abnormal Progenitor Proliferation, Neuronal and Network Excitability and Behavior, Modeling Human Neuro-Cardio-Facial-Cutaneous and Related Syndromes. *Journal of Neuroscience*, *32*(25), 8663–8677. https://doi.org/10.1523/JNEUROSCI.1107-12.2012

Pucilowska, J., Vithayathil, J., Tavares, E. J., Kelly, C., Karlo, J. C., & Landreth, G. E. (2015). The 16p11.2 Deletion Mouse Model of Autism Exhibits Altered Cortical Progenitor Proliferation and Brain Cytoarchitecture Linked to the ERK MAPK Pathway. *Journal of Neuroscience*, *35*(7), 3190–3200. https://doi.org/10.1523/JNEUROSCI.4864-13.2015

Qureshi, A. Y., Mueller, S., Snyder, A. Z., Mukherjee, P., Berman, J. I., Roberts, T. P. L., Nagarajan, S. S., Spiro, J. E., Chung, W. K., Sherr, E. H., Buckner, R. L., & Simons VIP Consortium. (2014). Opposing brain differences in 16p11.2 deletion and duplication carriers. *The Journal of Neuroscience: The Official Journal of the Society for Neuroscience*, *34*(34), 11199–11211. https://doi.org/10.1523/JNEUROSCI.1366-14.2014

Rauen, K. A. (2013). The RASopathies. *Annual Review of Genomics and Human Genetics*, *14*(1), 355–369. https://doi.org/10.1146/annurev-genom-091212-153523

Reh, R. K., Dias, B. G., Nelson, C. A., Kaufer, D., Werker, J. F., Kolb, B., Levine, J. D., & Hensch, T. K. (2020). Critical period regulation across multiple timescales. *Proceedings of the National Academy of Sciences*, 201820836. https://doi.org/10.1073/pnas.1820836117

Rizvi, T. A., Akunuru, S., de Courten-Myers, G., Switzer, R. C., Nordlund, M. L., & Ratner, N. (1999). Region-specific astrogliosis in brains of mice heterozygous for mutations in the neurofibromatosis type 1 (Nf1) tumor suppressor. *Brain Research*, *816*(1), 111–123. https://doi.org/10.1016/s0006-8993(98)01133-0

Robbins, R. J., Brines, M. L., Kim, J. H., Adrian, T., De Lanerolle, N., Welsh, S., & Spencer, D. D. (1991). A selective loss of somatostatin in the hippocampus of patients with temporal lobe epilepsy. *Annals of Neurology*, *29*(3), 325–332. https://doi.org/10.1002/ana.410290316

Rogan, S. C., & Roth, B. L. (2011). Remote Control of Neuronal Signaling. *Pharmacological Reviews*, *63*(2), 291–315. https://doi.org/10.1124/pr.110.003020

Rogers, S., Rozman, P. A., Valero, M., Doyle, W. K., & Buzsáki, G. (2021). Mechanisms and plasticity of chemogenically induced interneuronal suppression of principal cells. *Proceedings of the National Academy of Sciences*, *118*(2), e2014157118. https://doi.org/10.1073/pnas.2014157118

Rosina, E., Battan, B., Siracusano, M., Di Criscio, L., Hollis, F., Pacini, L., Curatolo, P., & Bagni, C. (2019). Disruption of mTOR and MAPK pathways correlates with severity in idiopathic autism. *Translational Psychiatry*, *9*(1), 50. https://doi.org/10.1038/s41398-018-0335-z

Roth, B. L. (2016). DREADDs for Neuroscientists. *Neuron*, *89*(4), 683–694. https://doi.org/10.1016/j.neuron.2016.01.040

Ryu, H.-H., Kang, M., Park, J., Park, S.-H., & Lee, Y.-S. (2019). Enriched expression of NF1 in inhibitory neurons in both mouse and human brain. *Molecular Brain*, *12*(1), 60. https://doi.org/10.1186/s13041-019-0481-0

Ryu, H.-H., Kim, T., Kim, J.-W., Kang, M., Park, P., Kim, Y. G., Kim, H., Ha, J., Choi, J. E., Lee, J., Lim, C.-S., Kim, C.-H., Kim, S. J., Silva, A. J., Kaang, B.-K., & Lee, Y.-S. (2019). Excitatory neuron–specific SHP2-ERK signaling network regulates synaptic plasticity and memory. *Science Signaling*, *12*(571), eaau5755. https://doi.org/10.1126/scisignal.aau5755

Saitta, S. C., Harris, S. E., McDonald-McGinn, D. M., Emanuel, B. S., Tonnesen, M. K., Zackai, E. H., Seitz, S. C., & Driscoll, D. A. (2004). Independent de novo 22q11.2 deletions in first cousins with DiGeorge/velocardiofacial syndrome. *American Journal of Medical Genetics*, *124A*(3), 313–317. https://doi.org/10.1002/ajmg.a.20421

Samuels, I. S., Karlo, J. C., Faruzzi, A. N., Pickering, K., Herrup, K., Sweatt, J. D., Saitta, S. C., & Landreth, G. E. (2008). Deletion of ERK2 Mitogen-Activated Protein Kinase Identifies Its Key Roles in Cortical Neurogenesis and Cognitive Function. *Journal of Neuroscience*, *28*(27), 6983–6995. https://doi.org/10.1523/JNEUROSCI.0679-08.2008

Samuels, I. S., Saitta, S. C., & Landreth, G. E. (2009). MAP'ing CNS Development and Cognition: An ERKsome Process. *Neuron*, *61*(2), 160–167. https://doi.org/10.1016/j.neuron.2009.01.001

Sánchez, A. I., García-Acero, M. A., Paredes, A., Quero, R., Ortega, R. I., Rojas, J. A., Herrera, D., Parra, M., Prieto, K., Ángel, J., Rodríguez, L.-S., Prieto, J. C., & Franco, M. (2020). Immunodeficiency in a Patient with 22q11.2 Distal Deletion Syndrome and a p.Ala7dup Variant in the ***MAPK1*** Gene. *Molecular Syndromology*, *11*(1), 15–23. https://doi.org/10.1159/000506032

Sanchez-Ortiz, E., Cho, W., Nazarenko, I., Mo, W., Chen, J., & Parada, L. F. (2014). NF1 regulation of RAS/ERK signaling is required for appropriate granule neuron progenitor expansion and migration in cerebellar development. *Genes & Development*, *28*(21), 2407–2420. https://doi.org/10.1101/gad.246603.114

Sanz, E., Yang, L., Su, T., Morris, D. R., McKnight, G. S., & Amieux, P. S. (2009). Cell-type-specific isolation of ribosome-associated mRNA from complex tissues. *Proceedings of the National Academy of Sciences*, *106*(33), 13939–13944. https://doi.org/10.1073/pnas.0907143106

Selcher, J. C. (2001). Mice Lacking the ERK1 Isoform of MAP Kinase Are Unimpaired in Emotional Learning. *Learning & Memory*, *8*(1), 11–19. https://doi.org/10.1101/lm.37001

Shimamura, K., & Rubenstein, J. L. (1997). Inductive interactions direct early regionalization of the mouse forebrain. *Development*, *124*(14), 2709–2718. https://doi.org/10.1242/dev.124.14.2709

Sik, A., Hajos, N., Gulacsi, A., Mody, I., & Freund, T. F. (1998). The absence of a major Ca2+ signaling pathway in GABAergic neurons of the hippocampus. *Proceedings of the National Academy of Sciences*, *95*(6), 3245–3250. https://doi.org/10.1073/pnas.95.6.3245

Silva, A. I., Ehrhart, F., Ulfarsson, M. O., Stefansson, H., Stefansson, K., Wilkinson, L. S., Hall, J., & Linden, D. E. J. (2022). Neuroimaging Findings in Neurodevelopmental Copy Number Variants: Identifying Molecular Pathways to Convergent Phenotypes. *Biological Psychiatry*, *92*(5), 341–361. https://doi.org/10.1016/j.biopsych.2022.03.018

Smith, S. J., Sümbül, U., Graybuck, L. T., Collman, F., Seshamani, S., Gala, R., Gliko, O., Elabbady, L., Miller, J. A., Bakken, T. E., Rossier, J., Yao, Z., Lein, E., Zeng, H., Tasic, B., & Hawrylycz, M. (2019). Single-cell transcriptomic evidence for dense intracortical neuropeptide networks. *ELife*, *8*, e47889. https://doi.org/10.7554/eLife.47889

Song, Y.-H., Hwang, Y.-S., Kim, K., Lee, H.-R., Kim, J.-H., Maclachlan, C., Dubois, A., Jung, M. W., Petersen, C. C. H., Knott, G., Lee, S.-H., & Lee, S.-H. (2020). Somatostatin enhances visual processing and perception by suppressing excitatory inputs to parvalbumin-positive interneurons in V1. *Science Advances*, *6*(17), eaaz0517. https://doi.org/10.1126/sciadv.aaz0517

Song, Y.-H., Yoon, J., & Lee, S.-H. (2021). The role of neuropeptide somatostatin in the brain and its application in treating neurological disorders. *Experimental & Molecular Medicine*, *53*(3), 328–338. https://doi.org/10.1038/s12276-021-00580-4

Southwell, D. G., Paredes, M. F., Galvao, R. P., Jones, D. L., Froemke, R. C., Sebe, J. Y., Alfaro-Cervello, C., Tang, Y., Garcia-Verdugo, J. M., Rubenstein, J. L., Baraban, S. C., & Alvarez-Buylla, A. (2012). Intrinsically determined cell death of developing cortical interneurons. *Nature*, *491*(7422), 109–113. https://doi.org/10.1038/nature11523

Spiegel, I., Mardinly, A. R., Gabel, H. W., Bazinet, J. E., Couch, C. H., Tzeng, C. P., Harmin, D. A., & Greenberg, M. E. (2014). Npas4 Regulates Excitatory-Inhibitory Balance within Neural Circuits through Cell-Type-Specific Gene Programs. *Cell*, *157*(5), 1216–1229. https://doi.org/10.1016/j.cell.2014.03.058

Sun, Y., Qian, L., Xu, L., Hunt, S., & Sah, P. (2020). Somatostatin neurons in the central amygdala mediate anxiety by disinhibition of the central sublenticular extended amygdala. *Molecular Psychiatry*. https://doi.org/10.1038/s41380-020-00894-1

Tallent, M. K., & Qiu, C. (2008). Somatostatin: An endogenous antiepileptic. *Molecular and Cellular Endocrinology*, *286*(1–2), 96–103. https://doi.org/10.1016/j.mce.2007.12.004

Talley, M. J., Nardini, D., Qin, S., Prada, C. E., Ehrman, L. A., & Waclaw, R. R. (2021). A role for sustained MAPK activity in the mouse ventral telencephalon. *Developmental Biology*, *476*, 137–147. https://doi.org/10.1016/j.ydbio.2021.03.019

Taniguchi, H., He, M., Wu, P., Kim, S., Paik, R., Sugino, K., Kvitsani, D., Fu, Y., Lu, J., Lin, Y., Miyoshi, G., Shima, Y., Fishell, G., Nelson, S. B., & Huang, Z. J. (2011). A Resource of Cre Driver Lines for Genetic Targeting of GABAergic Neurons in Cerebral Cortex. *Neuron*, *71*(6), 995–1013. https://doi.org/10.1016/j.neuron.2011.07.026

Tasic, B., Menon, V., Nguyen, T. N., Kim, T. K., Jarsky, T., Yao, Z., Levi, B., Gray, L. T., Sorensen, S. A., Dolbeare, T., Bertagnolli, D., Goldy, J., Shapovalova, N., Parry, S., Lee, C., Smith, K., Bernard, A., Madisen, L., Sunkin, S. M., … Zeng, H. (2016). Adult mouse cortical cell taxonomy

revealed by single cell transcriptomics. *Nature Neuroscience*, *19*(2), 335–346. https://doi.org/10.1038/nn.4216

Tereshko, L., Gao, Y., Cary, B. A., Turrigiano, G. G., & Sengupta, P. (2021). Ciliary neuropeptidergic signaling dynamically regulates excitatory synapses in postnatal neocortical pyramidal neurons. *ELife*, *10*, e65427. https://doi.org/10.7554/eLife.65427

Thomas, G. M., & Huganir, R. L. (2004). MAPK cascade signalling and synaptic plasticity. *Nature Reviews Neuroscience*, *5*(3), 173–183. https://doi.org/10.1038/nrn1346

Tidyman, W. E., & Rauen, K. A. (2016). Pathogenetics of the RASopathies. *Human Molecular Genetics*, *25*(R2), R123–R132. https://doi.org/10.1093/hmg/ddw191

Ting, A. K., Chen, Y., Wen, L., Yin, D.-M., Shen, C., Tao, Y., Liu, X., Xiong, W.-C., & Mei, L. (2011). Neuregulin 1 Promotes Excitatory Synapse Development and Function in GABAergic Interneurons. *Journal of Neuroscience*, *31*(1), 15–25. https://doi.org/10.1523/JNEUROSCI.2538-10.2011

Topolnik, L. (2012). Dendritic calcium mechanisms and long-term potentiation in cortical inhibitory interneurons: Calcium in interneuron dendrites. *European Journal of Neuroscience*, *35*(4), 496–506. https://doi.org/10.1111/j.1460-9568.2011.07988.x

Topolnik, L., Azzi, M., Morin, F., Kougioumoutzakis, A., & Lacaille, J.-C. (2006). mGluR1/5 subtype-specific calcium signalling and induction of long-term potentiation in rat hippocampal oriens/alveus interneurones: MGluR1/5 Ca^{2+} signalling and LTP in interneurones. *The Journal of Physiology*, *575*(1), 115–131. https://doi.org/10.1113/jphysiol.2006.112896

Tripp, A., Kota, R. S., Lewis, D. A., & Sibille, E. (2011). Reduced somatostatin in subgenual anterior cingulate cortex in major depression. *Neurobiology of Disease*, *42*(1), 116–124. https://doi.org/10.1016/j.nbd.2011.01.014

Tucker, E. S., Segall, S., Gopalakrishna, D., Wu, Y., Vernon, M., Polleux, F., & LaMantia, A.-S. (2008). Molecular Specification and Patterning of Progenitor Cells in the Lateral and Medial Ganglionic

Eminences. *Journal of Neuroscience*, *28*(38), 9504–9518. https://doi.org/10.1523/JNEUROSCI.2341-08.2008

Tuncdemir, S. N., Wamsley, B., Stam, F. J., Osakada, F., Goulding, M., Callaway, E. M., Rudy, B., & Fishell, G. (2016). Early Somatostatin Interneuron Connectivity Mediates the Maturation of Deep Layer Cortical Circuits. *Neuron*, *89*(3), 521–535. https://doi.org/10.1016/j.neuron.2015.11.020

Tyson, J. A., Goldberg, E. M., Maroof, A. M., Xu, Q., Petros, T. J., & Anderson, S. A. (2015). Duration of culture and sonic hedgehog signaling differentially specify PV versus SST cortical interneuron fates from embryonic stem cells. *Development*, *142*(7), 1267–1278. https://doi.org/10.1242/dev.111526

Urban-Ciecko, J., & Barth, A. L. (2016). Somatostatin-expressing neurons in cortical networks. *Nature Reviews Neuroscience*, *17*(7), 401–409. https://doi.org/10.1038/nrn.2016.53

Vithayathil, J., Pucilowska, J., Goodnough, L. H., Atit, R. P., & Landreth, G. E. (2015). Dentate Gyrus Development Requires ERK Activity to Maintain Progenitor Population and MAPK Pathway Feedback Regulation. *Journal of Neuroscience*, *35*(17), 6836–6848. https://doi.org/10.1523/JNEUROSCI.4196-14.2015

Vogt, D., Cho, K. K. A., Lee, A. T., Sohal, V. S., & Rubenstein, J. L. R. (2015). The Parvalbumin/Somatostatin Ratio Is Increased in Pten Mutant Mice and by Human PTEN ASD Alleles. *Cell Reports*, *11*(6), 944–956. https://doi.org/10.1016/j.celrep.2015.04.019

Vong, L., Ye, C., Yang, Z., Choi, B., Chua, S., & Lowell, B. B. (2011). Leptin Action on GABAergic Neurons Prevents Obesity and Reduces Inhibitory Tone to POMC Neurons. *Neuron*, *71*(1), 142–154. https://doi.org/10.1016/j.neuron.2011.05.028

Wei, Y., Han, X., & Zhao, C. (2020). PDK1 regulates the survival of the developing cortical interneurons. *Molecular Brain*, *13*(1), 65. https://doi.org/10.1186/s13041-020-00604-6

Wengert, E. R., Miralles, R. M., Wedgwood, K. C. A., Wagley, P. K., Strohm, S. M., Panchal, P. S., Idrissi, A. M., Wenker, I. C., Thompson, J. A., Gaykema, R. P., & Patel, M. K. (2021). Somatostatin-Positive Interneurons Contribute to Seizures in SCN8A Epileptic Encephalopathy.

The Journal of Neuroscience, *41*(44), 9257–9273. https://doi.org/10.1523/JNEUROSCI.0718-21.2021

Wonders, C. P., & Anderson, S. A. (2006). The origin and specification of cortical interneurons. *Nature Reviews Neuroscience*, *7*(9), 687–696. https://doi.org/10.1038/nrn1954

Wong, F. K., Bercsenyi, K., Sreenivasan, V., Portalés, A., Fernández-Otero, M., & Marín, O. (2018). Pyramidal cell regulation of interneuron survival sculpts cortical networks. *Nature*, *557*(7707), 668–673. https://doi.org/10.1038/s41586-018-0139-6

Wu, G.-Y., Deisseroth, K., & Tsien, R. W. (2001). Activity-dependent CREB phosphorylation: Convergence of a fast, sensitive calmodulin kinase pathway and a slow, less sensitive mitogen-activated protein kinase pathway. *Proceedings of the National Academy of Sciences*, *98*(5), 2808–2813. https://doi.org/10.1073/pnas.051634198

Xing, J., Ginty, D. D., & Greenberg, M. E. (1996). Coupling of the RAS-MAPK Pathway to Gene Activation by RSK2, a Growth Factor-Regulated CREB Kinase. *Science*, *273*(5277), 959–963. https://doi.org/10.1126/science.273.5277.959

Xing, L., Larsen, R. S., Bjorklund, G. R., Li, X., Wu, Y., Philpot, B. D., Snider, W. D., & Newbern, J. M. (2016). Layer specific and general requirements for ERK/MAPK signaling in the developing neocortex. *ELife*, *5*, e11123. https://doi.org/10.7554/eLife.11123

Xu, Q., Guo, L., Moore, H., Waclaw, R. R., Campbell, K., & Anderson, S. A. (2010). Sonic Hedgehog Signaling Confers Ventral Telencephalic Progenitors with Distinct Cortical Interneuron Fates. *Neuron*, *65*(3), 328–340. https://doi.org/10.1016/j.neuron.2010.01.004

Xu, Q., Tam, M., & Anderson, S. A. (2008). Fate mapping Nkx2.1-lineage cells in the mouse telencephalon. *The Journal of Comparative Neurology*, *506*(1), 16–29. https://doi.org/10.1002/cne.21529

Xu, Q., Wonders, C. P., & Anderson, S. A. (2005). Sonic hedgehog maintains the identity of cortical interneuron progenitors in the ventral telencephalon. *Development*, *132*(22), 4987–4998. https://doi.org/10.1242/dev.02090

Yamamoto, K. K., Gonzalez, G. A., Biggs, W. H., & Montminy, M. R. (1988). Phosphorylation-induced binding and transcriptional efficacy of nuclear factor CREB. *Nature*, *334*(6182), 494–498. https://doi.org/10.1038/334494a0

Yap, E.-L., & Greenberg, M. E. (2018). Activity-Regulated Transcription: Bridging the Gap between Neural Activity and Behavior. *Neuron*, *100*(2), 330–348. https://doi.org/10.1016/j.neuron.2018.10.013

Yu, W., Wang, Y., McDonnell, K., Stephen, D., & Bai, C. B. (2009). Patterning of ventral telencephalon requires positive function of Gli transcription factors. *Developmental Biology*, *334*(1), 264–275. https://doi.org/10.1016/j.ydbio.2009.07.026

Zeyda, T., Diehl, N., Paylor, R., Brennan, M. B., & Hochgeschwender, U. (2001). Impairment in motor learning of somatostatin null mutant mice. *Brain Research*, *906*(1–2), 107–114. https://doi.org/10.1016/S0006-8993(01)02563-X

Zhu, H., Aryal, D. K., Olsen, R. H. J., Urban, D. J., Swearingen, A., Forbes, S., Roth, B. L., & Hochgeschwender, U. (2016). Cre-dependent DREADD (Designer Receptors Exclusively Activated by Designer Drugs) mice. *Genesis (New York, N.Y.: 2000)*, *54*(8), 439–446. https://doi.org/10.1002/dvg.22949

Zou, D., Chen, L., Deng, D., Jiang, D., Dong, F., McSweeney, C., Zhou, Y., Liu, L., Chen, G., Wu, Y., & Mao, Y. (2016). DREADD in Parvalbumin Interneurons of the Dentate Gyrus Modulates Anxiety, Social Interaction and Memory Extinction. *Current Molecular Medicine*, *16*(1), 91–102. https://doi.org/10.2174/1566524016666151222150024